



Pontificia Universidad Católica del Perú

Escuela de Posgrado

Development of a measurement setup for
quantification of the vibration characteristics of the
hand-arm-system by inertial measurement units

Tesis para obtener el grado académico de Maestro en Ingeniería Mecánica que
presenta:

Carlos Gianpaul Rincón Ruiz

Asesor PUCP (PUCP): ***Jorge Hernán Alencastre Miranda***

Co-Asesor TU ILMENAU: ***Hartmut Witte***

Lima, 2024

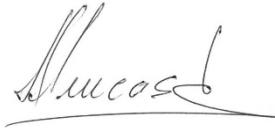
Informe de Similitud

Yo, Jorge Hernan Alencastre Miranda, docente de la Escuela de Posgrado de la Pontificia Universidad Católica del Perú, asesor de la tesis titulada Development of a measurement setup for quantification of the vibrational characteristics of the hand-arm-system by inertial measurement units, del autor Carlos Gianpaul Rincon Ruiz, dejo constancia de lo siguiente:

- El mencionado documento tiene un índice de puntuación de similitud de 8%. Así lo consigna el reporte de similitud emitido por el software *Turnitin* el 24/01/2025.
- He revisado con detalle dicho reporte y la Tesis o Trabajo de investigación, y no se advierte indicios de plagio.
- Las citas a otros autores y sus respectivas referencias cumplen con las pautas académicas.

Lugar y fecha:

Lima, 24 de enero de 2025.

| | |
|--------------------------------------------------------------------------------------------|-----------------------------------------------------------------------------------------------|
| Apellidos y nombres del asesor / de la asesora: <u>Alencastre Miranda, Jorge Hernán</u> | |
| DNI: 10588073 | Firma  |
| ORCID: 0000-0001-8442-8255 | |



*A mi madre, Maruja Ruiz,
cuyo amor trasciende toda distancia y tiempo,
es tanto lo que me has brindado, que este mérito es más tuyo que mío.*

Resumen

Dos síntomas caracterizan la enfermedad de Parkinson: el temblor patológico y la espasticidad en las extremidades. Ambos síntomas influyen significativamente en las actividades de movimiento deseadas, especialmente en el sistema mano-brazo (HAS, por sus siglas en inglés). Desde un punto de vista biomecánico, las características dinámicas del HAS pueden representarse mediante su impedancia. Una condición anormal podría manifestarse en un cambio de impedancia fuera del rango normal. En este sentido, la caracterización del comportamiento dinámico del HAS proporciona información crucial no solo para la determinación de un estado, sino también para cuantificar dicho comportamiento a través de parámetros que pueden representarse en un modelo biomecánico. Estos parámetros respaldan el desarrollo de soluciones de ingeniería actuales contra el temblor patológico, como dispositivos amortiguadores de vibraciones para mejorar el control del movimiento de las extremidades.

En esta investigación, se realizó el desarrollo de un sistema de medición para cuantificar el comportamiento dinámico del HAS bajo condiciones de vibración. La concepción de un método de caracterización formó parte de la fase conceptual del desarrollo. A través de la revisión de la literatura, se identificó que la tensión muscular es una de las variables más significativas en la respuesta dinámica del HAS. La tensión muscular controla los grados de libertad (DoF) de los elementos de la extremidad. Además, se investigaron la postura y las condiciones de perturbación como variables influyentes. El sistema de medición se implementó a nivel de prototipo para validar el concepto desarrollado en una fase experimental, en la que se evaluaron las principales capacidades del sistema. Los datos experimentales de un sujeto de prueba mostraron que el sistema de medición puede cuantificar de manera efectiva la respuesta dinámica, la influencia de la tensión muscular (indirectamente a través de la medición de fuerza), la postura y la perturbación (vibración generada por un shaker). Los datos medidos (a través de IMUs) pueden utilizarse para la estimación de los parámetros dinámicos de un modelo biomecánico del HAS. En una siguiente fase, se requiere análisis adicional con más sujetos de prueba para cuantificar las tendencias de influencia de las variables e identificar rangos de comportamiento promedio.

Abstract

Two symptoms characterize the Parkinson disease: pathological tremor and spasticity in the limbs. Both symptoms influence the desired motion activities significantly, specially on the hand-arm-system (HAS). From a biomechanical point of view, the dynamic characteristics of the HAS can be represented by its impedance. An abnormal condition could be manifested in an impedance change out of the normal range. In this sense, the characterization of the dynamic behaviour of the HAS provides critical information not only for the determination of a state, but also to quantify the behaviour through parameters that can be represented in a biomechanical model. These parameters support the development of current engineered solutions against the pathological tremor as vibration absorber devices to improve the motion control of limbs.

In this research, the development of a measurement setup was carried out to quantify the dynamic behaviour of the HAS under vibration conditions. The conception of a characterization method was part of the concept phase of the development. Identified through literature research, the muscle tension is one of the most significant variables in the dynamic response of the HAS. The muscle tension controls the degrees of freedom (DoF) of the limb elements. Furthermore, posture and perturbation conditions were also investigated as influential variables. The measurement setup was implemented in a prototype level to validate the concept developed through an experimental phase where main capabilities of the setup were tested. The experimental data from one test subject showed that the measurement setup can effectively quantify the dynamic response, the influence of the muscle tension (indirectly via force measurement), posture and perturbation (vibration initiation via shaker). The measured data (IMU data) can be used for the estimation of the dynamic parameters of a biomechanical model of the HAS. Further analysis with more test subjects are required to quantify tendencies of the variables influence and identify ranges of average behaviour.

Kurzfassung

Zwei Symptome charakterisieren eine Parkinson-Erkrankung: ein pathologischer Tremor und eine Spastik in den Extremitäten. Beide Symptome haben einen starken Einfluss auf die gewünschten Bewegungsaktivitäten, besonders auf das Hand-Arm-System (HAS). Aus biomechanischer Perspektive können die dynamischen Eigenschaften des HAS durch seine Impedanz dargestellt werden. Anormale Zustände könnten sich in einer Impedanzänderung außerhalb des normalen Bereichs zeigen. In diesem Sinne ermöglicht die Charakterisierung des dynamischen Verhaltens des HAS nicht nur die Bestimmung eines Zustands, sondern auch die Quantifizierung des Verhaltens durch Parameter, die in einem biomechanischen Modell dargestellt werden können. Diese Parameter unterstützen die Entwicklung aktueller technischer Lösungen zur Verringerung des pathologischen Tremors in Form von Schwingungsdämpfern zur Verbesserung der Bewegungskontrolle der Gliedmaßen.

In dieser Forschungsarbeit wurde ein Messaufbau entwickelt, um das dynamische Verhalten des HAS während Vibrationen zu quantifizieren. Die Konzeption einer Charakterisierungsmethode war Teil der Konzeptphase der Entwicklung. Aus der Literaturrecherche ergab sich als eine der wichtigsten Variablen für die dynamische Reaktion des HAS die Muskelspannung. Mittels muskulärer Anspannung werden die Freiheitsgrade (DoF) der Gliedmaßelemente gesteuert. Des Weiteren werden die Körperhaltung und die Störungsbedingungen als beeinflussende Variablen untersucht. Der Messaufbau wurde als Prototyp implementiert, um das entwickelte Konzept durch eine experimentelle Phase zu validieren, in der die wichtigsten Eigenschaften des Aufbaus getestet wurden. Die Experimentaldaten eines Probanden zeigen, dass der Messaufbau die dynamische Reaktion, den Einfluss der Muskelspannung (indirekt über Kraftmessung), der Körperhaltung und der Störung (Schwingungseinleitung mittels Shaker) effektiv quantifizieren kann und die gemessenen Daten (IMU-Daten) für die Bestimmung der dynamischen Parameter eines biomechanischen Modells des HAS verwendet werden können. Weitere Analysen mit mehr Probanden sind erforderlich, um die Tendenzen des Einflusses der Variablen zu quantifizieren und die Bereiche des Normalen zu identifizieren.

Agradecimientos

Es difícil agradecer sólo con palabras a tantas personas que han contribuido a mi desarrollo durante este periodo. En la TU Ilmenau, quiero expresar mi agradecimiento al Prof. Dr. Hartmut Witte por su invaluable contribución académica y mentoría en el desarrollo de este trabajo. Me gustaría agradecer con la misma intensidad a la M.Sc. Sabine Bruchmueller por su cercana tutoría en el trabajo diario, por el conocimiento compartido en el área anatómica y su paciencia en las explicaciones. Agradezco también al Dipl.- Ing. Sebastian Koehring por el constante soporte en el desarrollo constructivo y optimización. Extiendo mis gracias al Dr. Emanuel Andrada, no sólo por el conocimiento compartido en Biomecánica, sino también por su consejo y apoyo personal.

Quiero también expresar mi más sincero agradecimiento al Prof. Dr. René Theska por su guía en este periodo y por hacer posible este crecimiento académico en la TU Ilmenau.

En la PUCP, quiero expresar mi profundo agradecimiento a mi estimado Prof. Dr. Alencastre, por su continuo soporte, no sólo en el área académica, sino también por toda la ayuda brindada personalmente y también por la mentoría a lo largo de los años. Asimismo, expreso mi profundo agradecimiento al Prof. Dr. Jorge Rodriguez, por todo su invaluable soporte, dedicación con el desarrollo académico de sus estudiantes y hacer posible esta oportunidad. De la misma forma, quiero agradecer a Enrique Carrillo, Enrique Pujada y Daniel Lavayen por el soporte en estos años de trabajo.

Mi gratitud también se extiende profundamente a mis amigos, Carlos P., César H., Karla H., Moisés M., Elizabeth B. y Martín A. Gracias por todo su apoyo.

A mi familia, especialmente mis padres y hermana, quiero desde lo más profundo de mi corazón. A mi madre, Maruja, cuya resiliencia y fortaleza me inspiran a continuar cada día. A mi padre, Carlos, por mostrarme con su ejemplo que el esfuerzo carece de límites. A mi hermana, quien -aunque tal vez no lo sepa- fue parte de la razón por la que inicié este viaje. Continua excediendo en tus metas, solamente no seas tan dura contigo misma. A mi novia, Ingrid, por su confianza e incondicional soporte, no limitado a la distancia, pues cruzaste un continente para estar aquí. Gracias por hacerme sentir cerca de casa, Rini.

A todos, gracias. Espero algún día poder retribuir lo que han hecho por mí, aunque temo que nunca será suficiente.

Ilmenau, Julio 2024
Gianpaul Rincón

Content

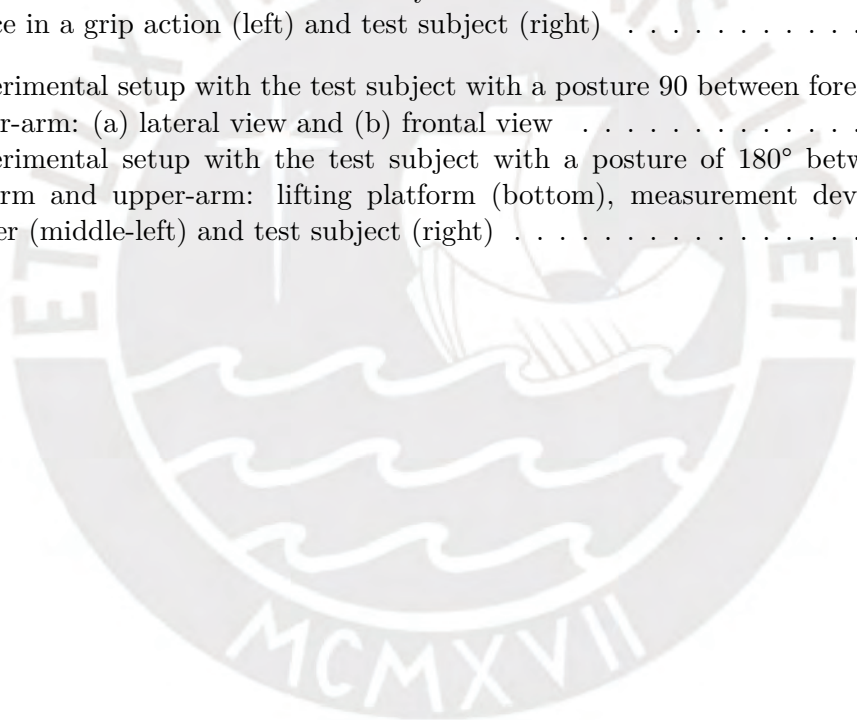
| | | |
|----------|----------------------------------------------------------------------------|-----------|
| 1 | Introduction | 12 |
| 2 | Fundamentals | 14 |
| 2.1 | The hand-arm-system: from the anatomy to the biomechanics | 14 |
| 2.1.1 | Planes of motion | 14 |
| 2.1.2 | Functional aspects | 14 |
| 2.1.3 | Hand mechanics: the grip action | 17 |
| 2.2 | Dynamics of the hand-arm-system | 18 |
| 2.3 | Mechanical vibrations (tremor) in the hand-arm-system | 21 |
| 2.3.1 | Physiological condition | 21 |
| 2.3.2 | Pathological condition | 21 |
| 2.4 | Technical fundamentals | 23 |
| 2.4.1 | Instrumentation and drive | 23 |
| 2.4.2 | System identification | 25 |
| 3 | State of the Art and Technology | 26 |
| 3.1 | Characterization of a vibration condition in the hand-arm-system | 26 |
| 3.1.1 | Physiological and pathological condition | 26 |
| 3.1.2 | Occupational environment | 29 |
| 3.1.3 | Classification | 30 |
| 3.2 | Characterization of the hand-arm-system parameters | 31 |
| 3.3 | Vibration absorption devices for the hand-arm-system | 32 |
| 3.3.1 | Passive devices | 32 |
| 3.3.2 | Active devices | 33 |
| 3.3.3 | Parameters | 33 |
| 4 | Clarification of the task | 35 |
| 5 | Method of characterization | 37 |
| 5.1 | Method establishment | 37 |
| 5.2 | Experimental layout | 39 |
| 5.3 | Dynamic parameters determination | 41 |
| 5.3.1 | Hand-arm-system modelling | 41 |
| 5.3.2 | Experimental identification procedure | 43 |
| 6 | Measurement setup concept | 46 |
| 6.1 | Introduction | 46 |
| 6.2 | List of requirements | 46 |
| 6.3 | Structure of functions | 49 |
| 6.4 | Technical principle | 50 |
| 6.5 | Measurement setup implementation | 51 |

| | | |
|-----------|------------------------------------------------------------|------------|
| 6.5.1 | First approach | 51 |
| 6.5.2 | Second measurement setup concept | 55 |
| 6.5.3 | Final measurement setup | 58 |
| 7 | Experimental design | 64 |
| 7.1 | Experimental setup | 64 |
| 7.2 | Protocol | 65 |
| 7.3 | Transition study | 66 |
| 7.4 | Variables influence study | 67 |
| 7.4.1 | Muscle tension and posture study | 67 |
| 7.4.2 | Frequency study | 68 |
| 8 | Results | 69 |
| 8.1 | Transient dynamics | 69 |
| 8.1.1 | Muscle tension transition | 69 |
| 8.1.2 | Posture transition | 70 |
| 8.2 | Grip force and posture influence | 73 |
| 8.3 | Frequency influence | 78 |
| 8.4 | Estimation of dynamic parameters | 78 |
| 9 | Discussion | 80 |
| 9.1 | Setup prototype performance | 80 |
| 9.2 | Characterization method | 81 |
| 9.3 | Vibration characteristics of the hand-arm-system | 82 |
| 9.4 | Observations and limitations | 84 |
| 10 | Conclusions and Outlook | 85 |
| | Bibliography | 86 |
| | Appendix | 90 |
| A | Matlab codes | 91 |
| B | Grip study results | 97 |
| C | DVD | 106 |
| D | Technical documents | 107 |

List of Figures

| | | |
|------|---------------------------------------------------------------------------------------------------------------------------------------------------------------------------------------------------------------------------|----|
| 1.1 | Methodology of the master thesis | 13 |
| 2.1 | Reference planes of motion for the human body Kaiser (2018) | 15 |
| 2.2 | Main elements of the hand-arm-system Earthlabs (2019) | 15 |
| 2.3 | Shoulder elements (a) and possible motion (b) Gerhard (2010) | 16 |
| 2.4 | Elbow elements (a) and possible motion (b) Gerhard (2010) | 17 |
| 2.5 | Wrist elements (a) and possible motion (b) Gerhard (2010) | 17 |
| 2.6 | Power (a) and precision (b) grip pattern Napier (1956) | 18 |
| 2.7 | Grip strength measurement Basaraba (2024) | 18 |
| 2.8 | Biomechanical model of the hand-arm-system Tsotsis (1987) | 19 |
| 2.9 | Natural frequencies of a human body Fayyad et al. (2020) | 20 |
| 2.10 | Commercial example and theoretic principles of an IMU Vectornav (2024) | 23 |
| 2.11 | Commercial example and theoretic principles of force sensor | 23 |
| 2.12 | Shaker overview | 24 |
| 3.1 | ES for physiological tremor on surgical applications Veluvolu & Ang (2011) | 27 |
| 3.2 | ES for physiological tremor on surgical applications Yang et al. (2015) | 27 |
| 3.3 | ES for the characterization of a pathological tremor Rocon et al. (2006) | 28 |
| 3.4 | ES for pathological tremor simulation Rudraraju & Nguyen (2018) | 28 |
| 3.5 | ES of physiological and pathological tremor Lukšys et al. (2018) | 29 |
| 3.6 | ES of wrist transmissibility: study of angular position (a) and study of postures (b) influence Wu et al. (2022) | 29 |
| 3.7 | ES of transmissibility through the hand-arm-system Xu et al. (2009) | 30 |
| 3.8 | ES for the determination of wrist stiffness in a relaxed state Formica et al. (2012) | 31 |
| 3.9 | ES for the determination of wrist stiffness in a writing position Kuchenbecker et al. (2003) | 32 |
| 4.1 | Requirements plan of the measurement setup | 36 |
| 5.1 | Scheme of experimental method: interaction of the test subject with the measurement device concept(left), final implementation of the device(right) | 38 |
| 5.2 | Analytical model of the hand-arm-system | 41 |
| 6.1 | Functions structure of the measurement setup | 49 |
| 6.2 | Optimal technical principle | 50 |
| 6.3 | Design prototype for first approach | 52 |
| 6.4 | First approach of measurement setup: shaker amplifier and DAQ (left behind), computer (left front), shaker with simplified device prototype and micro-controller with IMU (middle behind) and IMU (right) | 53 |
| 6.5 | Scheme of IMUs connections | 54 |

| | | |
|------|-------------------------------------------------------------------------------------------------------------------------------------------------------------------------------------------------------------------------------------------------|----|
| 6.6 | Test configurations with the hand attached to the simplified measurement device coupled to the shaker | 54 |
| 6.7 | Main views of the prototype A | 55 |
| 6.8 | Second measurement setup concept: shaker amplifier and power source(left); computer and shaker with measurement device (mid front); force amplifier and DAQ (mid behind); IMUs with micro-controllers(right) | 56 |
| 6.9 | Example of the configuration of the second concept implemented in a posture of 180°: Scheme of the test procedure (left) and implementation with the second prototype (right bottom and top) | 57 |
| 6.10 | Measurement device in the final setup | 58 |
| 6.11 | Constructive details of the measurement device | 60 |
| 6.12 | Final measurement setup for experimental characterization: shaker amplifier and power source(left); computer and shaker with measurement device (mid front); force amplifier and DAQ (mid behind); IMUs with micro-controllers(right) | 61 |
| 6.13 | Control of shaker signal with Matlab Simulink | 62 |
| 6.14 | Force sensors implemented on the measurement device | 63 |
| 6.15 | Position of MPUs on the hand-arm-system: hand attached to the measurement device in a grip action (left) and test subject (right) | 63 |
| 7.1 | Experimental setup with the test subject with a posture 90 between forearm and upper-arm: (a) lateral view and (b) frontal view | 64 |
| 7.2 | Experimental setup with the test subject with a posture of 180° between the forearm and upper-arm: lifting platform (bottom), measurement device with shaker (middle-left) and test subject (right) | 65 |



| | | |
|-----|---------------------------------------------------------------------------------------------------------------------------------------------------------------------------------------------------------------------------------------------------------------|-----|
| 7.3 | Transition test of muscle tension and posture | 67 |
| 7.4 | Muscle tension test during a stationary dynamic response with two postures: (a) 90° and (b) 180° between the forearm and the upper-arm | 68 |
| 8.1 | Dynamic response to an excitation of 8Hz during a change of hand-arm-system muscle tension from relaxed to high tension level: (a-b) force measurement, (c-d) hand, (e-f) forearm (g-h) upper-arm acceleration and spectrogram | 71 |
| 8.2 | Dynamic response to an excitation of 8Hz during a change of hand-arm-system posture from 180° to 90°: (a-b) force measurement, (c-d) hand, (e-f) forearm, (g-h) upper-arm acceleration and spectrogram | 72 |
| 8.3 | Dynamic response during a 50% grip force condition with 90° posture: (a-b) force measurement, (c-d) hand, (e-f) forearm, (g-h) upper-arm | 74 |
| 8.4 | Dynamic response during a 50% grip force condition with 180°: (a-b) force measurement, (c-d) hand, (e-f) forearm, (g-h) upper-arm | 75 |
| 8.5 | Influence of the grip force on the acceleration response along the hand-arm-system with a posture (a) 180° and (b) 90° | 76 |
| 8.6 | Influence of the grip force on the frequency spectrum along the hand-arm-system with a posture of (a), (c), (e) 180° and (b), (d), (f) 90° | 77 |
| 8.7 | Influence of the perturbation frequency on the dynamic response the hand-arm-system with a posture of 180°, (a) acceleration in rms, (b), (c) and (d) the frequency spectrum of the acceleration signal of hand, forearm and upper-arm respectively | 78 |
| B.1 | Dynamic response during a relaxed condition (0% grip force) with a posture of 90°: (a-b) force measurement, (c-d) hand, (e-f) forearm (g-h) upper-arm acceleration and frequency spectrum | 98 |
| B.2 | Dynamic response during a 25% grip force condition with a posture of 90°: (a-b) force measurement, (c-d) hand, (e-f) forearm (g-h) upper-arm acceleration and frequency spectrum | 99 |
| B.3 | Dynamic response during a 75% grip force condition with a posture of 90°: (a-b) force measurement, (c-d) hand, (e-f) forearm (g-h) upper-arm acceleration and frequency spectrum | 100 |
| B.4 | Dynamic response during a 100% grip force condition with a posture of 90°: (a-b) force measurement, (c-d) hand, (e-f) forearm (g-h) upper-arm acceleration and frequency spectrum | 101 |
| B.5 | Dynamic response during a relaxed muscle tension condition and posture 180°:(a-b) force measurement, (c-d) hand, (e-f) forearm (g-h) upper-arm acceleration and frequency spectrum | 102 |
| B.6 | Dynamic response during a 25% grip force condition with a posture of 180: (a-b) force measurement, (c-d) hand, (e-f) forearm (g-h) upper-arm acceleration and frequency spectrum | 103 |
| B.7 | Dynamic response during a 75% grip force condition and posture 180°: (a-b) force measurement, (c-d) hand, (e-f) forearm (g-h) upper-arm acceleration and frequency spectrum | 104 |
| B.8 | Dynamic response during a 100% grip force condition and posture 180°: (a-b) force measurement, (c-d) hand, (e-f) forearm (g-h) upper-arm acceleration and frequency spectrum | 105 |
| C.1 | DVD files | 106 |

List of Tables

| | | |
|-----|---------------------------------------------------------------------------------------------------------------------------------------------------------------------------------------------------------------------------------------------------|----|
| 2.1 | Tremor in hand-arm-system for different conditions: physiological condition (PYC), pathological condition (PAC), represented by Essential Tremor (ET) and Parkinson Disease (PD), occupational environment (OE) and natural motion (NM) | 22 |
| 3.1 | Quantified variables during characterization of tremor in hand-arm-system | 30 |
| 3.2 | Current studies in vibration absorption | 34 |
| 5.1 | Variables for characterization | 38 |
| 5.2 | Variables in the experimental setup | 39 |
| 6.1 | Simplifications in the first approach test | 51 |
| 6.2 | Components used for the experimental first approach | 53 |
| 6.3 | Final measurement setup components | 62 |
| 7.1 | Configuration of tests | 66 |
| 8.1 | Transmissibility during in a transient muscle tension in % | 70 |
| 8.2 | Estimated joint stiffness and damping for each condition | 79 |
| 8.3 | Estimated natural frequencies for each condition with a posture 180° | 79 |

1. Introduction

One of the conditions that affects the performance of human limbs motion is the presence of tremor. It can be described as a non-desired vibration behaviour of the limbs, specially in the hand-arm-system (HAS) Bhatia et al. (2018). Tremor can be caused by different sources of mechanical vibrations or pathological conditions as Parkinson Disease (PD) or Essential Tremor (ET), where it is a significant symptom. As consequence of a pathological condition, tremor impacts to the common daily physical activities resulting in a large amount of effort and necessary assistance. To date PD does not have a cure, treatments are addressed to improve quality of life and reduce the impact of symptoms. Current treatments as pharmacological and surgical can be considered invasive for patients Diaz & Louis (2010). In this sense, different engineering-oriented approaches have been developed as non-invasive devices in order to reduce the tremor amplitude and improve the motion control Mo & Priefer (2021). The development of these devices requires a previous knowledge of the dynamic behaviour of the (HAS).

The anatomic study of the (HAS) establishes that the motion control of its skeleton structure is performed through the muscle tissue net, each muscles group related to a specific degree of freedom (DoF) Gerhard (2010). From a biomechanical perspective, the dynamic behavior can be represented by its impedance. The impedance is consisted of a set of characteristic parameters involving the inertia, stiffness and damping of a system. Since the motion is performed through the muscle tissue behaviour, different possible impedance states depend on it. In this sense, a change of a HAS state would be reflected on the values of the impedance parameters. This idea is used in this work for the parameters quantification through the measurement of the dynamic response to a standard excitation.

The biological character of the HAS produces a non-linear behaviour of the impedance. Different levels of muscle tension are generated according to the activity performed and the instant requirements of the physical action. This non-linear behaviour makes the task of the characterization complex and establishes the necessity of each possible condition isolation that involves variables as, mainly, posture, muscle tension level and, in the case of a pathological condition, perturbation characteristics. The influence of these variables has been studied in the field of occupational disease, where the HAS is continuously exposed to vibration sources from tools and machines. However, the same conditions are not suitable for natural motion with a pathological condition since tremor behaviour is usually within a low frequency range and daily physical activities not only involve middle-high push force generation.

Therefore, in this work, a method and its technical implementation to quantify the dynamic characteristics of the HAS during vibration conditions were developed. Main variables that influence significantly on the movement quality were identified in the literature and set as design variables for the design engineering process. The quantification of the dynamic behaviour improves the conception and evaluation of devices oriented to tremor reduction during the design engineering since it allows to simulate and predict the dynamic response of the HAS.

Methodology

This work was divided in four main phases shown in Figure 1.1. In the first phase, the study of the current state of art and technology regarding the characterization methods oriented to specific areas was carried out in order to obtain the main variables that influence significantly on the HAS dynamics and set the requirements for the design. In the second phase, the conception of a solution was carried out and the characterization method was elaborated. The structure and form of the measurement setup were established according to the characterization method and an experimental proof of concept with simplified functions was carried out. In the third phase, the technical constructive design was carried out. The elements in terms of form and geometry were established oriented to the technical implementation. In the final phase, a prototype of the measurement setup was tested. A test procedure was elaborated and results processing was carried out and presented as a first approach with one test subject.

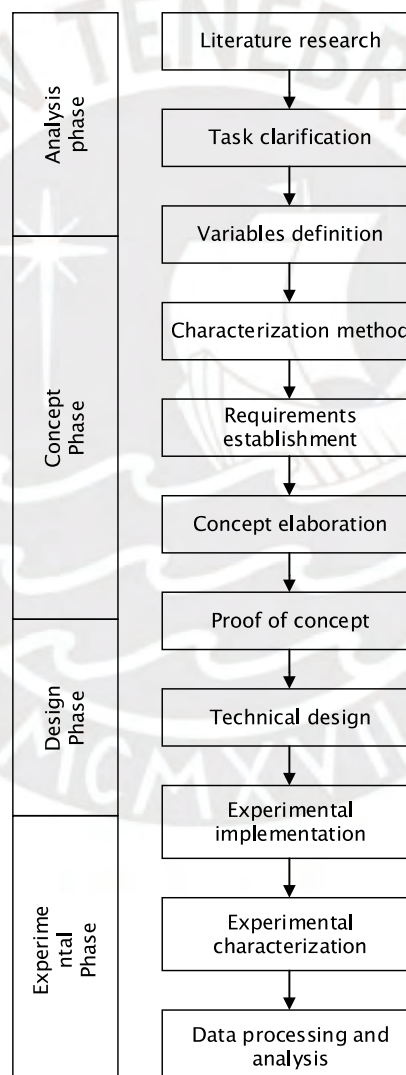


Figure 1.1.: Methodology of the master thesis

2. Fundamentals

This chapter describes the fundamental knowledge required for the comprehension of the following chapters and terms used in the development of the measurement setup. The current stage of theoretical and experimental knowledge regarding the hand-arm-system (HAS) is presented in order to extract the useful information for the concept phase elaboration. Current strategies of data processing for system identification and the instrumentation used are also presented in order to provide the background for the characterization method formulation in this work.

2.1. The hand-arm-system: from the anatomy to the biomechanics

The mechanics of motion of the HAS has its foundations on the anatomical study of the human body. For its characterization, it is necessary a previous understanding of how this system and its element are related each other. In Gerhard (2010) a meticulous description of the arm elements and functional aspects were presented. The understanding of the mechanics of the HAS motion allows its representation through a biomechanical model, where complex series of characteristics become into simple parameters useful for numerical simulations.

2.1.1. Planes of motion

The description of the motion, specially in a 3D space, needs reference planes. In the description is referred to the human body, the planes used are the following as shown in Figure 2.1.

- Sagittal: plane which divides the person body into left and right.
- Frontal: plane which divides the person body into back and front.
- Transversal: plane which divides the person body into inferior and superior.

2.1.2. Functional aspects

The HAS elements coupled to the thorax are shown in Figure 2.2. It is consisted of the upper-arm, forearm and hand connected by the shoulder, elbow and wrist joints. The upper-arm is mainly composed of the humerus bone while the forearm, of the radius and ulna bones. Muscle tissues are not considered for simplification purposes. Hand fingers bones are not considered for the explanation since the hand function is limited to a grip action in this research and does not impact to the main mobility of the HAS. The motion of each element is performed by the muscle tissue net along the arm and thorax. Each muscle has its own function to produce a determined motion of a bone within the arm, or in other words, to a determined DoF. The muscle tissue net therefore commands the motion of each element and produces the different arrangement according to the physical activity. The geometric characteristic of each bones connection in the shoulder, elbow and wrist acts as physical constrain and determines the number of DoF of the joint.

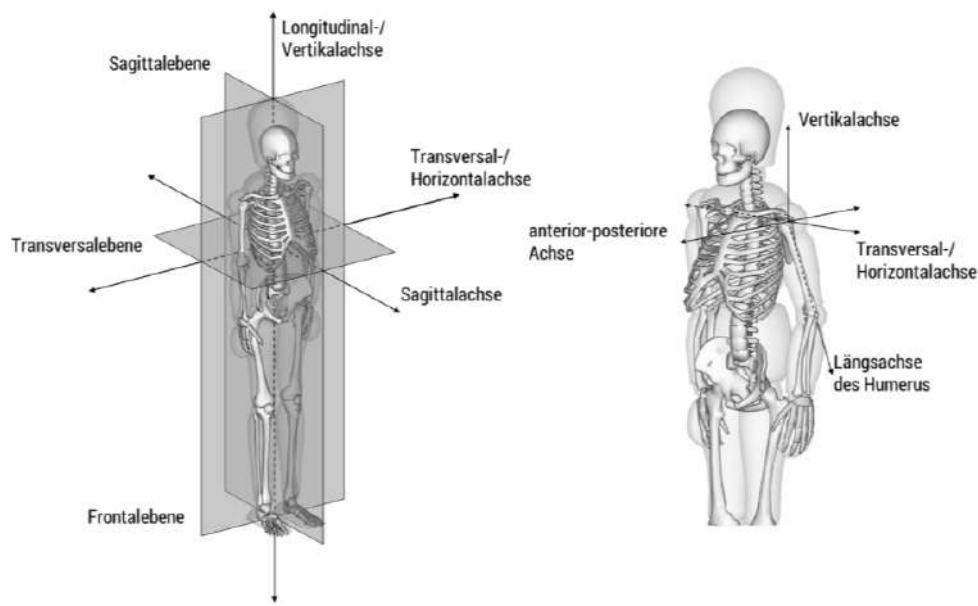


Figure 2.1.: Reference planes of motion for the human body Kaiser (2018)

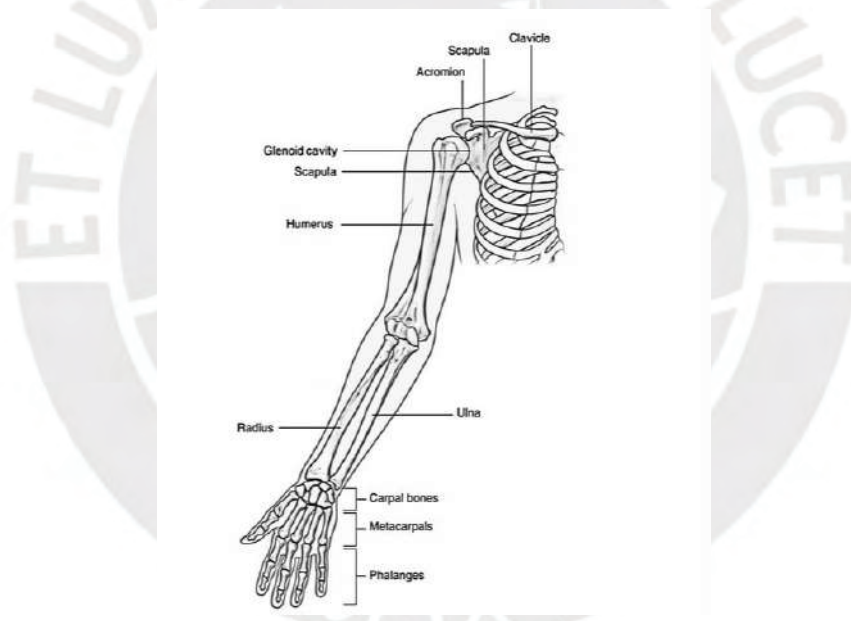


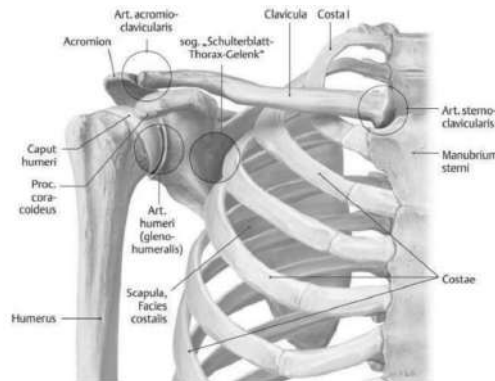
Figure 2.2.: Main elements of the hand-arm-system Earthlabs (2019)

Shoulder

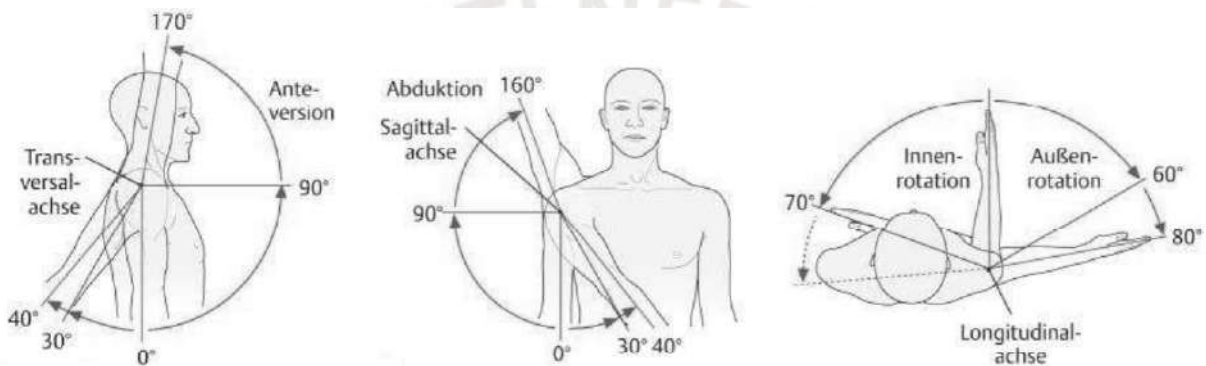
In Figure 2.3(a), it is shown an overview of the shoulder elements. The shoulder articulation can be considered as a universal joint with three DoF since the humerus is in conically in contact to the acromion. However, the great level of mobility of the arm is also due to the mobility of the shoulder joint through the motion of the scapula Gerhard (2010). The types of motion are classified as shown in Figure 2.3(b).

- Anteversion and retroversion take place in the sagittal plane.
- Abduction and adduction take place in the transversal plane.
- Internal and external rotation take place in the transversal plane with the vertical upper-

arm as vertical axis.



(a) Shoulder overview



(b) Classification of possible motions: anteversion and retroversion (left), abduction and adduction (middle) and internal and external rotation (right)

Figure 2.3.: Shoulder elements (a) and possible motion (b) Gerhard (2010)

Elbow

In Figure 2.4(a), it is shown an overview of the elbow elements. The articulation can be considered a joint with two DoF. This is consisted of the contact of three surfaces since the forearm is consisted of two bones, radius and ulna. The types of motion are classified as shown in Figure 2.4(b).

- Flexion and extension take place in the plane formed by the upper-arm and fore-arm axis.
- Pronation und supination take place in the ulna axis.

Wrist

In Figure 2.5, it is shown an overview of the wrist elements. The articulation can be considered a joint with two DoF. This is consisted of the surfaces of the proximal and distal wrist. Both surfaces, in spite of the contact between different bones, form the articulation in a functional aspect Gerhard (2010). The types of motion are classified as shown in Figure 2.5

- Dorsal and palmar flexion take place in a plane formed by the hand axis and the forerarm axis.
- Radial and ulnar abduction take place in a plane of the hand.

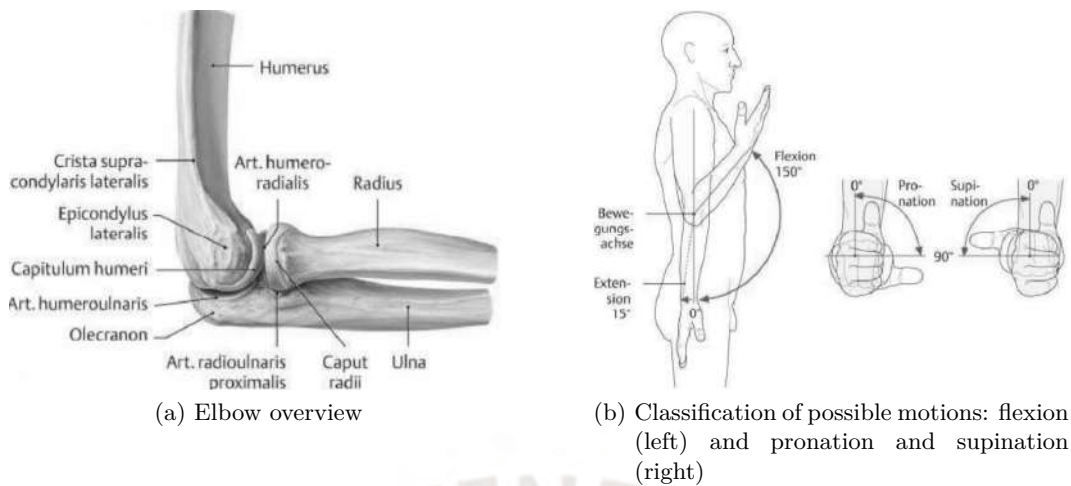


Figure 2.4.: Elbow elements (a) and possible motion (b) Gerhard (2010)

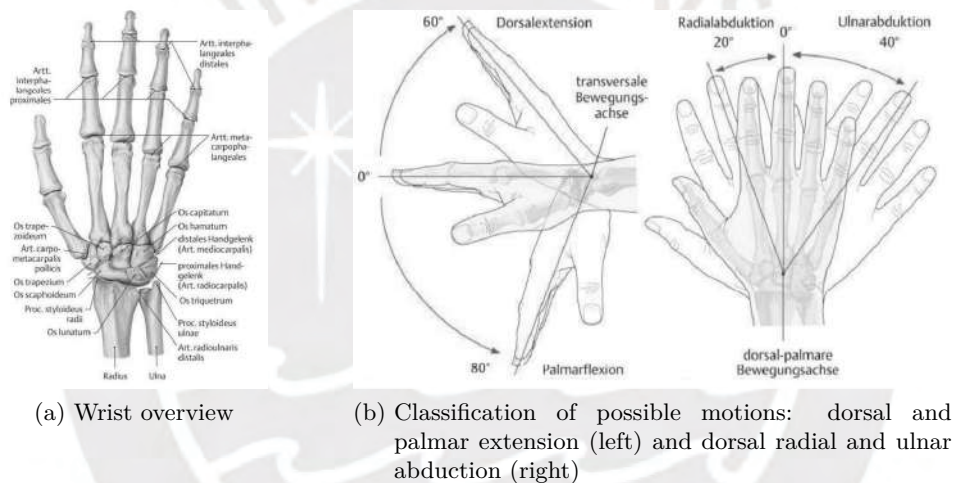


Figure 2.5.: Wrist elements (a) and possible motion (b) Gerhard (2010)

2.1.3. Hand mechanics: the grip action

The interaction with objects in the environment is performed mainly by the hand. In this sense, the hand functions need a deeply description in order to identify the variables which defines how these functions are mechanically performed. Mechanically in this context can be understood as the sequence of physical operations of kinematic chain's elements in order to perform an action. The activities performed by the hand involve a prehensile and a non-prehensile behaviour. Prehensile indicates the use of a certain grade of strength in order to hold an object. The prehensile behaviour can be classified according to two main pattern groups proposed by Napier (1956): power or precision grip, Figure 2.6.

Power grip involves a group of patterns where the holding is the most important objective while the positioning and orientation of the object in the hand is a secondary objective. On the other hand, precision grip involves a group of patterns where the trajectory, shape, orientation and more characteristics related to the positioning are the most important. In terms of force, a power grip is focused on holding an object with much more force than a precision grip. Precision grip requires also a special distribution of fingers involved in contact to the object held; therefore, the

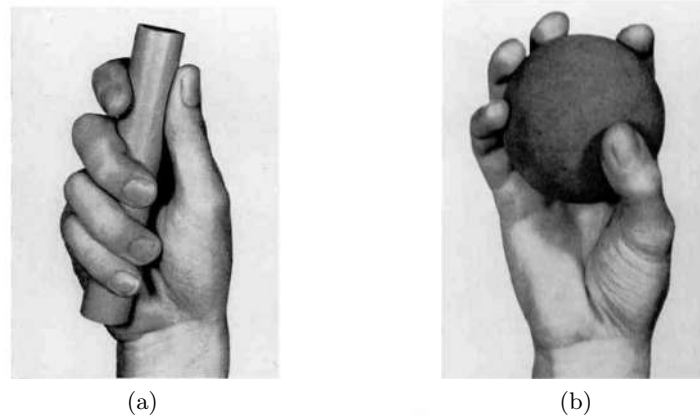


Figure 2.6.: Power (a) and precision (b) grip pattern Napier (1956)

are more possibilities of grips. The selection of a pattern group is an intuitive action depending of factors as size, shape, weight and even the objective of the motion Napier (1956).

In the HAS, the muscle tension is performed in order to control the kinematic motion by using the wrist, elbow and shoulder as joints of the HAS kinematic chain as explained in previous section. Likewise, the same behaviour is presented in the kinematic chain of fingers within the hand. In this case, a grip action in the hand is used in almost any daily activity as picking up objects. In occupational therapy, the grip strength is measured through a dynamo-meter and the value is used as an indicator of a condition related to weakness, Figure 2.7.



Figure 2.7.: Grip strength measurement Basaraba (2024)

2.2. Dynamics of the hand-arm-system

The study of dynamics seeks to the determine quantitatively the motion of a system in a space and its variables as position, velocity and acceleration (kinematics) as well as the relation between the motion of the HAS elements and the forces that produce it (kinetics) in order to have a better comprehension of the HAS motion. The study of dynamics in the field of Bio-mechanics provides useful information for applications related to human physical activities. In this sense, the bio-mechanical modelling of the HAS has been area of interest for many years, specially in the field of health to characterize its motion and perform numerical calculations and predict the behaviour under different conditions through a systematical mathematical procedure.

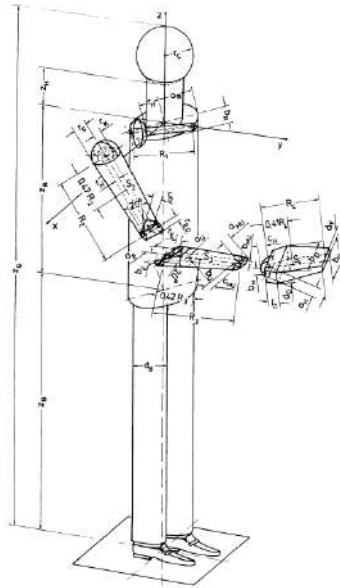


Figure 2.8.: Biomechanical model of the hand-arm-system Tsotsis (1987)

In Tsotsis (1987), it was developed a bio-mechanical model of the HAS simplifying the anatomical aspect of the human body by only focusing on the elements which contribute to the motion. A complex joint as the shoulder or elbow which are composed of different bones surfaces in contact were simplified according to the possible DoF due to the geometry constrains, see Section 2.1. Thus, the HAS can be represented as a kinematic chain of the upper-arm, forearm and hand connected by joints, each joint with a determined DoF, Figure 2.8. Once the biomechanical model is formulated, different studies can be carried out as the calculation of moment and forces related to a trajectory performing as in Tsotsis (1987), for instance. Another example of a biomechanical model can be found in Rincon & Alencastre (2023). It was developed a 3D model to simulate the addition of vibration absorber in order to improve the control of motion under presence of perturbation signals produced by a pathological condition. Lagrange mechanics is useful for the analysis and solving the system of differential equations of the biomechanical model since the motion of the HAS takes place in a 3D space where many DoF are involved.

One of the most important parameters used for describing the dynamical behaviour is the natural frequency or eigenfrequency since it determines an excitation frequency that must be avoid in order not to produce a structural damage to the system, a phenomenon named resonance. Previous works have estimated the natural frequencies of each element of the kinematic chain of the human body and a summary is shown in Figure 2.9.

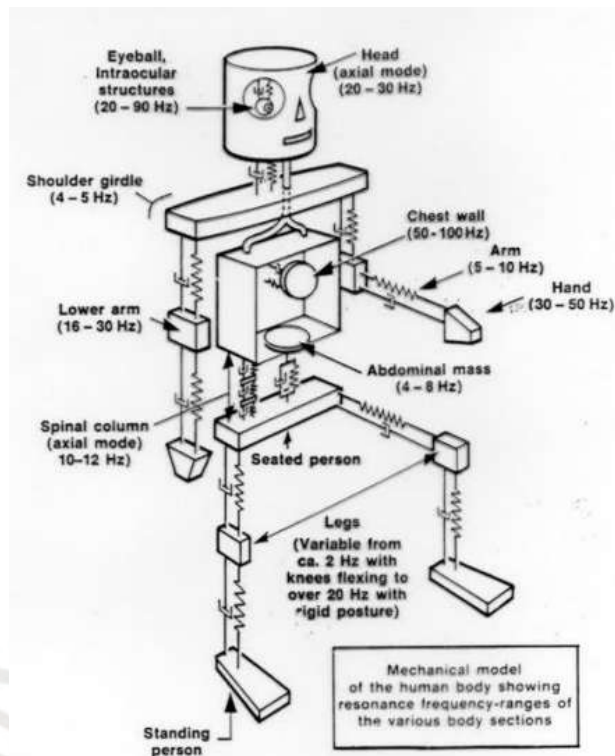


Figure 2.9.: Natural frequencies of a human body Fayyad et al. (2020)

2.3. Mechanical vibrations (tremor) in the hand-arm-system

Tremor can be described as an involuntary oscillating motion in Limbs. It is manifested on each limb element which are hand, fore-arm and upper-arm including the joints between each element. The main dynamic characteristics used for quantifying and describing the state of the condition are frequency and amplitude(magnitude of oscillating motion) which depends on the source of dynamic forces and limbs parameters. The term tremor is in essence a mechanical vibration produced by a self condition of humans. According to the condition, tremor can be classified in physiological or pathological condition. Both refers to a stationary condition which can not be eliminated, where physiological refers to a normal condition and pathological refers to the tremor caused by a disease. On the other hand, vibration can be also produced by an external condition with a mechanical vibration source during a determined period of time. This condition is studied in occupational health since long exposures to machines and vibration tools cause damage to the workers limbs and can lead to a disease as the Hand-Vibration Syndrome.

The study of tremor involves a quantitatively characterization of the phenomenon by its mechanical behaviour. Mechanical in this context is understood as the study of motion and how it is produced by the action of forces.

2.3.1. Physiological condition

Physiological tremor is manifested in any human activity. It is part of the natural motion of a human. It is characterized by motion oscillations along the HAS with very small amplitudes Veluvolu & Ang (2011). During daily activities, it is not considered a problem since small amplitudes of vibration do not impact to people's desired motion. However, it does impact negatively when repeatability and precision are required in specific tasks. For instance, this kind of tremor has been deeply studied in the field of precision movement for surgical applications, where it is required a position accuracy of at least 10um, since it can impact significantly to patients Veluvolu & Ang (2011). Authors characterize the physiological tremor by the measurement of motion frequency during different tasks of the HAS. In Table 2.1, it is shown the experimental values for postural and kinetic tremor.

2.3.2. Pathological condition

Pathological tremor is caused by a medical condition as a disease. It is manifested permanently in the limbs of patients. Tremor in pathological condition has significantly higher amplitudes than values reported in physiological tremor. The specific characteristics of tremor as amplitudes and frequencies depend highly on each person's parameters, the performed activity, type of disease and stage as well as external factors related to the tremor motion. Parkinson Disease (PD) and Essential Tremor (ET) are medical conditions characterized by the presence of tremor. Both have been studied and characterized mainly by the frequencies presented during different activities. In a Parkinson condition, a tremor signal can be consisted of multiple excitation signals with a specific frequency; however, only the dominant frequency is usually used for characterization purposes Zhou et al. (2016). Previous researches have classified three types of activity condition for tremor characterization Lukšys et al. (2018) Rocon et al. (2006) Veluvolu & Ang (2011). Rest tremor, if the tremor is produced with a relaxed limb; kinetic tremor, if it is produced during a desired motion and postural tremor, if it is produced during a posture holding. In Table 2.1, it is shown the experimental values of some of researches carried out for the mentioned types of the activities.

Table 2.1.: Tremor in hand-arm-system for different conditions: physiological condition (PYC), pathological condition (PAC), represented by Essential Tremor (ET) and Parkinson Disease (PD), occupational environment (OE) and natural motion (NM)

| Tremor | Cond. | Type | Task | Freq. (Hz) | Ref. |
|--------|-------|----------|-------------|---------------------------------|----------------------------|
| PYC | | Postural | | 2,29 - 6,56 | Lukšys et al. (2018) |
| | | Kinetic | circle path | 7 - 11 | Veluvolu & Ang (2011) |
| | | Kinetic | trajectory | 1,75 - 3,28 | Lukšys et al. (2018) |
| PAC | ET | | | 8 - 12 | Veluvolu & Ang (2011) |
| | | | stretched | main 5 | Rocon et al. (2006) |
| | | | | 5 - 10 | Puschmann & Wszolek (2011) |
| | PD | | | 3 - 5 | Puschmann & Wszolek (2011) |
| | PD | Resting | | main 5 | Rocon et al. (2006) |
| | PD | Resting | | 3 - 7 | Morrison et al. (2008) |
| | PD | Resting | | 1st 3.5 - 5.8 2nd 6.9 - 11.5 | Zhou et al. (2016) |
| | PD | Postural | | 3,86 - 7,61 | Lukšys et al. (2018) |
| | PD | Postural | | 5 - 12 | Morrison et al. (2008) |
| | PD | Postural | | 1st 3.9 - 7.7 2nd 7.7 - 11.5 | Zhou et al. (2016) |
| | PD | Kinetic | trajectory | 3 - 10 | Rocon et al. (2006) |
| | PD | Kinetic | trajectory | 1,65 - 3,52 | Lukšys et al. (2018) |
| | PD | | | 4,5; 5,5 | Rudraraju & Nguyen (2018) |
| OE | | | | 16 - 50 | Wu et al. (2022) |
| NM | | | | <2 | Rocon et al. (2006) |

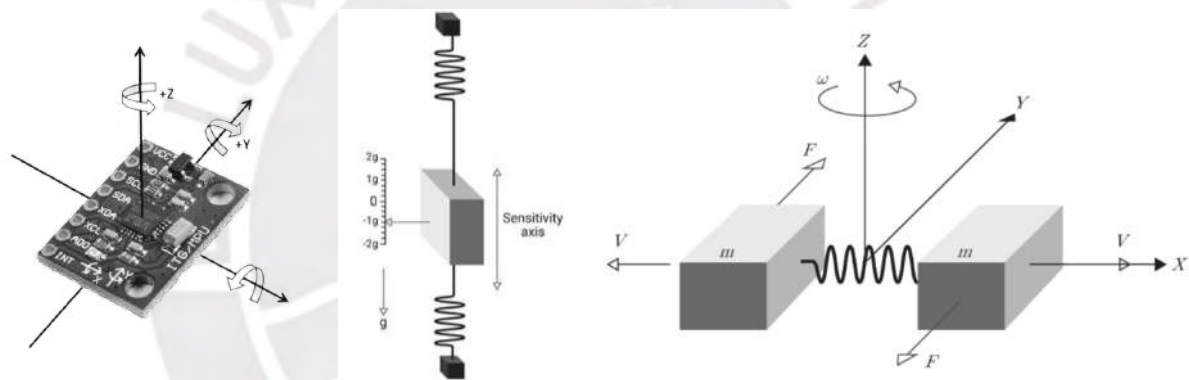
2.4. Technical fundamentals

2.4.1. Instrumentation and drive

IMU

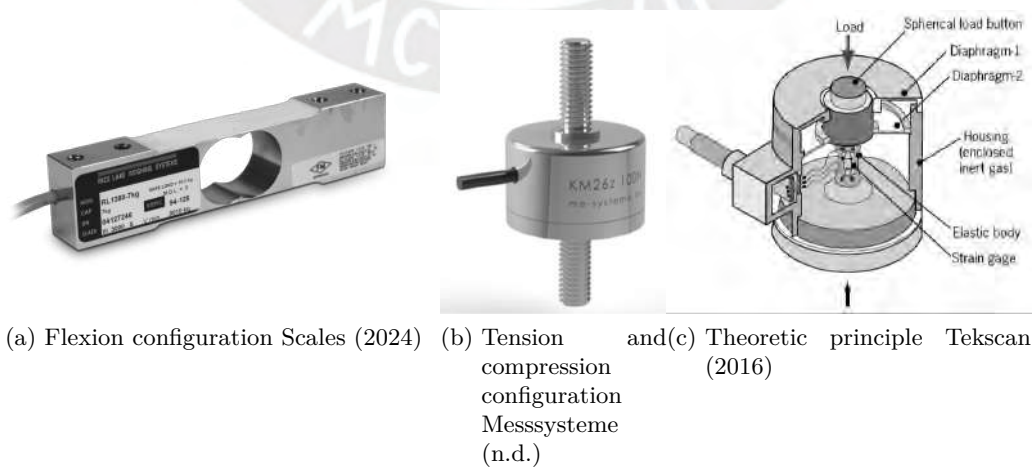
The Inertial Measurement Unit IMU is a sensor able to measure the change of the main variables of motion by using the known behaviour of material properties and how they response to a determined change. Figure 2.10(a) shows an example of a commercial IMU commonly used in a prototype stage. An IMU typically consists on the following elements:

- Accelerometer: it provides the acceleration value through the measurement of the inertial force to the motion in a specific direction, Figure 2.10(b).
- Gyroscope: it provides the angular velocity through the measurement of the centripetal force during a rotation motion, Figure 2.10(c).
- Magnetometer: it provides the measurement of the magnetic field through the change of the resistance due to magnetic properties of materials.



(a) Example of a commercial IMU (b) Accelerometer (c) Gyroscope

Figure 2.10.: Commercial example and theoretic principles of an IMU Vectornav (2024)



(a) Flexion configuration Scales (2024) (b) Tension and (c) Theoretic principle Tekscan
compression configuration Messsysteme (2016)
(n.d.)

Figure 2.11.: Commercial example and theoretic principles of force sensor

Force sensor

A force sensor, also known as load cell, provides the value of a force change applied to the device with a rate established by the mechanical properties of deformable materials. In Figures 2.11 (a-b), it is shown a pair of commercial sensors. It uses the measurement of the deformation with strain gauges to quantify the force as a proportion, Figure 2.11(c). A strain gauge is a material sheet with a determined electric resistance which depends on its geometry. An elongation or compression produces a change of the resistance value which can be calibrated with the stress value applied.

Shaker

It is an electro-mechanical device used to produce an oscillation signal over time. Figure 2.12(a) shows an example of a commercial shaker TIRA TV 51110 which was used in this work. A shaker commonly uses the principle of the Electromagnetism to create a drive force as a function of the current intensity. Figure 2.12(b) shows a typical structure of a shaker. The vibration plate is a suspended mass fixed to a coil of wire which envelope an arrange of permanent magnets. The current through the coil creates a magnetic field which interacts with the magnetic field created by the permanent magnets. As a result, the vibration plate moves as function of the current.

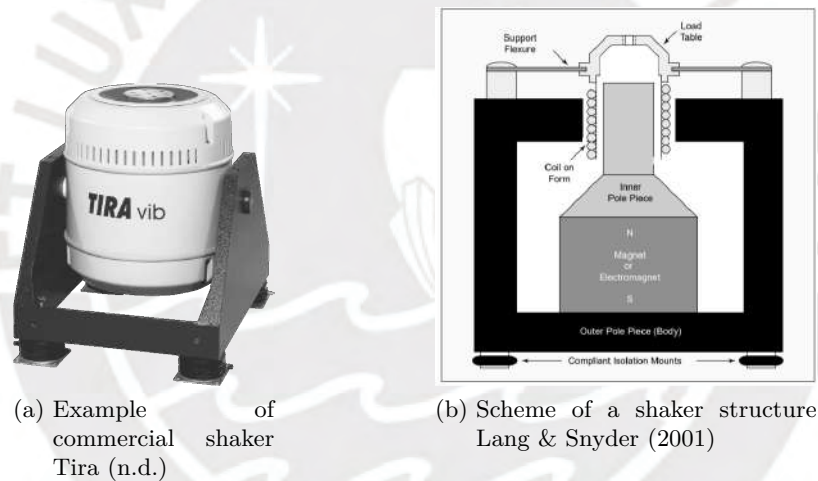


Figure 2.12.: Shaker overview

2.4.2. System identification

The system identification is the process of the dynamic parameters determination of a system based on experimental measurement of its input and output data Pappalardo & Guida (2018). The development of dynamical systems require a previous knowledge of a model and the values of its dynamical parameters which can represent the dynamic behaviour with results enough close to the real behaviour as the application demands. The model allows to perform simulation and predict the dynamical behaviour. This is especially needed for control applications where the control algorithm and its parameters are setting according to the dynamical behaviour of the system. The system identification are usually divided into two groups of procedures based on the domain used Pappalardo & Guida (2018).

- Frequency domain.- It is focused on the frequency response characteristics. It is used for a non-parametric identification, there is no a mathematical function which describes the relation between the input and output Reynders (2012). The application helps more to structural analysis where natural frequencies must be avoid and where the frequency values are more important Pappalardo & Guida (2018).
- Time domain.- It is used for a parametric identification which involves the determination of the parameters of a mathematical function which describes the relation Reynders (2012). Here the dynamical behaviour of the system over time is the most important object of analysis. The differential equation which represented this behaviour is determined. This is focused on solving the vibration control problem and is specially useful for control purposes Pappalardo & Guida (2018).

Input and output data of unknown system are measured and can be fitted according to different strategies Reynders (2012). In a mechanical context, this an often procedure for the analysis of structures under dynamical loads. The input data could be easily identified but the output data requires a previous knowledge of the dynamics of the system in order to establish the number of variables measured and the exact location of these variables. For instance a structure with multiple degrees of freedom is supposed to be measure in a variable related to each degree of freedom. The input and output data are obtained after a experimental procedure. In this sense, a setup with special characteristics according to the system variables during different well-controlled conditions must be developed. Different procedures and techniques are presented in the literature for the system identification. Operational Modal Analysis is one of the most known procedures highly used for industry applications. Operational Modal Analysis (OMA) can be understood as estimation of modal parameters of a system by using measured data during operation conditions Reynders (2012). OMA is specially used for structures in order to determine the natural frequencies and modal shapes, which are indicators of the structural health analysis over time Reynders (2012). The technique is based on theoretical fundamentals of modal decomposition. The vibration motion of a compliant system is the result of the superposition of its modal shapes with determined weights per shape according to the excitation frequency and direction of forces in the operating condition. In this sense, the dynamic behaviour of a system can be represented by only the modal shapes and their corresponding natural frequencies with high influence which allows to experimentally find a reduced modal model Reynders (2012).

3. State of the Art and Technology

The study of the hand-arm-system HAS has been carried out by different approaches according to the research field. Exoskeleton, robotics, motion precision assistance, tremor condition, occupational disease are examples of fields which study the HAS dynamics. Characterization of the dynamic behaviour of the HAS in presence of vibrations is specially required in the study of a tremor condition and occupational disease.

In this chapter, it is presented a review of previous approaches and current studies up to date in the field of the characterization of the HAS's vibration behaviour. Experimental approaches for quantification are analyzed in the field of physiological condition, pathological condition and occupational disease, which shares some characteristic related to our objective. In the literature, the term tremor is used as the representation of mechanical vibrations when it is related to the oscillation of the limbs in the human body.

The formulation of characterization method and the variables involved are studied and classified in order to establish the most important for quantifying. This information is necessary as an input to the concept elaboration, see Chapter 6. Current applications of the characterization are also presented and analyzed from a biomechanical point of view with focus on the attenuation of undesired tremor caused by a pathological condition.

3.1. Characterization of a vibration condition in the hand-arm-system

Current approaches in characterization have been carried out according to the important variables in the study of tremor and what the aim of the research is. In this sense, different experimental setups (ES) have been developed with specific functions according to the variables to quantify. The nature of the tremor is important for the design of the test. There aren't external sources of vibration in physiological and pathological conditions; however, there is in a work environment with tools and machines. The following subsections present the different variables used in the study of specific conditions, where the HAS is under the influence of vibration sources, can be classified as physiological, pathological and occupational environment.

3.1.1. Physiological and pathological condition

In Veluvolu & Ang (2011), it was characterized the tremor signal of two groups based on the precision of motion. First group was consisted of healthy subjects with no expertise in surgery. Second group was consisted of medical doctors. The setup was consisted of the measurement of acceleration signals, Figure 3.1. There was used a micro motion sensing system with a resolution 0.7 μ m, an accuracy 98% with a sampling speed of 250Hz. A setup was elaborated, Figure 3.1, where two tasks were performed. Tasks can be classified as stationary and tracing activities.

- Stationary.- Pointing a laser light at a center of the platform with a stylus for 30s.
- Tracing task.- Tracing a circumference for 30s in a platform with a realistic speed in surgical micro manipulation tasks. Then the data was processed with an algorithm for the

extraction of involuntary tremor from the signal.

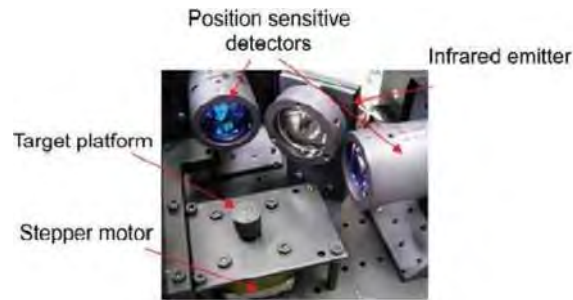


Figure 3.1.: ES for physiological tremor on surgical applications Veluvolu & Ang (2011)

In Yang et al. (2015), it was developed a manipulator for the compensation of physiological tremor oriented to precision on surgical applications. The setup was consisted of performing pointing and tracing task with and without a tremor cancellation device, Figure 3.2. The absolute position was measured by a high precision surgical microscope Zeiss OPMI with a magnification of 25x.

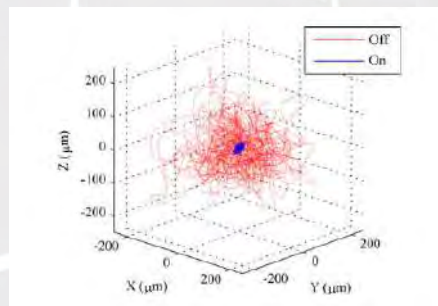


Figure 3.2.: ES for physiological tremor on surgical applications Yang et al. (2015)

In Rocon et al. (2006), it was determined an estimation of the tremor signal in a group of 31 subjects with pathological condition. Most patients were diagnosed with Essential Tremor (postural and kinetic tremor) and 3 with Parkinson Disease (postural and resting). Measurement setup was consisted of 4 gyroscopes placed on the HAS, from the hand until the elbow specifically, Figure 3.3. The data was processed by an innovative procedure using Hilbert spectrum which allowed to identify directly the signal related to the tremor activity. The following tasks were performed for the determination of the tremor signal behaviour.

- (a) Rest.- Patients keep the arm in a rest position with hands resting on thighs.
- (b) Reaching for an object. - Patients perform a trajectory to reach an object.
- (c) Drawing a spiral.- Patients draw a spiral with the index finger.
- (d) Arm outstretched.- Patients keep the HAS outstretched with hands in supination.
- (e) Touching nose.- Patients touch their noses with the index finger from the rest position.
- (f) Moving a cup.-Patients move a cup from left side to right side.



Figure 3.3.: ES for the characterization of a pathological tremor Rocon et al. (2006)

In Rudraraju & Nguyen (2018), it was developed a setup for the simulation of a HAS with a pathological tremor condition oriented to quantify the tremor mitigation of a device also developed in their work, Figure 3.4. The setup was consisted of a fore-arm prototype excited by two linear shakers in the horizontal and vertical directions which simulate the tremor sources. Each lineal shaker was consisted of a motor and a mechanism to convert rotation motion into lineal motion. The lineal excitation displacement and the forearm prototype are coupled indirectly by springs which simulate the muscles effect. The response of the forearm was measured of two distance sensors in the vertical and horizontal direction.

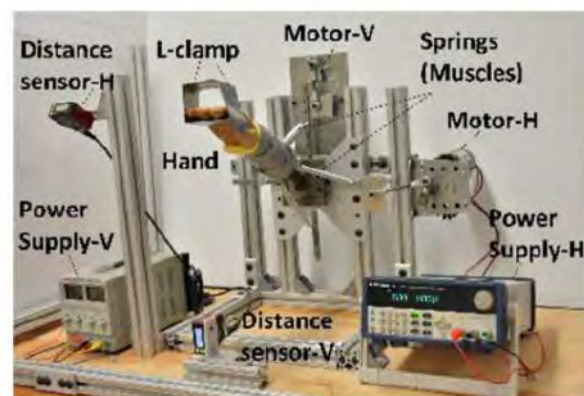


Figure 3.4.: ES for pathological tremor simulation Rudraraju & Nguyen (2018)

In Lukšys et al. (2018), it was measured the tremor produced by physiological and pathological conditions in order to determine the characteristic dynamic behaviour of tremor and the dominant frequencies, which are the main parameters to diagnose. The setup was consisted of IMUs (accelerometer and gyroscope signal measurement) placed on the hand, forearm and upper-arm of the subjects, Figure 3.5. The sample frequency was 51.2Hz via Bluetooth. For the data treatment, high pass filters were used for both group of signals. Two tasks were performed to quantify the kinetic and postural tremor, finger-hose and holding the outstretched arm.

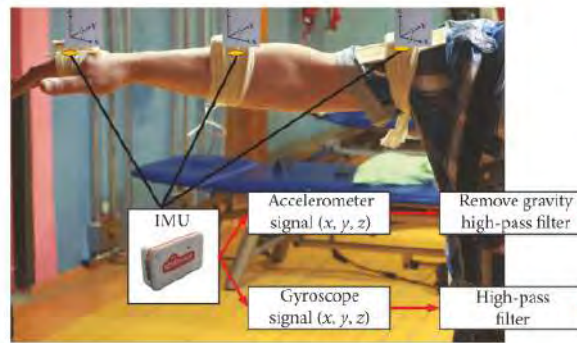


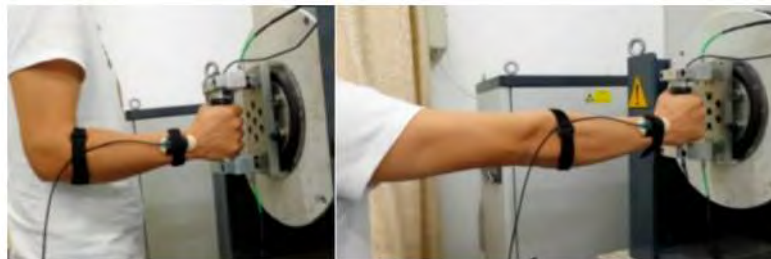
Figure 3.5.: ES of physiological and pathological tremor Lukšys et al. (2018)

3.1.2. Occupational environment

In Wu et al. (2022), it was characterized the transmissibility of the wrist under different conditions such as perturbation amplitude or position of the HAS. The aim was to determine the influence of these variables on the wrist damage during work with tools what produce mechanical vibrations. The setup was consisted of a shaker couple to the handle bracket for the HAS perturbation, Figure 3.6. The acceleration signals of the source and response close to the wrist were measured over time. The dynamic forces were also measured and its influence to the dynamic behaviour of the HAS was studied.



(a)



(b)

Figure 3.6.: ES of wrist transmissibility: study of angular position (a) and study of postures (b) influence Wu et al. (2022)

In Xu et al. (2009), it was characterized the transmissibility through the wrist and elbow in order also to determine the damage of a prolonged exposition during work with tools. It was measured and correlated the relation between torque and tremor due to the action of dynamical forces from tools. The setup was consisted of accelerometers placed on the forearm just after the wrist and before the elbow, force sensors for the measurement of the applied force by the

subject, Figure 3.7. The fundamental resonance frequency of the HAS was manifested during the excitation within the range of excitation frequencies.



Figure 3.7.: ES of transmissibility through the hand-arm-system Xu et al. (2009)

3.1.3. Classification

Each measurement setup developed in the literature was addressed to a specific variables set for quantifying according to the application. In Table 3.1, it was classified the main variables investigated in the measurement of tremor.

Table 3.1.: Quantified variables during characterization of tremor in hand-arm-system

| Reference | Motion signal over time | Natural frequencies | Tremor frequency | Voluntary motion | Involuntary motion | Transmissibility | Muscle tension | External forces | Limb posture | Limb trajectory |
|----------------------------------------|-------------------------|---------------------|------------------|------------------|--------------------|------------------|----------------|-----------------|--------------|-----------------|
| Kalyana2011Veluvolu & Ang (2011) | x | | x | x | x | | | | x | x |
| Rocon2006Rocon et al. (2006) | x | | x | x | | | | | | x |
| Mingzhong2022Wu et al. (2022) | x | | x | | | x | x | x | x | |
| Xu2009Xu et al. (2009) | x | x | x | | | x | x | x | x | |
| Sungwook2015Yang et al. (2015) | x | | | | | | | | | x |
| Rudraraju2018Rudraraju & Nguyen (2018) | x | x | x | | | | | x | | |
| Donatas2018Lukšys et al. (2018) | x | | x | | | | | | x | x |

3.2. Characterization of the hand-arm-system parameters

Characterization is a fundamental step for the comprehension of a phenomenon. In the context of the HAS, characterization can be understood as the quantification of its dynamic parameters in a specific state. Previously, it has been studied the characterization of tremor, which quantified the vibration condition or, in other words, the perturbation condition of the system. Likewise, characterization of tremor has quantified the dynamic response in variables of motion and force signals. However, it is also needed a model to explain the reason of a determined dynamic response.

In this sense, in order to have a complete comprehension, the HAS behaviour must be quantified to predict different external conditions or analyze the influence of each variables within the HAS. The aim in a dynamic system is to determine the set of parameters which governs the motion. These parameters can be used then in a dynamic model to predict the response in any condition. This characterization process is also known as system identification since the quantified parameters can be used for a structured mathematical model Pappalardo & Guida (2018).

The characterization also allows to understand the different compensation mechanisms of non-desired dynamic behaviour along the arm which is reached by a set of feedback variables inherent to a human body as muscles, reflex or motion adaptation Formica et al. (2012). In an analytical model of the dynamic behaviour of a HAS, the dynamic behaviour of any response is governed by three parameters: stiffness, damping and mass matrix. The mass matrix could be measured directly; however, stiffness and damping matrix require a experimental procedure to be quantified. Stiffness is a parameter closely related to the level of muscle tension in the HAS. It along the mass, almost determines the natural frequencies of the system, since the damping only produces a small displacement of the frequency value and the motion amplitude attenuation.

In Formica et al. (2012), it was quantified the passive wrist stiffness simplified as a 1 DoF model as well as a 2D combining flexion-extension and and radial-ulnar deviation, Figure 3.8. The method consisted of producing a slow motion of the hand while the rest of the arm was fixed. Muscle activity was measured to assure a relaxed state of the HAS.



Figure 3.8.: ES for the determination of wrist stiffness in a relaxed state Formica et al. (2012)

In Kuchenbecker et al. (2003), it was proposed a characterization of a simple 1 DoF model addressed to the development of remote control systems. A pulse was generated while a stylus is maintained by a grip force. This test condition simulates a writing position, where a small

muscle tension is applied to generate the required grip force.

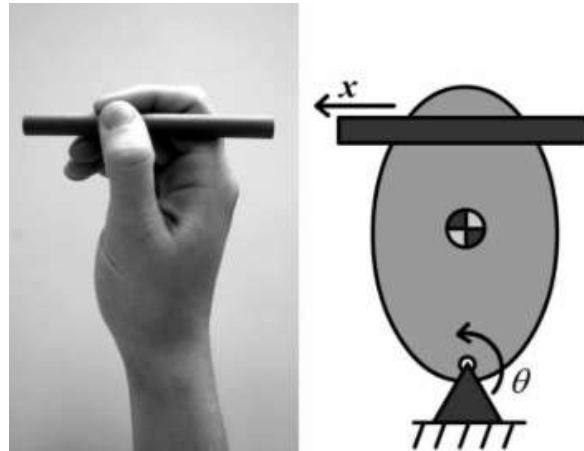


Figure 3.9.: ES for the determination of wrist stiffness in a writing position Kuchenbecker et al. (2003)

3.3. Vibration absorption devices for the hand-arm-system

Devices for attenuation of tremor were addressed to reduce the vibration amplitude of patients in order to improve the quality of life during their daily activities. The non-invasive characteristics of the devices are shown in the flexibility to be used when patients decide to use. Conventional treatments can result extremely aggressive for patients since the negative secondary effects impact their lives or they suppose a high risk as in a surgery. In this sense, absorption devices have been developed which seek a balance within conventional treatments Mo & Priefer (2021).

Several authors have proposed non-invasive devices against the tremor produced by a pathological condition and can be classified as passive, semi-active and active devices according to the tuning characteristics for different requirements. Passive devices use the principle of vibration absorption which does not require a source of energy. Active devices, on the other hand, require a source of energy in order to be able to change the dynamical parameters of the HAS in real time. Fundamentals of HAS modelling presented in Chapter 2 explains the analytical modelling that can be used for the design and simulation of these kind of devices after the determination of the dynamical parameters which govern the response of the HAS over time.

3.3.1. Passive devices

The technical principle commonly used is the vibration absorption. It consists of the attachment of a secondary mass to the system, in this case the HAS, in order to dissipate the energy produced by the dynamical forces produced by a pathological tremor Rincon et al. (2023). In this sense, the vibration amplitude is reduced along the HAS while the secondary mass has the highest vibration amplitude. The limbs are stabilized and the control is improved during the desired motion of the person. These devices are almost completely mechanical devices. Then, they do not require external energy source for working. However, they are not able to adapt its parameters and change the dynamic parameters of the HAS for different patients requirements. Mass, stiffness and damping matrix are unique for each person as established in the HAS model. However, the vibration amplitude can be still reduced in spite of the parameters are not the optimal Rincon & Alencastre (2023).

There are two devices available in the market based on this concept: Tremelo and Steadi One. Both are based on a passive vibration absorption principle and report a 85% and 85...90% amplitude attenuation respectively Fivemicrons (2021) Rudraraju & Nguyen (2018) Mo & Prierer (2021). Bot can be modelled by its differential equation on motion and implemented to a HAS model for calculation and simulation.

3.3.2. Active devices

Active devices, on the other hand, are able to adapt their parameters as a function of the patient requirements. These devices are based on the principle of producing an active force in counter-phase to the dynamic force produced by the pathological condition. In other words, they adapt the inertia force over time in order to reduce the dynamic response. This active force is produced by an actuator. This kind of devices require a strong control algorithm in order to tune the actuator over time. In this sense, simulation of the HAS is specially required for the control development.

One of the most simple devices was named WOTAS, which used a DC motor as an actuator and reported an amplitude attenuation of 40% Rocon et al. (2007). However, the device volume was big for practical application and could affect the natural motion of patients by producing fatigue. Different types of actuators have been also tested. In Taheri et al. (2015), it was proposed an pneumatic actuator controlled by an adaptive strategy and reported an attenuation of 74.3...98.1% in test bench conditions. In Zamanian & Richer (2017), it was proposed permanent magnets for the actuator and reported an attenuation of 97.6 % also in test bench conditions.

3.3.3. Parameters

The reason behind a characterization of a HAS is to be able to use the information in a model for predicting the dynamic behaviour under different conditions. Current initiatives focus on the development of vibration absorption devices are addressed to reduce the tremor amplitude of pathological disease as PD or ET without the use of an invasive treatment. A general dynamic system is represented by its differential equation, where parameters are the stiffness, damping and mass matrix. In Table 3.2, it was classified the different approaches and results of current vibration absorption devices for a HAS in a pathological condition. process.

In Rudraraju & Nguyen (2018) there was no a characterization process of the HAS, the stiffness value used for the calculation was assumed according to the setup fabricated. In Hosseini et al. (2014) it was used parameters from the literature, but it was not reported the procedure to obtain it. A constant value of the joint stiffness was used for simulation purposes. Tremelo is one of the available devices for a passive vibration absorption Fivemicrons (2021), it was validated by experimental tests with patients. In Matsumoto et al. (2013), it was developed an exoskeleton for the assistance of the desired motion in a person with a pathological condition. In this case, the device was tested with patients with ET. HAS Parameters were not used since the device used a control loop with a targeted tremor amplitude. In Taheri et al. (2015), it was also developed an exoskeleton. An analytical model of the HAS was formulated for control. HAS parameters from literature were used for numerical simulation. Authors established that HAS parameters are not constant and depends on the conditions during real motion, although constant parameters as stiffness and damping were used for numerical simulation purposes in a specific case. In Zamanian & Richer (2017), it was a control procedure for the attenuation of the Parkinson disease. An analytical model was formulated and the dynamic parameters were

assumed according to previous calculated range from literature Kuchenbecker et al. (2003). In Herrnsstadt & Menon (2016), it was also developed an exoskeleton in order to compensate the involuntary motion. HAS parameters were not used since the control used a PID algorithm with vibration amplitude as input.

Table 3.2.: Current studies in vibration absorption

| Type | Attenuation (%) | Characterization of HAS parameters | Constant parameters assumed | Experimental validation with test bench | Experimental validation patients | Reference |
|-----------------|-----------------|------------------------------------|-----------------------------|-----------------------------------------|----------------------------------|----------------------------|
| Pharmacological | 54.1...59 | | | | | Deuschl et al. (2011) |
| Passive devices | 85 | | x | x | x | Rudraraju & Nguyen (2018) |
| | 74...82 | | x | x | x | Fromme et al. (2020) |
| | 75 | | | x | | Hosseini et al. (2014) |
| | 85...90 | | x | x | x | Fivemicrons (2021) |
| Active devices | 50...80 | | | x | | Matsumoto et al. (2013) |
| | 74.3...98.1 | | x | x | | Taheri et al. (2015) |
| | 82.7...97.6 | | x | x | | Zamanian & Richer (2017) |
| | 99.8 | | | x | | Herrnsstadt & Menon (2016) |

4. Clarification of the task

The development of engineering solutions for reducing non desired vibrations in the hand-arm-system (HAS) requires the characterization of the parameters which govern the dynamical response of the system. Since the HAS involves a non-linear behaviour, the characterization highly depends on the specific set of internal and external conditions where the physical activity takes place. In this sense, measurement setup for characterization must simulate as close as possible the physical activity performed.

In this research field, most current approaches focus on the measurement of the dynamic response of the HAS under the influence of a vibration source addressed to the quantification of damage caused by machines and tools. This condition is characterized by a high frequency behaviour and middle-high muscle tension to perform the task. However, a complete comprehension of the dynamical behavior of the HAS needs, additional to the quantification of the dynamic response in low frequencies, the determination of its parameters in an analytical model in order to predict the dynamic response under the influence of different conditions. It has been found that muscle tension along the HAS is one of the main variables which has a significant influence on the dynamical response; in this sense, part of this work is to quantify this influence through the parameter stiffness.

Therefore, the task is formulated as following: a measurement setup for the quantification of the dynamic characteristics and the influence of the muscle tension in its dynamical response in presence of a controlled perturbation is going to be developed. This proposal will contribute to the comprehension of the dynamic behaviour of the HAS. Not only the dynamic response will be quantified, but also the parameters of a biomechanic model are going to be estimated with the measured data as a validation of the characterization method established. The goal is to develop a setup able to provide useful parameters for numerical simulation purposes in the development of engineered-oriented solutions for the attenuation of non-desired tremor.

After an analysis of the literature regarding different approaches and methods for HAS characterization, it was clarified the main variables oriented to the design of devices for tremor mitigation produced by pathological conditions. A requirements plan was elaborated as a graphical representation of the desired setup frame in Figure 4.1, which is an important input for the concept phase. In the development of the measurement setup, the items to elaborate in this work are the following:

- Analysis of the state of the art and technology regarding the characterization of the hand-arm-system.
- Formulation of a method for the hand-arm-system characterization.
- Design of a measurement setup for characterization.
- Implementation of a measurement setup prototype.
- Implementation of data processing algorithms in Matlab for the characterization with experimental data.

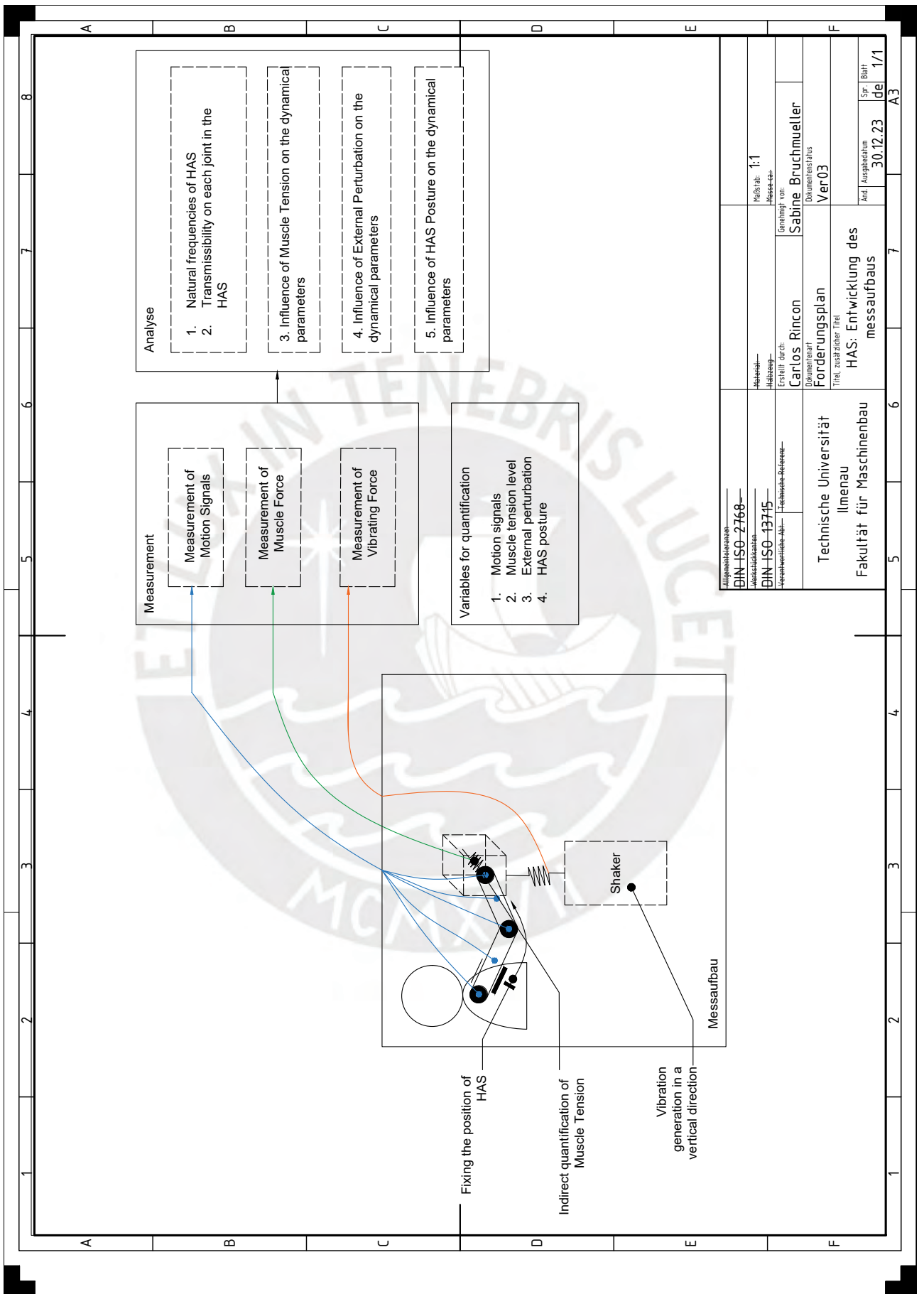


Figure 4.1.: Requirements plan of the measurement setup

5. Method of characterization

5.1. Method establishment

The comprehension of the hand-arm-system (HAS) dynamics involves a experimental determination of its motion behaviour, specifically how the arm responses to a determined excitation and be able to predict it. On the basis of biomechanics, see Chapter 2, the dynamics of HAS is governed by its set of differential equations with a set of parameters that constitutes the mechanical impedance. The mechanical impedance is not directly measured, but can be related to the motion response as a biomechanical model establishes since the HAS can be represented as a kinematic chain of linked elements: hand, forearm and upper-arm. The procedure for characterization seeks to quantify the influence of different possible scenarios on the HAS motion response. This chapter, therefore, elaborate the strategy used for the characterization.

For a characterization method conception, the set of variables that govern a phenomenon must be identified. In the case of the HAS, different authors have studied the motion response in different conditions depending on the characterization context, see Section 3.2. A condition is set by a group of significant variables. Most of authors addressed to the quantification in an occupational environment, where tool and machine frequencies, arm posture, muscle tension applied are significant variables quantified trough the measurement of force and the dynamic response quantified through the measurement of motion signals. In the context of this study, the important variable were identified from the physical activities that the HAS performs. During a physical task, the biological character of the HAS produces a non-linear behaviour, which make the characterization complex. The muscle tension, which governs the HAS motion, is continuously adapted according to the task requirement. Different muscle tension levels along the HAS are performed and depend on external requirements as the force required to pick up an object with hands or the required rigidity of the posture. Likewise, geometry arrangement of the HAS is the purpose of motion during a task. Different postures are performed and involve a series of combinations of relative position between each element of the kinematic chain. These variables are controlled by human intuitively. However, the motion of the HAS is always under external factors which can also be considered as non-controlled conditions and can perturb the desired motion and produce vibrations as explained in the Section 2.3. In this sense, the most significant conditions in this study in order characterize are summarized in Table 5.1. Some conditions are complex to be directly quantified as the muscle tension. Then an indirect quantification was selected through the force performed since it is closely related to the muscle tension.

The selected variables can represent common and characteristic conditions in a real behaviour during motion perform. In an ideal case, the condition should be as close as possible to the natural motion of the HAS. In a natural motion, all the variables act simultaneously, which makes difficult the determination of the influence of a determined variable. Therefore, the strategy is consisted of the isolation of each variable during the experiment while others are maintained as constant as possible.

The conception of a system that performs the method and integrates the quantification of

Table 5.1.: Variables for characterization

| Condition | Quantified variable | Measurement | |
|-----------------------|-----------------------------------|----------------|---------------|
| | | Motion signals | Force signals |
| Geometric posture | Representative posture | x | x |
| Muscle tension level | Indirect force | x | x |
| External perturbation | Frequency of vibration excitation | x | x |

the mentioned variables is essentially an iterative design process which requires feedback from experimental tests due to the high non-linear behaviour of the HAS. In this sense, the method establishes the frame of the design process and the capabilities as part of the requirements. The method and the measurement setup design development were subject to continuously be improved with feedback from experimental implementations and tests. In Figure 5.1, it is shown a scheme of the experimental method with the mentioned variables after the concept establishment in Chapter 6 in order to illustrate the strategy. The influence of these variables are quantified through the measurement of the dynamic response of the HAS under the different combinations of the external variables. The motion signals are measured in each mass center element of the HAS. Due to the rigidity of bones, the upper arm and forearm can be considered rigid elements coupled by flexible joints. Then, only a motion sensor per element is enough. The muscle tension is quantified through the measurement of force performed at the hand, usually known as grip force, and the force performed against the shaker motion. The grip force can be considered more related to the parameter of wrist stiffness and it is measured with a force sensor in a device designed for this purpose. The total force against the shaker can be considered more related to the superposition of the shoulder and elbow stiffness with a specific weighting which depends on the other conditions. It is measured with a second force sensor placed between the perturbation source, known as shaker since here, and the gripper device designed. The shaker produces a sinusoidal excitation signal as vibration source to the HAS while the motion and force signals are measured.

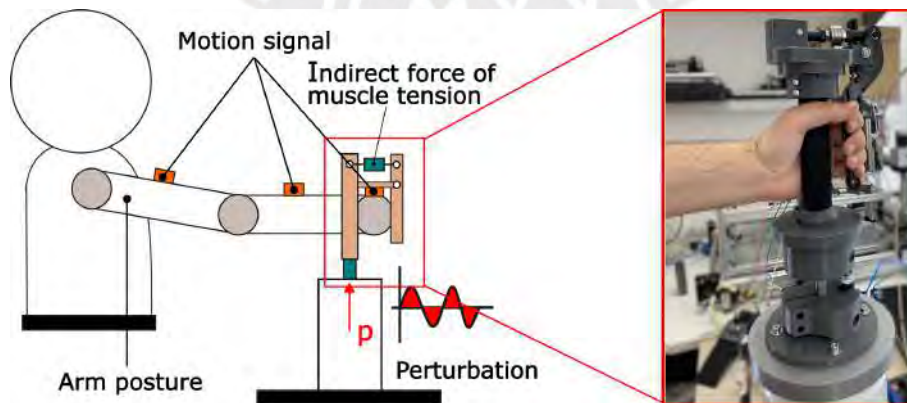


Figure 5.1.: Scheme of experimental method: interaction of the test subject with the measurement device concept(left), final implementation of the device(right)

5.2. Experimental layout

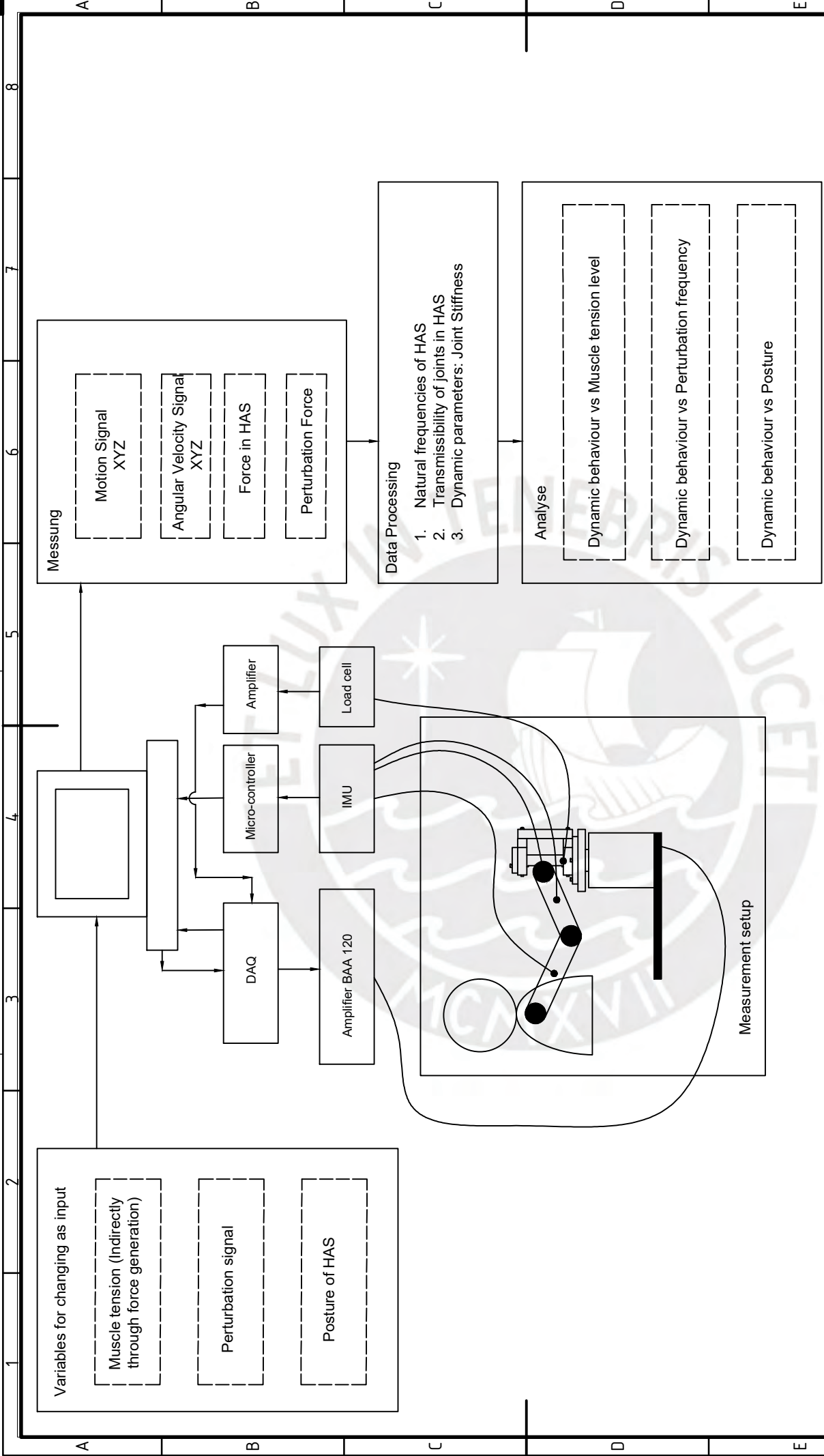
The implementation of the method requires an integration of hardware elements, which perform or assist the measurement, and software, which processes the experimental data in order to obtain useful information. In following page, it is attached the experimental layout proposal as an integrated overview of all the measurement setup elements that are discussed in detail in the Chapter 6. The method required the design of a special device for the measurement of the defined variables. The experimental layout shows how this device is going to interact the subject test and other hardware elements. Although the complete elements were not defined in this stage, main components, specially of electric components were known in parallel to the development.

Measurement of the HAS response with IMUs requires a controller to communicate the sensor with the computer for data recording. The shaker, in this case a fixed available element in the laboratory, receives the excitation signal through an amplifier. The amplifier requires a data acquisition box to receive the excitation signal (form and amplitude) from the computer. Force sensors require also an amplifier and a data acquisition to send the data to the computer.

The formulated method uses the motion and force signal response to an standardized excitation. In this sense, the experimental procedure is divided in three main sections: input conditions, measurement of variables and analysis, Table 5.2. The motion is quantified by the measurement of acceleration and angular velocity signals in different areas of the HAS. Likewise, the motion parameters are measured for different conditions of muscle tension, external perturbation and posture in order to quantify the behaviour in ranges of different physical activities. These variables were defined as inputs in the layout since it depends on user. With the data measured, the data processing includes the calculation of characteristics that represent the dynamic behaviour and can identify and quantify the change of the input variables. The analysis includes a correlation between the input conditions and their influence on the dynamic behaviour.

Table 5.2.: Variables in the experimental setup

| Layout section | Items |
|------------------|---------------------------------------------------------------------------------------------------|
| Input conditions | Muscle tension Posture Perturbation |
| Measurement | Acceleration signal Angular velocity signal Force signal |
| Analysis | Response in time domain Response in frequency domain Transmissibility Dynamic parameters |



| | | | |
|--------------------------------------------------|--|---------------------------------------------------------------------------|--|
| Allgemeinbezeichnung: DIN ISO 2768 | | Maßstab: 1:1 | |
| Maschinenzeichnung: DIN ISO 13745 | | Abbildung: 1:1 | |
| Verantwortliche Abt.: Technische Referenz | | Genehmigt von: Sabine Bruchmüller | |
| Erstellt durch: Carlos Rincon | | Dokumententyp: Ver02 | |
| Technische Universität Ilmenau | | Layout des Aufbaus | |
| Fakultät für Maschinenbau | | Titel, zusätzlicher Titel Messaufbau fuer Charakterisierung | |
| 5 | | 6 | |
| 7 | | 7 | |
| 11.03.23 | | Spr. Blatt de 1/1 | |
| A3 | | A3 | |

5.3. Dynamic parameters determination

5.3.1. Hand-arm-system modelling

The description of the kinematics of the Hand-Arm-System was done by using the Euler coordinates. Figure 5.2 shows the proposal model of the HAS with three DoF corresponding to the shoulder, elbow and wrist joint in a vertical plane. Position vectors of the gravity center of the Hand, Fore-arm and Upper-arm with respect to the inertial system of coordinates XYZ0 are described by the equations 5.1, 5.2 and 5.3 respectively.

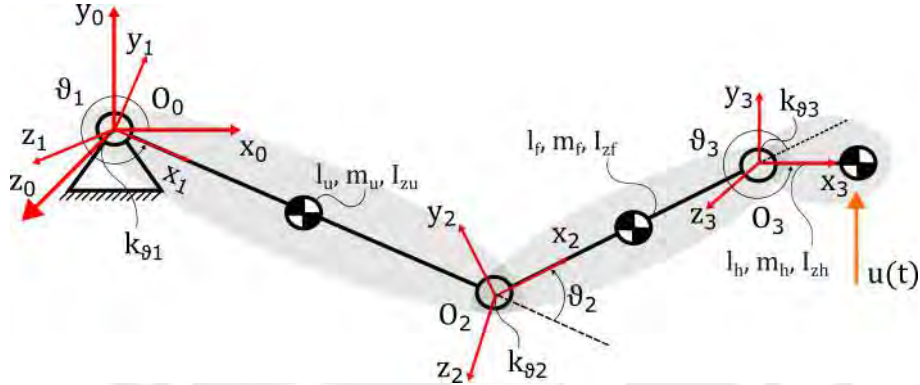


Figure 5.2.: Analytical model of the hand-arm-system

The position vectors of the mass center of the hand (H), forearm (F) and upper-arm (U) are described with the equations 5.1, 5.2 and 5.3.

$${}_{(0)}\vec{R}_H = {}^{03}R_{(3)}\vec{R}_H + {}_{(0)}\vec{R}_{03} \quad (5.1)$$

$${}_{(0)}\vec{R}_F = {}^{02}R_{(2)}\vec{R}_F + {}_{(0)}\vec{R}_{02} \quad (5.2)$$

$${}_{(0)}\vec{R}_U = {}^{01}R_{(1)}\vec{R}_U \quad (5.3)$$

The relative position vectors of the mass center with respect to the system of coordinates placed in each HAS element is described by the equations 5.4, 5.5 and 5.6.

$${}_{(1)}\vec{R}_U = l_{g1} \begin{pmatrix} 1 \\ 0 \\ 0 \end{pmatrix} \quad (5.4)$$

$${}_{(2)}\vec{R}_F = l_{g2} \begin{pmatrix} 1 \\ 0 \\ 0 \end{pmatrix} \quad (5.5)$$

$${}_{(3)}\vec{R}_H = l_{g3} \begin{pmatrix} 1 \\ 0 \\ 0 \end{pmatrix} \quad (5.6)$$

And the displacement vector between each coordinates system is described by the equations 5.7 and 5.8

$${}_{(0)}\vec{R}_{02} = {}_{(1)}\vec{R}_0 \quad (5.7)$$

$${}_{(0)}\vec{R}_{03} = {}_{(1)}\vec{R}_0 + {}_{(2)}\vec{R}_0 \quad (5.8)$$

Where

$${}_{(1)}\vec{R}_0 = l_1 \begin{pmatrix} \cos \theta_1 \\ \sin \theta_1 \\ 0 \end{pmatrix} \quad (5.9)$$

$${}_{(2)}\vec{R}_0 = l_2 \begin{pmatrix} \cos \theta_2 \\ \sin \theta_2 \\ 0 \end{pmatrix} \quad (5.10)$$

The Euler'matrixes are defined according to the model with the following equations

$${}^{01}R = \begin{bmatrix} \cos \theta_1 & -\sin \theta_1 & 0 \\ \sin \theta_1 & \cos \theta_1 & 0 \\ 0 & 0 & 1 \end{bmatrix} \quad (5.11)$$

$${}^{12}R = \begin{bmatrix} \cos \theta_2 & -\sin \theta_2 & 0 \\ \sin \theta_2 & \cos \theta_2 & 0 \\ 0 & 0 & 1 \end{bmatrix} \quad (5.12)$$

$${}^{23}R = \begin{bmatrix} \cos \theta_3 & -\sin \theta_3 & 0 \\ \sin \theta_3 & \cos \theta_3 & 0 \\ 0 & 0 & 1 \end{bmatrix} \quad (5.13)$$

Kinetic and Potential Energy

The kinetic energy is calculated with the equation 5.14

$$T = T_1 + T_2 + T_3 \quad (5.14)$$

where

$$T_i = \frac{m_i}{2} V_{g_i}^2 + \frac{J_i}{2} \theta_i^2 \quad (5.15)$$

The potential energy is calculated with the equation 5.16

$$U = U_1 + U_2 + U_3 \quad (5.16)$$

where

$$U_i = m_i g h_i + \frac{k_i}{2} \theta_i^2 \quad (5.17)$$

Lagrange equations

$$L = T - U \quad (5.18)$$

$$\frac{d}{dt} \frac{\partial}{\partial \dot{q}_i} L - \frac{\partial}{\partial q_i} L = Q_i \quad i = 1 \dots 3 \quad (5.19)$$

Finally, after a linearization process around a specific position of the HAS, the set of differential equations can be arranged in matrix form, equation 5.20, where M, C and F are the mass matrix, damping matrix, stiffness matrix and external forces matrix respectively.

$$[M] \{\ddot{\Theta}\} + [C] \{\dot{\Theta}\} + [K] \{\Theta\} = [F] \quad (5.20)$$

Model solution

The elaborated equations were implemented in Matlab for the solution of the mass, stiffness and damping matrix as a function of the dynamic parameters and dimensions of the arm. The code can be found in Section A in the Appendix.

5.3.2. Experimental identification procedure

Once the experimental data is obtained, datasets are pre-processed with a filtering. Then, the filtered data is used for the calculation of the dynamic parameters in the bio-mechanic model of the HAS based on an iterative approach of the stiffness and damping values until a cost function of the motion real and model response reaches its minimum.

The system of differential equations of the HAS was used as parametric model for identification. Excitation signal transmitted to the HAS is used as input to the model. Motion signals of angular velocity and angular position were used as output of the model. The procedure starts with guess values of stiffness and damping and calculate the model motion response. Then compute the cost function based on the minimum square values of the difference between model and experimental output. It is followed by the calculation of a new set of stiffness and damping values and the procedure is repeated until the cost function reaches its minimum designed.

Bio-mechanic model

```
1
2
3 function dxdt = odesystem(t, x,u_data,t_data, theta)
4     c1 = theta(4); % Damping in shoulder joint
5     c2 = theta(5); % Damping in elbow joint
6     c3 = theta(6); % Damping in wrist joint
7     k1 = theta(1); % Stiffness in shoulder joint
8     k2 = theta(2); % Stiffness in elbow joint
9     k3 = theta(3); % Stiffness in wrist joint
10
11     u = interp1(t_data, u_data, t); % Excitation force over time
12
13     % Set of differential equations based on bio-mechanic model
```

```

14 dx1dt = x(4);
15 dx2dt = x(5);
16 dx3dt = x(6);
17 dx4dt = -(19.960266 *c1 + 356.905226*c2)*x(4)
18 -(- 56.905226*c2 - 87.8990359*c3)*x(5)
19 - 87.8990359*c3*x(6)
20 - (19.960266 *k1 + 356.905226*k2)*x(1)
21 -(- 56.905226*k2 - 87.8990359*k3)*x(2) -87.899035*k3*x(3)
22 -0.33969384*u;
23
24 dx5dt = -(-36.944959*c1 - 149.3801751*c2)*x(4)
25 -(149.38017515*c2 + 338.90598660*c3)*x(5)
26 +338.90598660*c3*x(6)
27 - (-36.944959*k1 - 149.3801751*k2)*x(1)
28 -(149.38017515*k2 + 338.90598660*k3)*x(2)
29 +338.90598660*k3*x(3)
30 + 1.509805137*u;
31
32 dx6dt = -(50.9540768*c1 + 277.4248474*c2)*x(4)
33 -(- 277.424847*c2 - 1020.1148689*c3)*x(5)
34 -1020.1148689*c3*x(6)
35 - (50.9540768*k1 + 277.4248474*k2)*x(1)
36 -(- 277.424847*k2 - 1020.1148689*k3)*x(2)
37 -1020.1148689*k3*x(3)
38 + 17.85718749*u;
39
40 dxdt = [dx1dt; dx2dt; dx3dt; dx4dt; dx5dt; dx6dt];
41
42 end
43

```

System identification algorithm

```

1
2 t_data = sync_gyro3(:,1)'; % Data time
3 x6 = sync_gyro1(:,4) '-mean(sync_gyro1(:,4)')'; % Angular velocity of Hand
4 x5 = sync_gyro2(:,4) '-mean(sync_gyro2(:,4)')'; % Angular velocity of Forearm
5 x4 = sync_gyro3(:,4) '-mean(sync_gyro3(:,4)')'; % Angular velocity of Shoulder
6
7 u_data=sync_excforce(2,:);
8
9 % Angular position determination
10 dt = (sync_gyro1(:,1)); % Sample time
11 x3 = cumtrapz(dt, x6); % Angular position of Hand
12 x2 = cumtrapz(dt, x5); % Angular position of Hand
13 x1 = cumtrapz(dt, x4); % Angular position of Shoulder
14
15
16 % Initial guess for the parameters
17 initialGuess = [30, 30, 30,5,5,5];

```

```

18
19 % Use fminsearch to minimize the cost function and find the parameters
20 options = optimset('MaxIter', 20, 'MaxFunEvals', 200);
21 theta_estimated = fminsearch(@(theta) costFunction2(theta, t_data, x1, x2, x3,
22 x4,x5,x6,u_data), initialGuess,options);
23
24 % Display the result
25 disp(['Estimated parameters: ', num2str(theta_estimated)]);
26
27 % Optional: Plot the results
28 [t_fit, x_fit] = ode45(@(t, x) odesystem(t, x,u_data,t_data, theta_estimated),
29 linspace(0, t_data(end), 100), [x1(1); x2(2); x3(3); x4(4); x5(5); x6(6)]);

```



6. Measurement setup concept

6.1. Introduction

The aim of this research was to develop a setup with all the elements to be able to characterize the dynamic behaviour of the HAS in presence of vibrations. This development is essentially divided in the formulation of a method to characterize the vibration behaviour and a setup which materialize all the elements in order to perform the method. Since the setup is addressed to integrate a test subject Hand Arm System (HAS) in the execution, feedback is required due to the high level of non-linearity presented in the dynamic behaviour of the HAS. In this sense, the characterization method in Chapter 5 and the design process explained in this chapter were closely developed in an iterative process retro-alimented by experimental data with a test subject. Guidelines established by the Design Methodology VDI2221 were used in the conception of the measurement setup.

This chapter is structured as following. First, it is presented the list of requirements used for the delimitation of the measurement setup capabilities according to the information found in the literature and the resources available during this development, see Section 9.4 in order to found more information about the limitations. Once the list of requirements was established, the conception of the solution was carried out. The structure of functions was first established and the technical principle developed and optimized.

The development of a technical principle was retro-alimented by experimental prototypes of the measurement setup. For each prototype, it was carried out the integration between actuators, sensors, designed components and numerical procedure to process the experimental.

6.2. List of requirements

The aim of the measurement setup performance is to quantify the vibration characteristics in a standard well-controlled environment. The list of requirements pretends to delimited the capabilities that the measurement setup is going to have. After an analysis of the state of the art, the study variables were clarified in order to establish requirements oriented to measure them, see Chapter 5. The list of requirements also establishes the important study cases oriented to the characterization of the HAS. There were mandatory requirements critical to quantify the influence of the variables. These critical characteristics that must be considered were M (must) type.

List of Requirements

Master Thesis: Development of a measurement setup for quantification of the vibration characteristics of the hand-arm-system by inertial measurement units



Institution: Technische Universität Ilmenau Student: Carlos Rincon

Faculty: Maschinenbau Version: D-12.05.2024

Field: Biomechatronik Phase: Planning

| Organization | | | | Requirement | Values/Data | | | |
|--------------|---------|-------|------|--------------------------------------------------------------------------------------------------------------------------|-------------|--------------|--------|-------------------|
| Nr. | Source | Phase | Type | | Min | Should | Ideal | Unit |
| | | | | Physical Technical Function | | | | |
| F1 | Client. | K | M | Measurement setup for the quantification of the vibration characteristics of the Hand-Arm-System | | | | |
| F2 | SofT. | K | M | Positioning of the Hand-Arm-System for the physical task | | | | |
| F3 | SofT. | K | M | Quantification of the vibration signal in critical points of the Hand-Arm-System during the physical task | | 2D | 3D | mm/s ² |
| F4 | SofT. | K | M | Quantification of the muscle tension of the Hand-Arm-System during the physical task | | Indirect | Direct | N |
| F5 | SofT. | K | M | Possibility of changing the muscle tension level for each physical task | | 2 | | ranges |
| F6 | SofT. | K | K | Quantification of the vibration characteristics during a physical task for different trajectories of the Hand-Arm-System | | | | |
| | | | | Experimental Setup | | | | |
| E7 | SofT. | EP | K | 1. Measurement of the motion signals of the Hand-Arm-System during a physical task | | Acceleration | | mm/s ² |
| E8 | SofT. | EP | K | 1a. Characterization of the vibration characteristics of the Hand-Arm-System (impedance) during normal conditions | | | | |
| E9 | SofT. | EP | K | 1a1. Vibration measurement on critical points of the Hand-Arm-System during resting "Rest Tremor" | | 3 | | # |
| E10 | SofT. | EP | K | 1a2. Vibration measurement on critical points of the Hand-Arm-System during a posture holding "Postural Tremor" | | | | |
| E11 | SofT. | EP | K | 1a3. Vibration measurement on critical points of the Hand-Arm-System during a trajectory: "Kinematic Tremor" | | | | |
| E12 | SofT. | EP | K | 1a4. Measurement of the muscle tension in parallel with the activities performed | | Indirect | Direct | N |
| E13 | SofT. | EP | M | 1b. Characterization of the dynamical response of the Hand-Arm-System to external perturbations | | Acceleration | | mm/s ² |
| E14 | SofT. | EP | M | 1b1. During a external perturbation for different muscle tension levels | | 2 | | ranges |
| E15 | SofT. | EP | K | 1b2. During a external perturbation for different physical trajectories of the Hand-Arm-System | | | | |
| E16 | SofT. | EP | K | 1b3. During a external perturbation for different Hand-Arm-System's postures | | | | |
| E17 | SofT. | EP | M | 1b4. During different perturbations | | 2 | | # |
| E18 | SofT. | EP | K | 2. Determination of the stiffness through the measurement of motion and force signal | | | | Nm/rad |
| E19 | SofT. | EP | K | 2a. During different perturbations | | 2 | | # |

Requirement: M - must, S - should, K - could. Category: F - Technical Function, E - Experimental Setup, D- Design, S-State of the Art and Technology. Design Phase: An - Analysis, K - Concept, E- Technical Design, EP - Experimental Part

Ilmenau: Univ.-Prof. Dipl.-Ing. Dr. med. (habil.) Hartmut Witte

Respon. Prof. PUCP: Prof. Dr. Ing. Jorge Alencastre

Supervisor: Sabine Bruchmüller, M. Sc.

PREVIOUS Version C
Date 06.05.2024

Template Version: D - 12.05.2024 (English)

Seite 1 von 2

List of Requirements

Master Thesis: Development of a measurement setup for quantification of the vibration characteristics of the hand-arm-system by inertial measurement units



| | | | |
|--------------|--------------------------------|----------|---------------|
| Institution: | Technische Universität Ilmenau | Student: | Carlos Rincon |
| Faculty: | Maschinenbau | Version: | D-12.05.2024 |
| Field: | Biomechatronik | Phase: | Planning |

| Organization | | | | Requirement | Values/Data | | | |
|--------------|--------|-------|------|-------------------------------------------------------------------------------------------------------------|-------------|--------|----------------|-----------|
| Nr. | Source | Phase | Type | | Min | Should | Ideal | Unit |
| | | | | Experimentaleller Aufbau | | | | |
| E20 | Soft. | EP | K | 2b. During different activity trajectories | | | | |
| E21 | Soft. | EP | K | 2c. During different muscle tension level along the Hand-Arm-System | | 2 | | ranges |
| E22 | Int. | EP | M | Experimental Prototype with simplified characteristics for measurement the motion signals | | Motion | Muscle Tension | variables |
| | | | | Design | | | | |
| D23 | Int. | An | M | List of requirements of the design | | 1 | | # |
| D24 | Int. | K | M | Technical principle of the design | | 3 | | # |
| D25 | Int. | EP | M | Concept prototype design with 3D CAD | | 1 | | # |
| D26 | Int. | K | K | Concept prototype with simplified characteristics for testing the vibration measurement | | 1 | | # |
| D27 | Int. | E | M | List of parts | | 1 | | # |
| D28 | Int. | E | M | Optimal technical principle of the measurement setup | | 1 | | # |
| D29 | Int. | E | M | Technical design of the measurement setup | | 1 | | # |
| | | | | State of the Art and Technology | | | | |
| S30 | Int. | An | M | Description of different areas where the characterization of a Hand-Arm-System is applied | | | | |
| S31 | Int. | An | M | Classification of current procedures of Hand-Arm-System characterization | | | | |
| S32 | Int. | An | M | Identification of main variables for Hand-Arm-System characterization | | | | |
| S33 | Int. | An | M | Classification of current procedures for measurement of vibration conditions presented in a Hand-Arm-System | | | | |

Requirement: M - must, S - should, K - could. Category: F - Technical Function, E - Experimental Setup, D- Design, S-State of the Art and Technology. Design Phase: An - Analysis, K - Concept, E- Technical Design, EP - Experimental Part

| | | | |
|---------------------|--------------------------------------------------------|------------------|------------|
| Ilmenau: | Univ.-Prof. Dipl.-Ing. Dr. med. (habil.) Hartmut Witte | Previous Version | C |
| Respon. Prof. PUCP: | Prof. Dr. Ing. Jorge Alencastre | Date | 06.05.2024 |
| Supervisor: | Sabine Bruchmüller, M. Sc. | | |

6.3. Structure of functions

The functions structure is represented in Figure 6.1. The main idea is to quantify the parameters of the dynamic behaviour as a function of three variables in the HAS: perturbation, posture and muscle tension. These three variables are represented in each group in the structure. Each group are in parallel since the variables can be changed independently in order to quantify the influence of each one.

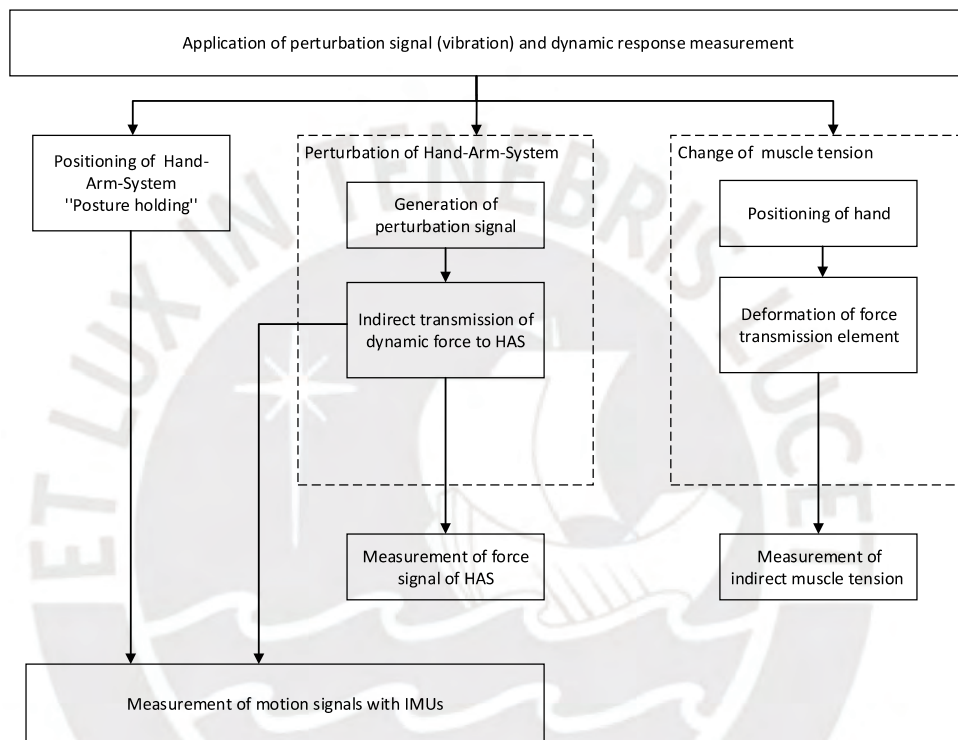


Figure 6.1.: Functions structure of the measurement setup

6.4. Technical principle

The materialization of the method was carried out through the formulation of a technical principle where the constructive elements are elaborated in order to fulfil the functions of the measurement setup. The technical principle is a continuous formulation and evaluation of all the possibilities to integrate the requirements established. In this research, it was possible also the implementation. This context established a frame of considerations to use available resources and components from the Laboratory which delimited the functions of the technical principle. In Section ??, it was discussed each technical principle elaborated. Then, the best technical principle was evaluated for implementation. Due to fabrication and components acquisition limitation, the technical principle capabilities were delimited to only focus on the most important variables in this study.

Once a basic primitive concept with limited functions was tested, see 6.5.1, the technical principle was improved considering the feedback from the prototypes in terms of how the device was related to the test subject. The functions include mainly the measurement of the arm vibration motion as well as the grip force and total force applied against the perturbation. Both were important values for the characterization of the influence of the force level to the dynamic response under a perturbation. In Figure 6.2, it is shown the final principle of the measurement device.

The hand strength is quantified by a force sensor (2) in the gripper (4) with a lever (1). It must be noticed that the lever amplifies the force measured at the force sensor (2). The shaker (6) produces a vibration force in the vertical direction, the vibration force is transmitted through a sensor force (5) to the gripper (4) in order to measure the force transmitted to the hand. A linear guide (3) was implemented to assure a fixed-free configuration in order to remove any interference to the force sensor (5). In this sense, the total force applied against the shake is only produced by the arm.

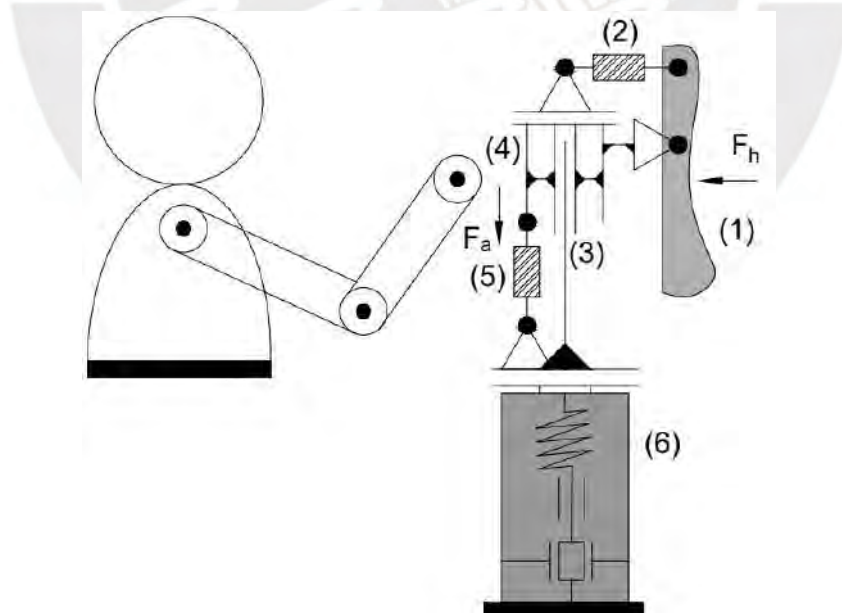


Figure 6.2.: Optimal technical principle

6.5. Measurement setup implementation

The design process included a constructive development of the technical principle retro-alimented mainly by experimental test with subjects in ergonomic and capabilities aspects. Some aspects can not be theoretically calculated and depends on each subject, such as the ergonomic behaviour of the grip action on the measurement device. This kind of aspects are strongly related to the person and the acquisition of experimental feedback is meaningful information. Therefore, the development of the setup was consisted on three levels of prototypes implementation. The first level was part of the concept phase where a first approach was carried out with a simplified design only focused on to test ergonomic aspects of the grip action while an excitation is transmitted to the arm. The second level was oriented to the technical design where the prototype included all the functions and desired capabilities to perform the measurement. Finally, in the third level, an optimization of the constructive elements were carried out oriented to the final implementation. This third prototype was a more sophisticated version with standard, commercial and sturdy elements as close as possible to the final design, where most parts are addressed to be manufactured with aluminum alloy in order to have a deformation as low as possible. However 3D printing was still used for most parts of the prototype due to manufacturing limitations.

6.5.1. First approach

Device description

As part of the concept development, the functions of the technical principle were tested. A simplified prototype of the setup was implemented with PLA parts by 3D-Printing focused only on the measurement of motion signals. In this sense, the first concept approach is focused on the following points:

- Measurement of motion signals: acceleration and angular velocity.
- Testing the electronic components.
- Development of a data acquisition procedure.
- Development of a data processing procedure.

This experimental first approach only takes into account functional and geometrical characteristics of the concept described in Table 6.1. Then the concept was significantly simplified.

Table 6.1.: Simplifications in the first approach test

| N | Description |
|---|---------------------------------------------------------------------------|
| | Characteristics taken into account |
| 1 | Power and amplitude produced by the shaker |
| 2 | Form and geometrical relation between subject and system (ergonomics) |
| 3 | Vibration force transmission through the mechanical components and joints |
| 4 | Guide alignment during the vibration produced by the shaker |
| | Characteristics not taken into account |
| 1 | Measurement of force transmitted from the shaker to the gripper |
| 2 | Measurement of grip force in the hand |

It was proposed a grip shape in order to measure the muscle tension indirectly through a grip force at the hand. Figure 6.3 shows the constructive design. All the elements were supposed to be printed, then the geometrical characteristics were based on simple primitive elements and the dimensions were established for a sturdy behaviour during vibration conditions. The main section is shown in the Figure 6.3b. It can be seen that there is a rigid coupling between the shaker and the gripper. In general, all the elements were supposed to have a rigid connection between each other.

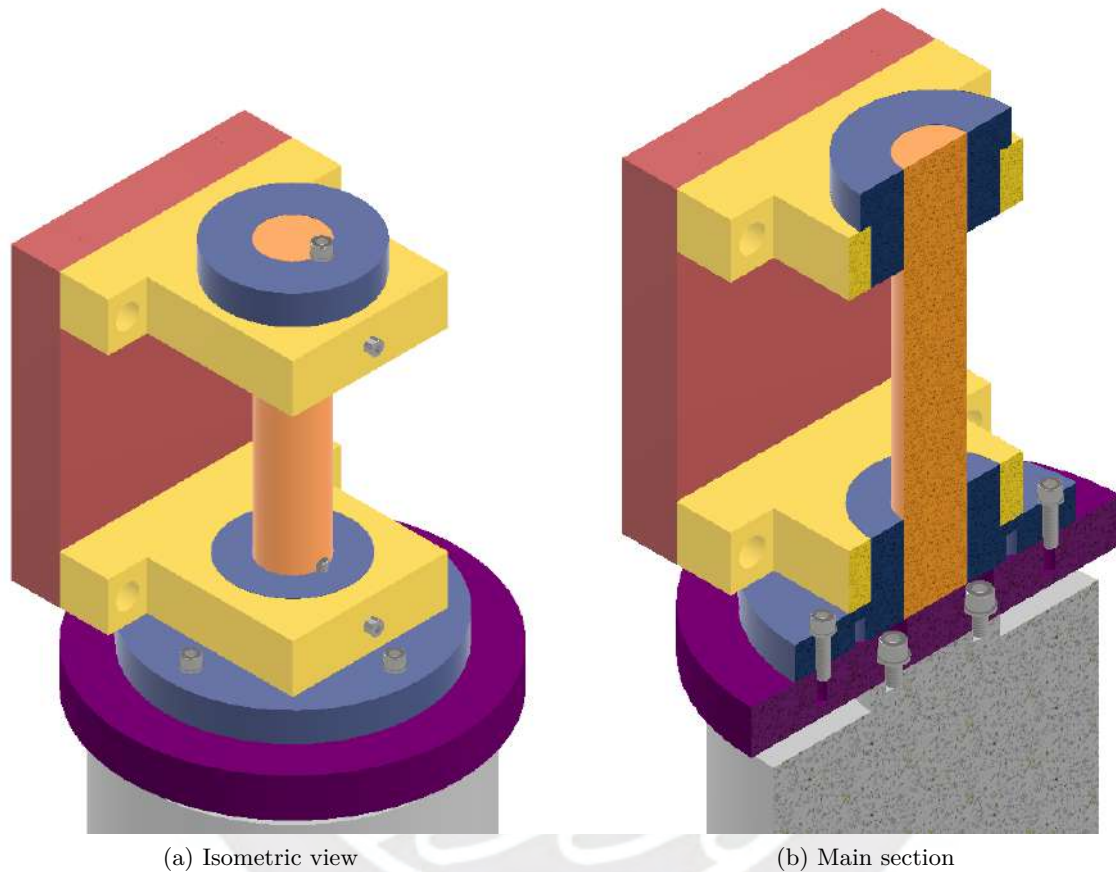


Figure 6.3.: Design prototype for first approach

Experimental test

The simplified design was implemented, Figure 6.4, and was consisted of the components in Table 6.2. For testing purposes, high frequency ranges were first generated in the shaker in order to find the mechanical limitations of the elements. Two IMUs were used for the measurement of hand and forearm, its connection scheme is shown in Figure 6.5.

Table 6.2.: Components used for the experimental first approach

| N | Components description |
|---|---------------------------------------------------------------------------------------------------------------------------------------|
| 1 | A computer for the excitation signal generation |
| 2 | A NI DAQ for the communication between the computer and the amplifier. |
| 3 | A ESP32 for the communication between the IMU MPU6050 and the computer. |
| 4 | Two IMU MPU6050 for the measurement of the acceleration and angular velocity in 3 coordinates XYZ placed on the hand and the forearm. |
| 5 | A shaker TIRA TV 51110 and its amplifier TIRA BAA 120 for the perturbation force generation |
| 6 | The simplified design of the gripper for the transmission of the perturbation force to the hand-arm-system |



Figure 6.4.: First approach of measurement setup: shaker amplifier and DAQ (left behind), computer (left front), shaker with simplified device prototype and micro-controller with IMU (middle behind) and IMU (right)

Two position configurations of the HAS were tested. Figure 6.6. In the first position, only the forearm can rotate with respect to the elbow joint and the hand with respect to the wrist joint. The test subject performed enough grip force in order to fix the wrist joint. In this case, the calculation of the elbow stiffness is simplified since the position simulates only a DoF case without consider the wrist as a joint. In the second case, the elbow joint was free. This condition allows the calculation of transmissibility along the HAS. The IMU were placed according to the orientation shown.

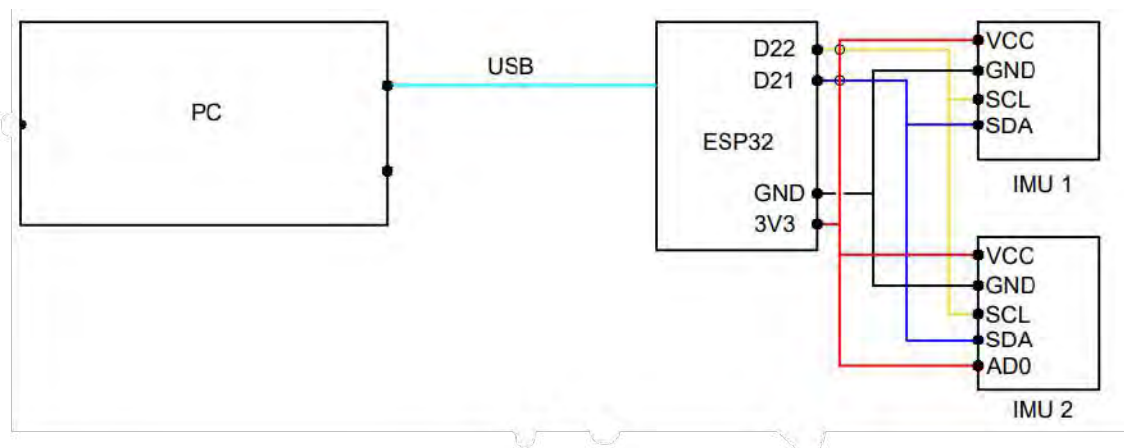


Figure 6.5.: Scheme of IMUs connections

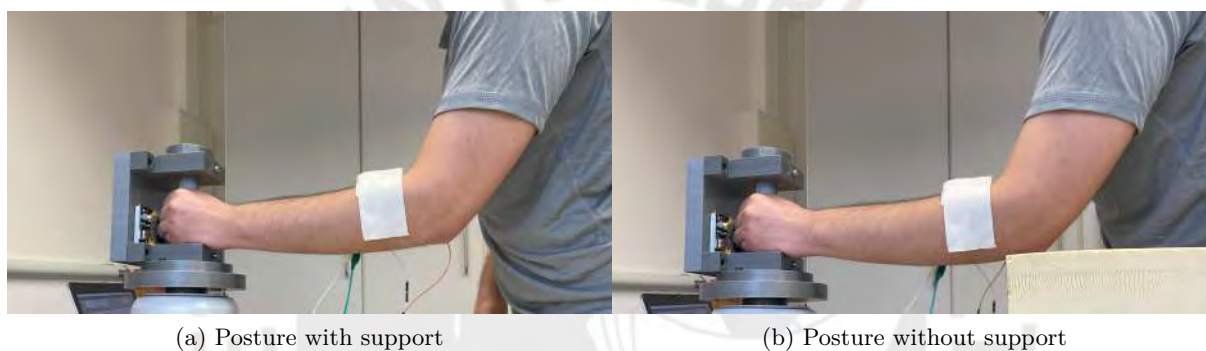


Figure 6.6.: Test configurations with the hand attached to the simplified measurement device coupled to the shaker

Main findings and highlights

Useful information regarding the existent components performance was found during the first approach. The available shaker showed a better behaviour for frequencies from 10 Hz maintaining the amplitude when the inertia of the impedance of the HAS increases. Below 10 Hz, it is able to work but the signal amplitude was not constant and also there were short periods without motion. Measurements were characterized by a high non-stationary behavior, mainly due to the non controlled conditions in this concept prototype. The dimensions of the PLA components were sturdy enough, there were no visible deformations. The measured signal was high and low frequency enough to be measured by the commercial IMUs. It was possible to process data obtained; however, high level of noise was found and it was required a filtering process. The internal linear bearing of the shaker was not as vertical as desired. The formulated characterization method has the assumption of a vertical excitation force as input; in this sense, the linear motion in a plane should be mechanically assisted or the motion of the HAS better controlled. In this first approach, as an example of a mechanical assistance, the block used in Figure 6.6 supported the motion control. Without a mechanical assistance that would change the boundary conditions of the motion, two positions were found that helped to maintain this linear vertical motion better and also to support a constant behaviour of the muscle tension: 90° and 180° between the forearm and upper-arm. Afterwards, these postures were used as a final method.

6.5.2. Second measurement setup concept

Device description

This prototype meets all the capabilities defined in the list of requirements, see Section 6.2. The constructive elements were designed in order to fulfil each function of the technical principle. A detailed explanation of each element in its final form and geometry is presented in Section 6.5.3.

The second prototype design is shown in Figure 6.7. The idea corresponds to the technical principle and was to integrate a device to measure the muscle tension force at hand while a standardized excitation signal is transmitted to through the hand. An internal linear bearing was implemented to fulfil the internal slide function and only measure the transmitted force to the HAS as shown in Figure 6.7(b). In contrast to the first approach, in this phase, both force sensors were implemented in order to measure the grip force and excitation force from the shaker. The device was designed in order to be printed with PLA filament. The lever of the gripper device was designed to have an ergonomic shape. This grip action can be seen in Figure 6.9.



Figure 6.7.: Main views of the prototype A

Experimental test

The experimental setup is shown in Figure 6.8. The addition of both force measurement sensors required an amplifier to record the data through a data acquisition box. The connections detail of all the electric components is shown in Appendix, Section D. The evaluation of this device consisted on the performance during the characterization of the muscle tension, posture and perturbation influence. A series of tests were carried out with each mentioned variable. In the muscle tension study, different grip forces were applied while the other variables as reaction force, posture and perturbation were fixed, Figure 6.9. The reaction force used corresponded to a normal muscle tension level, the posture was fixed as close as possible to 90 while test subject was seated and the perturbation was 6 Hz.

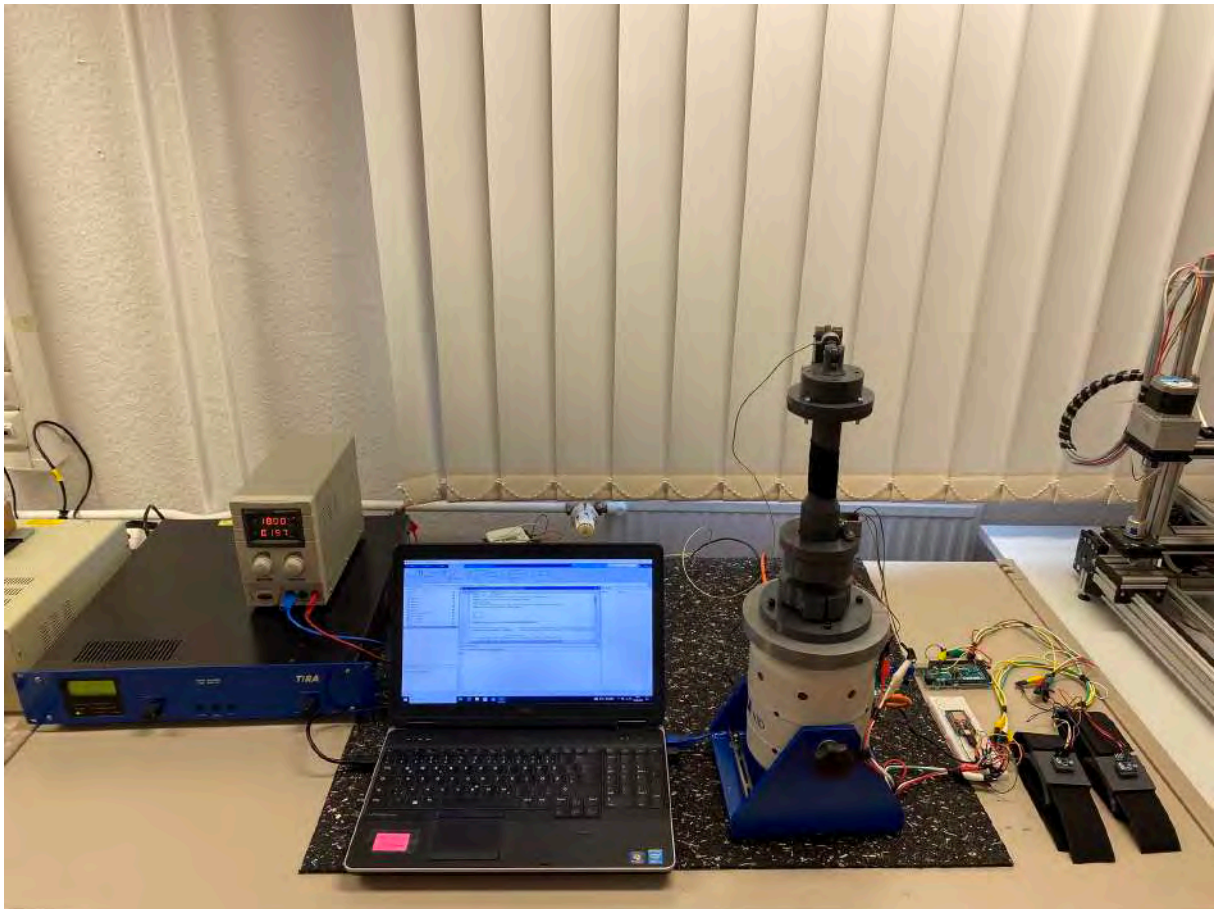


Figure 6.8.: Second measurement setup concept: shaker amplifier and power source(left); computer and shaker with measurement device (mid front); force amplifier and DAQ (mid behind); IMUs with micro-controllers(right)

Main findings and highlights

Part of the pre-processing required the synchronization of the acceleration and force signals measured since it is important for the system identification algorithm which uses the excitation signal to calculate the motion signals by using an analytical model, see Section A. The stiffness of the device elements must be as enough high in order not to affect the force measurement. It was observed significant deformation of the lever made by PLA when the grip force was applied.

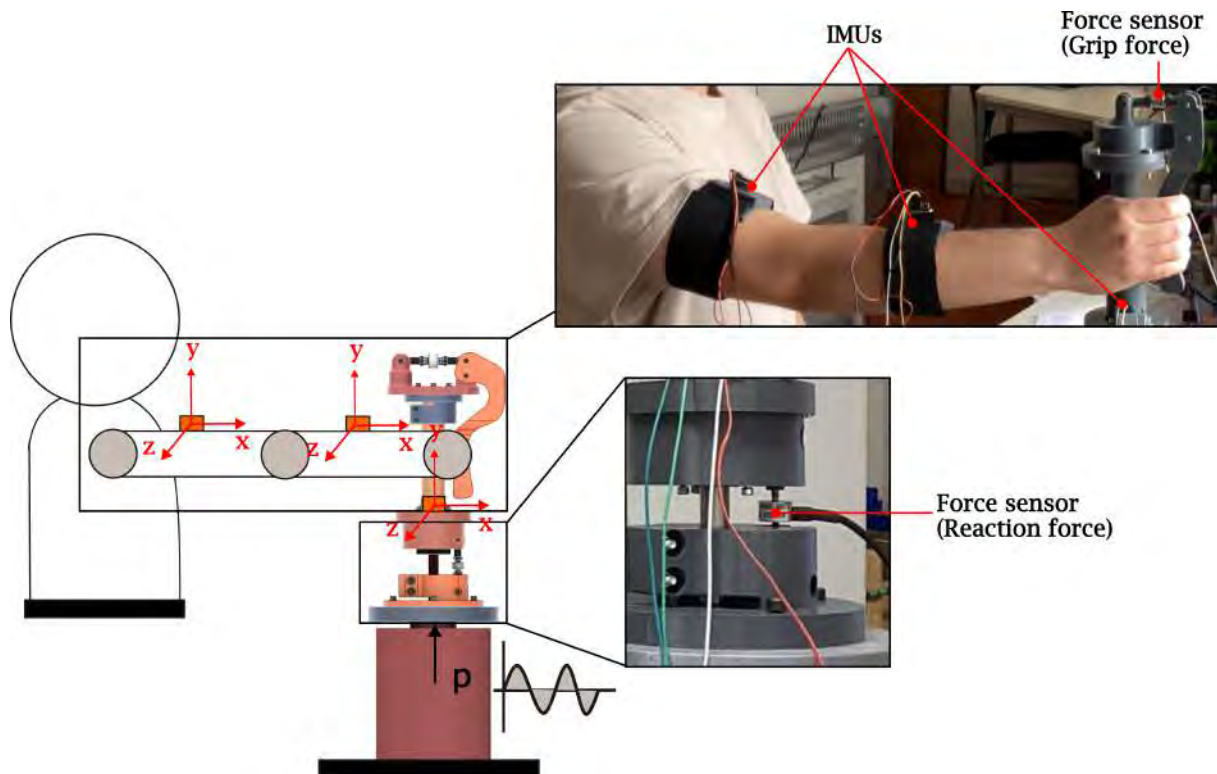


Figure 6.9.: Example of the configuration of the second concept implemented in a posture of 180°: Scheme of the test procedure (left) and implementation with the second prototype (right bottom and top)

This behaviour affect directly to the measurement of the real grip force applied. The structure of the device should be made also by low weight metal elements as alloy aluminum which has a good mechanical strength and weight rate. The filtering process had a high impact for the system identification procedure and the calculation of the frequency response. Due to the non-linear behaviour of the HAS variables that depends on the motion quality of control of the test subject, the dynamic response manifested different magnitudes and frequency over the whole measurement. In this sense, the analysis must be performed with a selected time period from the whole signal with a behavior as stationary and stable as possible. The shaker performance below 5 Hz was not good as expected. Its capacity to maintain a constant excitation amplitude tended to degrades in low frequencies. The system identification fit was significant better if the angular velocity values are higher. A cost function based on frequency domain was used instead a conventional time domain because of its main advantage not considering the delay between signals.

6.5.3. Final measurement setup

Constructive implementation

The core element of the measurement setup is the implementation of the measurement device for the excitation of the hand-arm-system (HAS) and, simultaneously, the measurement of the muscle tension performed. The technical principle of the device is materialized for a constructive implementation. In Figure 6.10(a), it is shown a the isometric view of the device while in Figure 6.10(b), the final implementation. The detail of the components and its constructive relation can be found in the assembly drawing in Appendix, Section D.

- Hand shaft: This component is fixed to a internal linear bearing with the DoF only in the vertical direction. The bearing provides enough vertical alignment for the experimental purposes.
- Fixing mass: The shaft of the linear bearing is fixed with this component by friction produced by screw joints.
- Adaptor: It is the connection between the force sensor and the housing of the linear bearing.
- Lever: The idea is to have an ergonomic design for manipulation. The subject generates the grip force by applying pressure load on the surface which generates a torque compensate by the reaction force from the force sensor at the top.

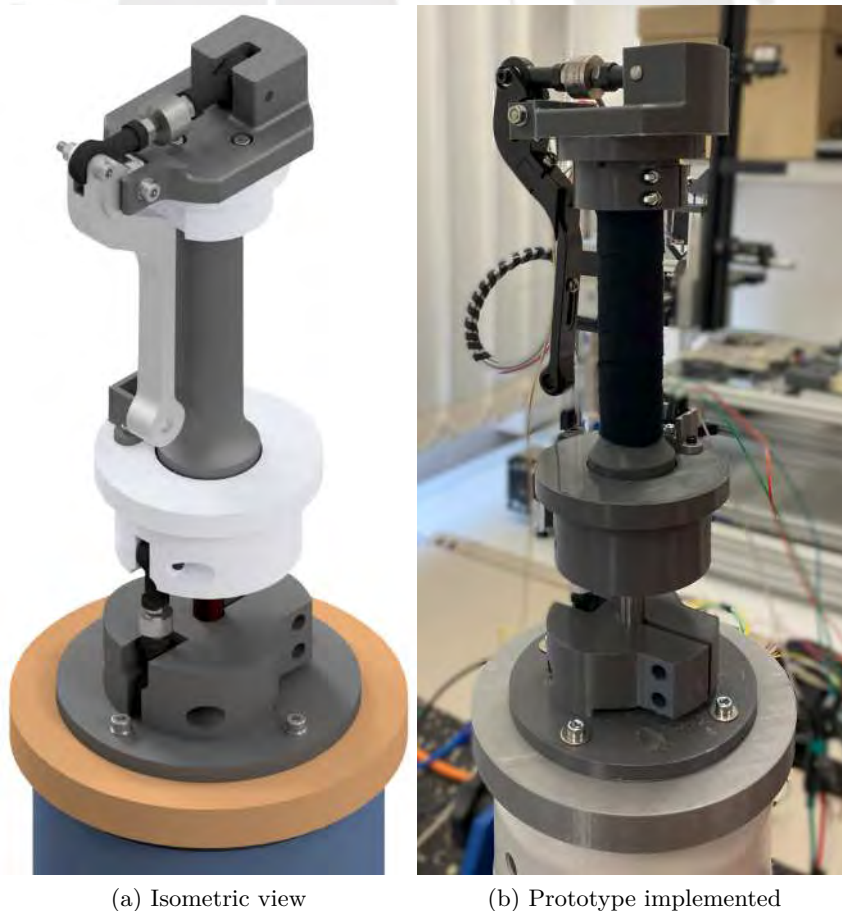
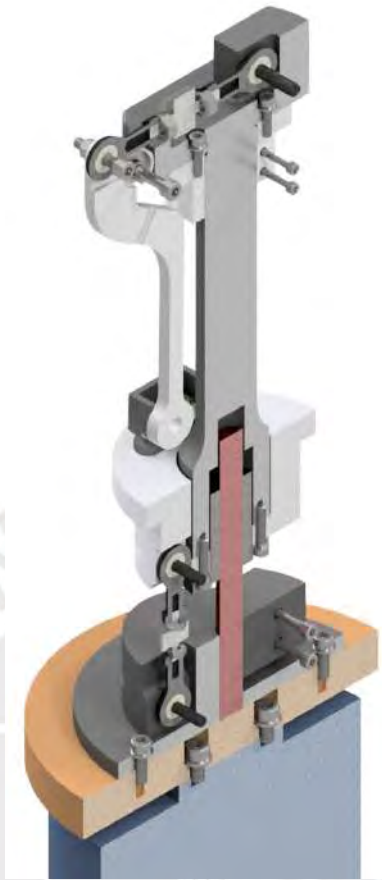


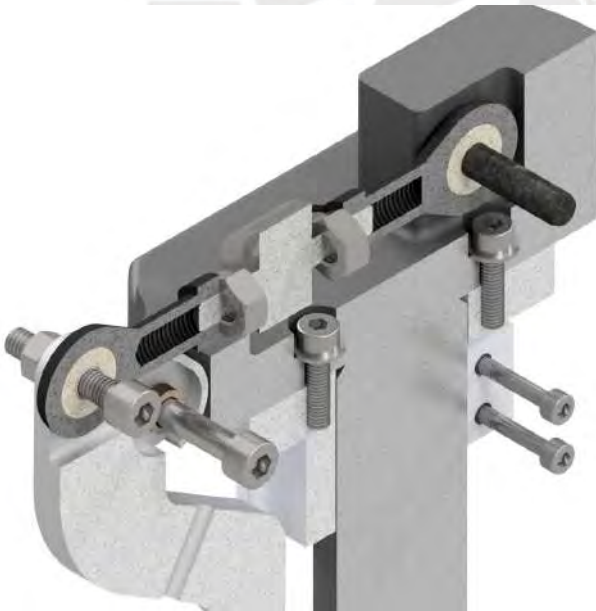
Figure 6.10.: Measurement device in the final setup

The analysis of the muscle tension influence requires the measurement of the force transmitted between the shaker and the HAS through the device. Thus, the measurement of this force is carried out by a load cell placed between the device and the shaker, Figure 6.11(c). The linear bearing within the device allows the free motion on the vertical axis, which is the excitation axis. In this sense, the load cell fixed the device with the shaker and transmit the excitation force to the device, therefore the HAS, through it. In order to guarantee that only the excitation force is measured, the configuration of the linear bearing shaft is fixed to the shaker and free to the hand shaft. The housing of the linear bearing, which is the element with the HAS, is fixed to the hand shaft by screw joints as shown in Figure 6.11(c). The only connection available with the shaker is through screw joints positioned in a small diameter. Thus a secondary element for the connection between the device and the shaker was included as shown in Figure 6.11(c). The muscle tension of the hand is quantified through the grip force measurement with a lever configuration, Figure 6.11(a). The hand subject produces a grip force with the device gripper generating a torque with respect to the lever rotation center, which is compensated by the force from the load cell at the top while it is measured, Figure 6.11(b).

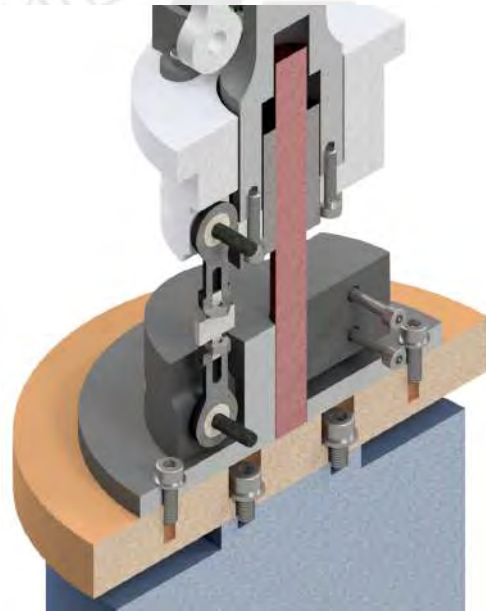




(a) Isometric section



(b) Force sensor implementation for hand



(c) Force sensor implementation for excitation force

Figure 6.11.: Constructive details of the measurement device

Integration of sensors and actuators

The measurement setup is consisted of its core element, the designed measurement device, integrated with other hardware elements that are necessary to perform measurement. The shaker and force sensors required amplifiers, power source and a data acquisition system to communicate the signals to the computer. In case of the motion sensors, there were required micro-controllers for the communication between sensors and computer. In Figure 6.12, it is shown the implementation of the prototype setup. The components of the setup are described in Table 6.3. The connections of each electronic component is detailed in the connections diagram in Section D.



Figure 6.12.: Final measurement setup for experimental characterization: shaker amplifier and power source(left); computer and shaker with measurement device (mid front); force amplifier and DAQ (mid behind); IMUs with micro-controllers(right)

Table 6.3.: Final measurement setup components

| N | Components description |
|---|-----------------------------------------------------------------------------------------------------------------------------------------|
| 1 | A computer for the excitation signal generation and motion signal recording |
| 2 | A NI DAQ for the communication between the computer and the force amplifier and the communication between shaker amplifier and computer |
| 3 | Three MPU 6050 for motion measurement placed on the measurement device, forearm and upper-arm |
| 4 | A ESP32 for the communication between two IMUs and the computer |
| 5 | An Arduino MEGA for the communication between the third IMU and the computer |
| 6 | A shaker TIRA TV 51110 and its amplifier TIRA BAA 120 for the perturbation force generation |
| 7 | Two force sensors NOVATECH F250 UFR0H0 and BURSTER 8417-6002 |
| 8 | A force signal amplifier SG-2K-KS-24E-010 |
| 9 | The developed measurement device made by PLA and standard mechanical components |

Shaker

The excitation of the HAS was performed with the available shaker TIRA TV 51110 and its amplifier TIRA BAA 120. The shaker meets the requirement of force range and frequency estimated in the design calculations with a natural frequency over 650 times the frequency working range. However, the large frequency range available from 2 to 7000 Hz is not the ideal for an accurate excitation within the HAS frequency range characterization of 3-10 Hz, see Section 3.2. The excitation frequencies and amplitudes produced by the shaker is controlled in communication with a program elaborated in Matlab Simulink, Figure 6.13. The excitation signal generated Simulink is sent to the shaker amplifier with a data acquisition system DAQ NI USB-6008.

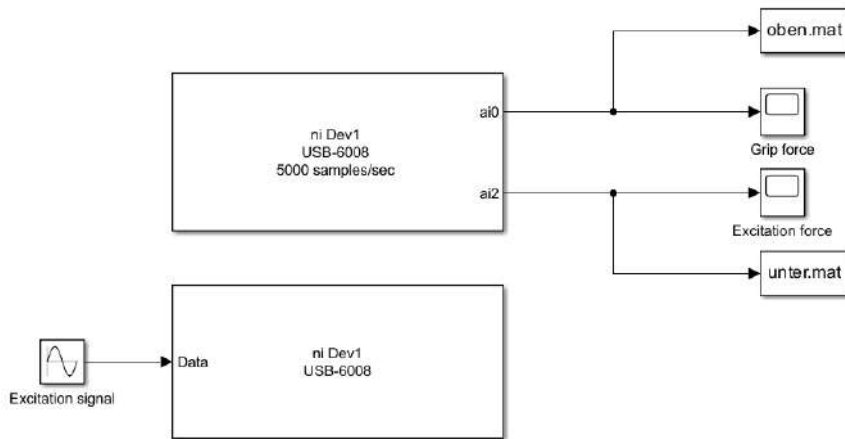


Figure 6.13.: Control of shaker signal with Matlab Simulink

Force measurement

The grip force performed by the hand is measured by the force sensor BURSTER 8417-6002 which is connected to the gripper shaft and the lever through two head rods IGUS KBRM-06, Figure 6.14(a). The force transmission from the shaker to the Hand-Arm-System is carried out through the force sensor NOVATECH F250 UFR0H0 which also fixes the measurement device with the shaker with two head rods IGUS KBRM-05-M4, Figure 6.14(b). The amplifier with two canals SG-2K-KS-24E-010 is used for the communication of the force signal measured to the same data acquisition system NI USB-6008 of the shaker.

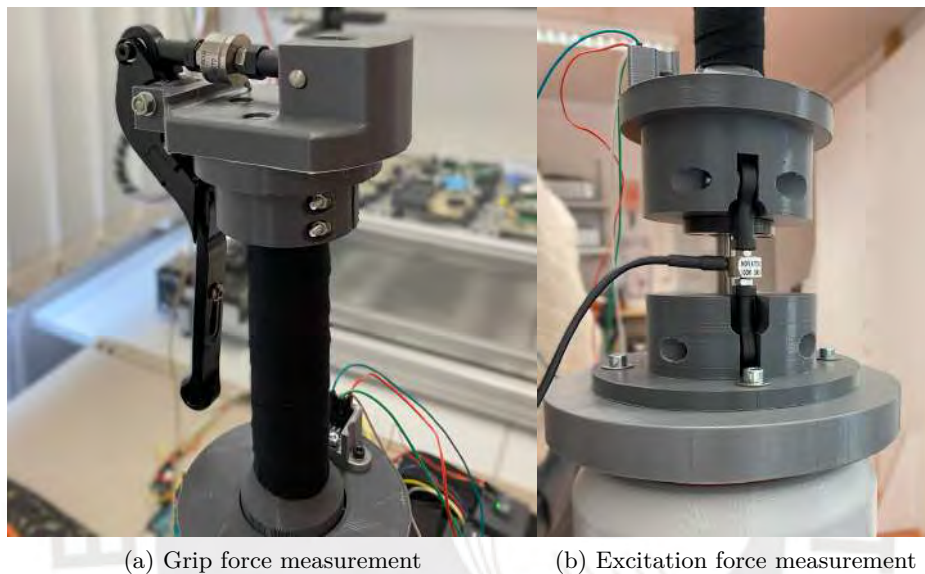


Figure 6.14.: Force sensors implemented on the measurement device

Motion measurement

Three MPU 6050 were used for the measurement of acceleration and angular velocity signals of the HAS. They are placed in the mass center of each element of the HAS as shown in Figure 6.15. According to Dempster & Gaughran (1967), mass centers take place in approximately 43.74% of the upper-arm and 42.93% of the forearm length. In the case of the Hand, the MPU is placed on the measurement device base which is fixed to the hand motion.



Figure 6.15.: Position of MPUs on the hand-arm-system: hand attached to the measurement device in a grip action (left) and test subject (right)

7. Experimental design

7.1. Experimental setup

The measurement setup designed was implemented with existent equipment in the Laboratory of Biomechanics at the TU Ilmenau. The measurement device in the setup was fabricated by standard components in combination with 3D printing for validation purposes. The implementation was described in detail in Section 6.5.3 and Figure 6.12 shows the experimental setup in the laboratory. This setup was designed to measure the dynamic response in force and motion signals while the excitation force is transmitted to the HAS. Excitation force and grip force along the motion response were measured over time according to a designed protocol. The excitation force also represents the reaction force performed by the HAS.



(a) Lifting platform for shaker positioning (bottom-behind), (b) shaker with measurement device (left-middle) footrest for 90° posture (bottom) and test subject and lifting platform (left-bottom) executing a grip action (middle-behind)

Figure 7.1.: Experimental setup with the test subject with a posture 90 between forearm and upper-arm: (a) lateral view and (b) frontal view

The implementation of the measurement device, shown in Figure 8.2, was carried out with



Figure 7.2.: Experimental setup with the test subject with a posture of 180° between the forearm and upper-arm: lifting platform (bottom), measurement device with shaker (middle-left) and test subject (right)

3D printed parts and involved a series of assumptions in order to compensate precision and robust behaviour with 3D printing. Dimensions of the device parts were designed with high cross sectional areas since polymer parts do not have mechanical properties as good as metal materials: strength and elasticity modulus values are significantly lower in polymer materials. Nevertheless, it was used the same constructive implementation developed for the device, see Section 6.5.3. Most parts were fabricated by PLA. On the other hand, standard mechanical components were used where form and geometry tolerance were required as the internal linear bearing in order to guarantee the assembly and performance during dynamic conditions.

7.2. Protocol

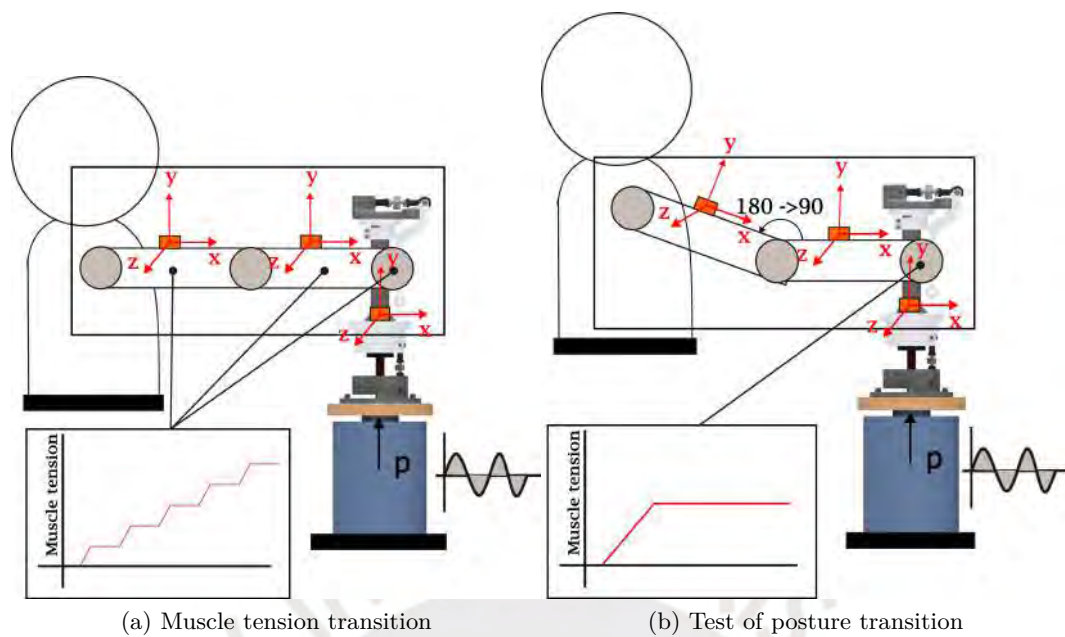
The experimental test designed in this work seeks the validation of the proposal measurement setup through the characterization of the dynamic behaviour of the HAS and the influence of the main variables identified in the literature, see Chapter 5. The variables selected are muscle tension, posture and perturbation in the HAS. The perturbation is quantified by its frequency. The muscle tension is quantified by the measurement of the grip force performed by the hand's subject and the reaction force against the shaker. Two different postures which are commonly involved in the natural motion of the HAS were studied. Each configuration of the variables set for each test is shown in Table 7.1 and are addressed to the characterization of a specific variable by isolating the influence of the others.

Table 7.1.: Configuration of tests

| Test | Description | Perturbation 4 Hz | Perturbation 6 Hz | Perturbation 8 Hz | Grip Tension 0% | Grip Tension 25% | Grip Tension 50% | Grip Tension 75% | Grip Tension 100% | Reaction Tension 0% | Reaction Tension 25% | Reaction Tension 50% | Reaction Tension 75% | Reaction Tension 100% | Elbow 90° | Elbow 180° |
|---------------------|--------------|-------------------|-------------------|-------------------|-----------------|------------------|------------------|------------------|-------------------|---------------------|----------------------|----------------------|----------------------|-----------------------|-----------|------------|
| Transition | Tension 1 | | | x | x | x | x | x | x | x | x | x | x | x | | x |
| | Posture 2 | | | x | | x | | | | | x | | | | x | x |
| Tension and Posture | Grip 90 3.1 | x | | | x | | | | | | x | | | | | x |
| | Grip 90 3.2 | x | | | | x | | | | | x | | | | | x |
| | Grip 90 3.3 | x | | | | | x | | | | x | | | | | x |
| | Grip 90 3.4 | x | | | | | | x | | | x | | | | | x |
| | Grip 90 3.5 | x | | | | | | | x | | x | | | | | x |
| | Grip 180 4.1 | x | | | x | | | | | | x | | | | | x |
| | Grip 180 4.2 | x | | | | x | | | | | x | | | | | x |
| | Grip 180 4.3 | x | | | | | x | | | | x | | | | | x |
| | Grip 180 4.4 | x | | | | | | x | | | x | | | | | x |
| | Grip 180 4.5 | x | | | | | | | x | | x | | | | | x |
| Perturbation | 4Hz 5.1 | x | | | | | x | | | x | | | | | | x |
| | 6Hz 5.2 | | x | | | | x | | | x | | | | | | x |
| | 8Hz 5.3 | | | x | | | x | | | x | | | | | | x |

7.3. Transition study

The first test seeks the characterization during conditions that can simulate a possible real condition. In a real condition, the characteristics of the HAS adapts their behaviour to the desired motion to perform. This non-linear behaviour produces that the dynamic response of the arm depends on the variables of muscle tension, posture geometry and perturbation. Since in a real condition all the variables that control the dynamic response are involved simultaneously, the experimental test should represent it, in a simplified and well controlled way. The influence of a muscle tension transition was measured by applying different levels of muscle tension simultaneously while the other variables are fixed. Perturbation was set in 8Hz while the posture was fixed in 180°. On the other hand, the influence of the posture was measured by applying two postures sequentially from 180° to 90° while the perturbation was also set in 8Hz and the muscle tension was maintained in a normal level (around 25 % of the possible maximum force). The reaction force was maintained as relaxed as possible close to 0%.



(a) Muscle tension transition

(b) Test of posture transition



(c) Posture transition

Figure 7.3.: Transition test of muscle tension and posture

7.4. Variables influence study

7.4.1. Muscle tension and posture study

The influence of the muscle tension and posture was quantified. Figure 7.4 shows the test cases for two postures 90° and 180° . The muscle tension was represented through an indirect measurement of the grip force and reaction force against the shaker. The ranges of possible forces that the subject can produce are measured offline without the perturbation from the shaker. According to these ranges, the muscle tension level is divided in steps of 25% from 0 to 100%. It was an assumption that the grip force was related to the wrist behaviour while the reaction force was an effect produced by the forearm and upper arm muscles. Two postures 90° and 180° between the forearm and upper-arm were selected since they can represent common activities related to pick objects up as an example.

In the first group, from Grip 90 3.1 to 3.5, the subject is asked to hold the reaction tension performed by the arm while the grip force is increased from 0 to 100 % for each test. The other variables of perturbation frequency and arm posture were set in 6Hz and 90° posture angle. In

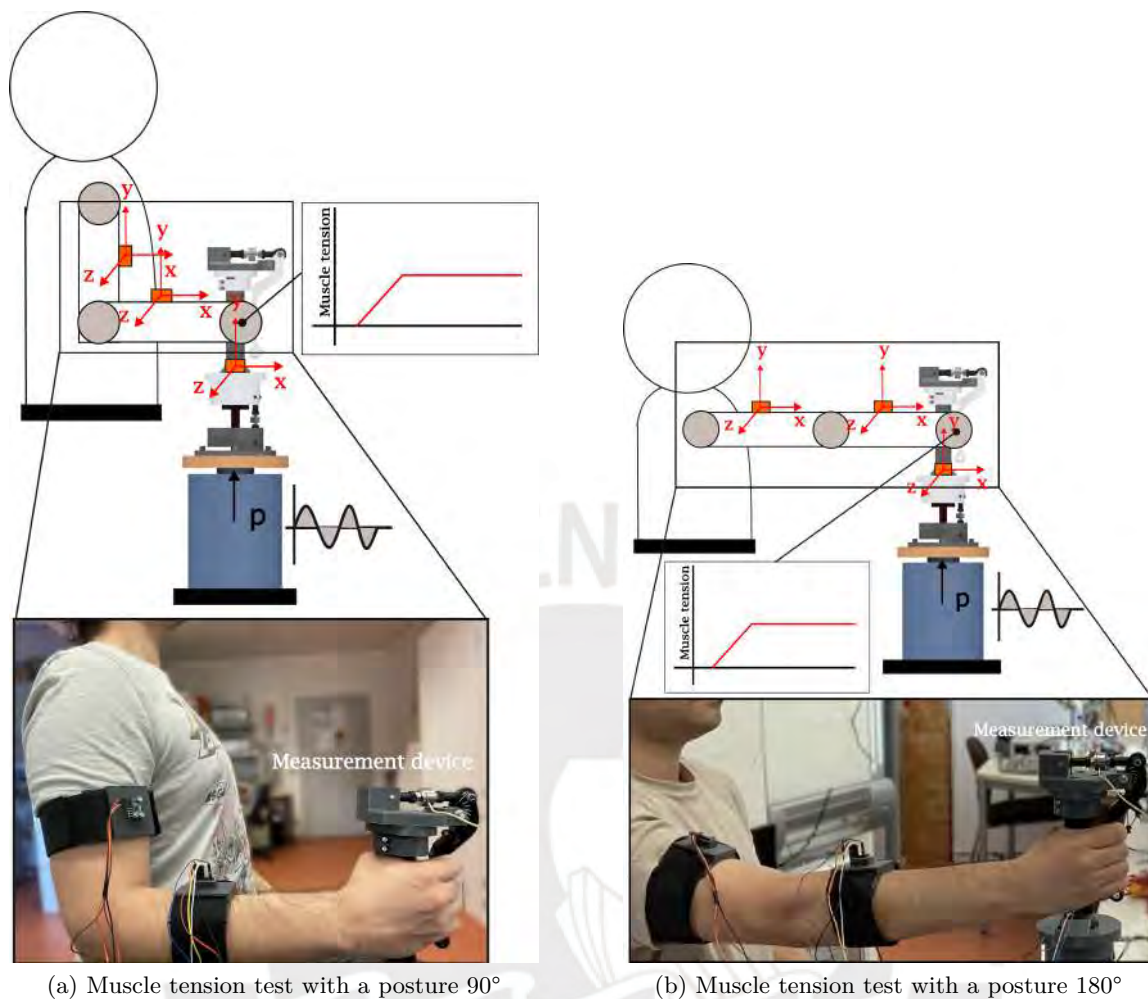


Figure 7.4.: Muscle tension test during a stationary dynamic response with two postures: (a) 90° and (b) 180° between the forearm and the upper-arm

the second group, from Grip 180 4.1 to 4.5, the subject was asked to hold the same conditions set of grip force, reaction force and perturbation while is arm posture was set in 180°. During the tests, it was found that the perform of a reaction force against shaker was physically difficult to maintain and also was imitated by the shaker power. In this sense, only 25% which corresponds to normal condition was used.

7.4.2. Frequency study

The influence of the perturbation frequency was quantified. Frequencies of a pathological condition were reported in the literature, see 2.1 in a range from 3-10 Hz. In this, the perturbation frequencies were set in 4,6 and 8 Hz while the other variables are maintained. Figure 7.4(b) represents also this case, where the muscle tension was set in a 50% for grip and the reaction force was maintained as close as possible to a relaxed condition (around 0%). The arm posture is set in 180°.

8. Results

In the measurement setup prototype, each test in Table 7.1 was carried out. Different condition of muscle tension, posture and perturbation were studied. Two dynamic cases were considered: transient and stationary response. Transient response was measured during a change of a condition while stationary response was measured once the test subject achieve the desired condition. The test subject was asked to maintain the value of two of the three variables during the test, see Section 5. The third variable of perturbation was controlled by the excitation signal generated in the shaker. Signals of motion and force were measured simultaneously while the perturbation was producing vertical vibration. The raw signals were processed offline by selecting a specific period of each signal. The data processing algorithm was implemented in Matlab and can be found in Section A. Results are structured as following: data sets plots of measured signals and the results after processing for each test.

8.1. Transient dynamics

The natural motion of the arm is a continuous change of its state. In order to quantify the influence in conditions as close as possible to real environment, it has been measured the dynamic response during the transition of muscle tension level along the HAS and arm posture.

8.1.1. Muscle tension transition

In this test, the influence of the muscle tension change over time was studied. The subject performed sequentially different levels of muscle tension quantified through grip force and vertical force against the shaker while other variables were maintained as constant as possible. Perturbation frequency was set in a nominal value of 8 Hz and the HAS posture was 180° (arm extended). In Figure 8.1, it is shown the measurement of the dynamic response over time. In Figure 8.1(a), each level of muscle tension is represented through the grip force and excitation force. There are 5 levels corresponding to relaxed, normal, middle, middle-high and high muscle tension level. Only for this transient test, the test subject performed the muscle tension intuitively around 0, 25, 50, 75 and 100% since the set of a specific value required a large setting time and the test wouldn't be transient. In Figure 8.1(b), it is shown the excitation force which can represent the reaction force performed by the HAS. It can be noticed also the gradually increase of the reaction force simultaneously to the grip force. It can be identified some peaks between each muscle tension level in Figures 8.1 (a) and (b) which represented the setting period performed by the test subject. From 20s, the reaction force in (b) was difficult to maintain and higher deviations are presented.

In Figure 8.1(c),(e),(f), it is shown the acceleration response of each HAS element and in (d),(f),(g), it is shown its corresponding spectrogram. The spectrograms show that the motion amplitude decreased with each muscle tension level, even for the hand which had the same signal as the excitation signal. This behaviour shows a non-constant behaviour of the shaker excitation signal generation as the muscle tension increases. It was observed during the experimental tests,

some mechanical defects regarding this aspect that could also included short periods without excitation, see Section 9.4. Spectrograms also show how the significant frequency signals were from 4 to 15 Hz and each period of muscle tension level was not as constant as desired in its dynamic response. The transmissibility along the HAS for each muscle tension level was calculated as the division of the acceleration rms value and it is shown in Table 8.1. It can be seen that the transmissibility through the wrist increase significantly as the muscle tension increased while the transmissibility through the elbow decreased, with the exception of middle and middle high muscle tension level out of the tendency. However, it can be explained due to the non-constant muscle tension level from 20s shown in Figure 8.1(b).

Table 8.1.: Transmissibility during in a transient muscle tension in %

| Muscle tension | Wrist | Elbow |
|-----------------------|--------------|--------------|
| Relaxed | 49.67 | 72.51 |
| Normal | 59.00 | 64.45 |
| Middle | 73.62 | 57.92 |
| Middle-High | 60.45 | 64.92 |
| High | 70.77 | 56.82 |

8.1.2. Posture transition

In this test, the influence of the posture change over time was studied. The subject performed two different postures from 180°(arm extended) to 90° while the other variables were maintained. The level of muscle tension was maintained in a middle tension level with 50 % grip force as well as 50 % reaction force. The perturbation was set with a nominal value of 8Hz. In Figure 8.2, it is shown the measurement of the dynamic response over time. Figure 8.2 (a-b) shows the setting time of the subject to reach the desired grip and reaction force until 10s. It must be noticed that it was required more time to set a determine average value of reaction force in (b). Close to 19s, the test subject changed the position from 180 to 90. This transition was reflected in a slightly change of the grip and excitation force in 19s, not as significant as the previous case with an increase of the 25% of the muscle tension in Figure 8.1(b).

Likewise, in Figure 8.2(c),(e),(g), it is shown the acceleration response of each HAS element and in (d),(f),(h), it is shown its corresponding spectrogram. The spectrograms show that the forearm and upper-arm acceleration were significantly decreased from 19s during the posture transition, Figure 8.2(f) and (h), even when the excitation force maintained its amplitude almost constant as the hand acceleration, Figure 8.2(b),(d). The upper-arm was the most decreased as shown in Figure 8.2(h). In Figure 8.2(e) and (f), the forearm tended to decrease its acceleration but some peaks were found, especially from 25 to 30. This behaviour was also reflected in the excitation signal from 25 to 30s where there were some peaks slightly higher than around 19s.

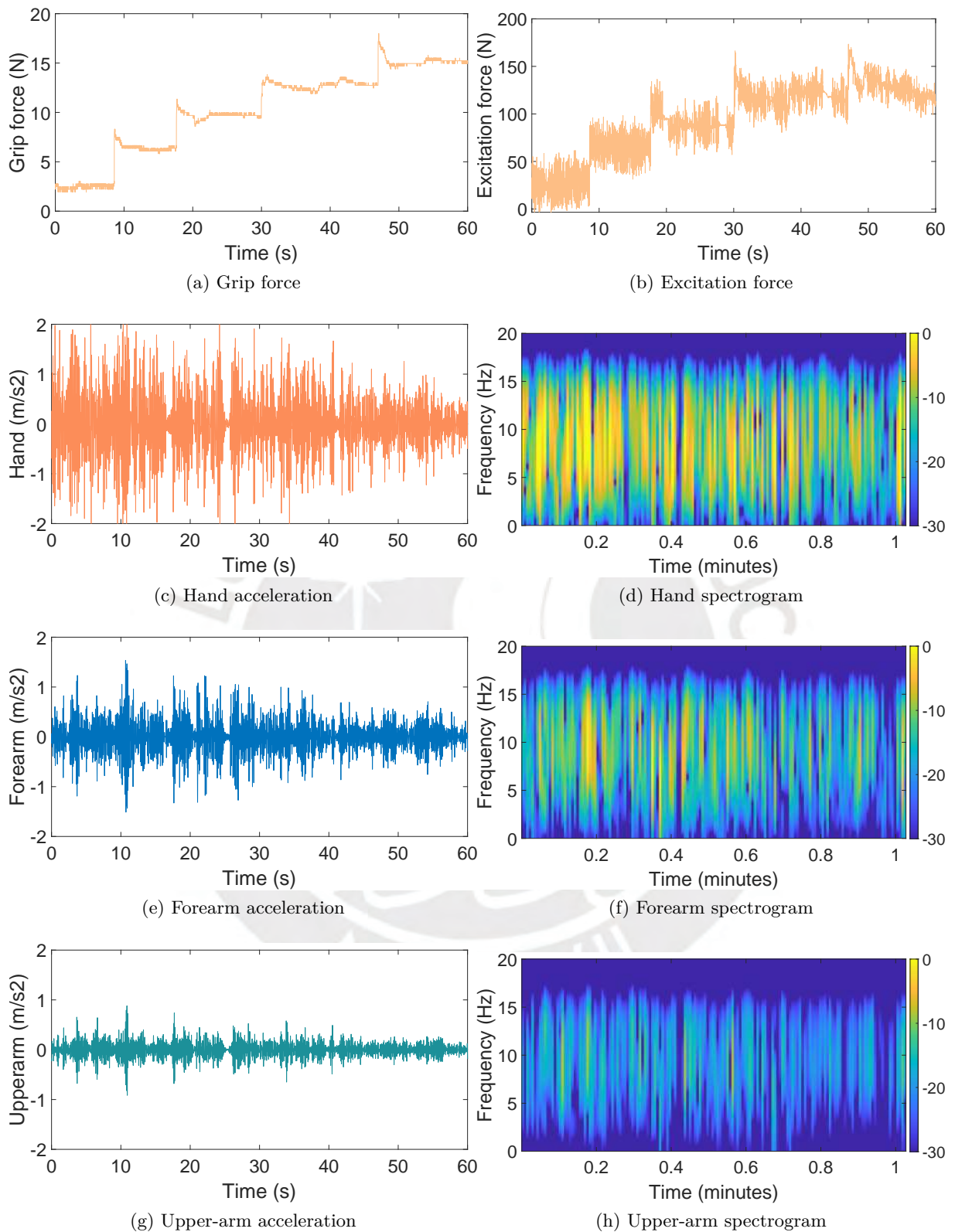


Figure 8.1.: Dynamic response to an excitation of 8Hz during a change of hand-arm-system muscle tension from relaxed to high tension level: (a-b) force measurement, (c-d) hand, (e-f) forearm (g-h) upper-arm acceleration and spectrogram

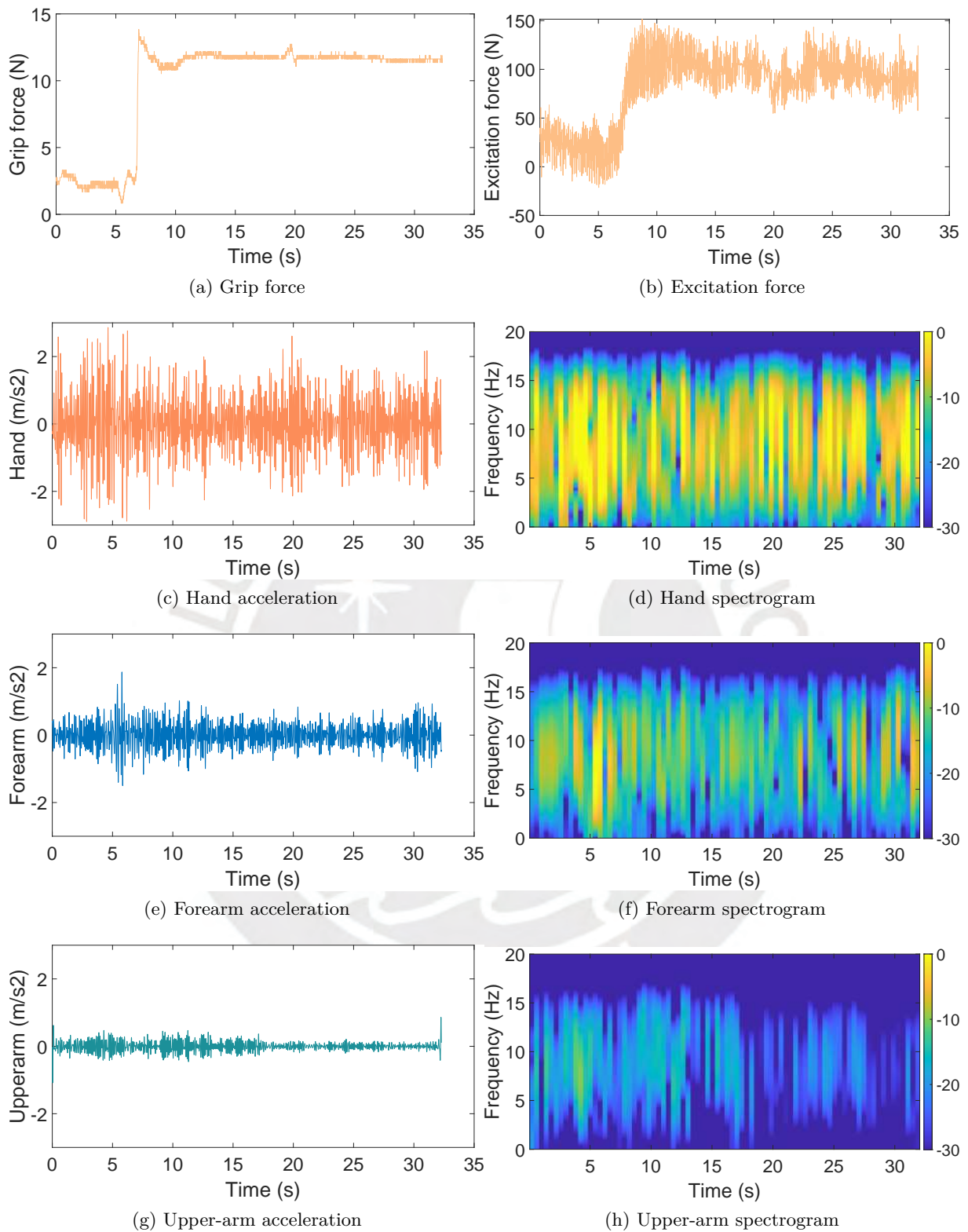


Figure 8.2.: Dynamic response to an excitation of 8Hz during a change of hand-arm-system posture from 180° to 90°: (a-b) force measurement, (c-d) hand, (e-f) forearm, (g-h) upper-arm acceleration and spectrogram

8.2. Grip force and posture influence

In contrast to the transient dynamics, the study of the variables influence was carried out with stationary data after a setting time period where the test subject manages a desired condition. A period of 5s where the dynamic response was as stationary as possible is selected for the analysis in each test. Two postures are evaluated according to the protocol in Table 7.1. For each posture, a relaxed condition for the reaction force was tried to maintain. Other reaction force was not tested due to the physical difficulty of manage and maintain a reaction force. A perturbation of 6Hz was used for all the tests in this section as an average condition in the available range. Different muscle tension level through the grip force was produced by the test subject between pauses of 5 minutes.

Raw signals were processed and the dynamic response of an average condition with a grip force 50% and posture 90° is shown in Figure 8.3. The other datasets of the complete test are shown in Section B. In Figure 8.3(a) and (b), it is shown the grip force and the excitation force over time. It can be seen that the grip force was almost constantly maintained while the excitation force presented some amplitude changes over time. Figures 8.3(c),(e) and (g) show the acceleration response over time and (d),(f) and (h) show the frequency spectrum of each signal. The acceleration signals were divided by the rms value of the excitation force in order to have a comparison between cases without the influence of the increase an increase of the excitation force. Figure 8.3(d) shows the frequencies range that are presented in the shaker excitation signal. A nominal value of 6Hz was established; however, more frequency peaks were found around 6Hz with the highest peak around 8.6 Hz. It must be noticed that the acceleration response decreased along the HAS and the lowest value was found in the upper-arm as expected. Frequency spectrum also show that there were many peaks in the upper-arm spectrum. It was observed during the experiment that the sensor placed on the upper-arm was influence significantly by the skin motion. These different frequencies signals presented in each signal show the non-linearity of each condition.

In Figure 8.4, it is shown the dynamic response with a grip force of 50% and a posture of 180° . Figure 8.3(a) shows the grip force over time which was also almost constant. Figure 8.3(b) shows the excitation force over time. It can be noticed that the posture 180° showed almost the double value of the excitation forces measured in the posture 90° case. This behaviour shows how the same test subject can not control a relaxed reaction force as well as the grip force. Figures 8.4(d) shows the hand acceleration spectrum, where the highest peak is presented around 3Hz. It can be noticed that it is significantly different to the posture 90° case. Figures 8.4(c),(e) and (g) show the acceleration response over time and (d),(f) and (h) show the frequency spectrum of each signal. In this case, the upper-arm spectrum presents lower peaks than the posture 90° .

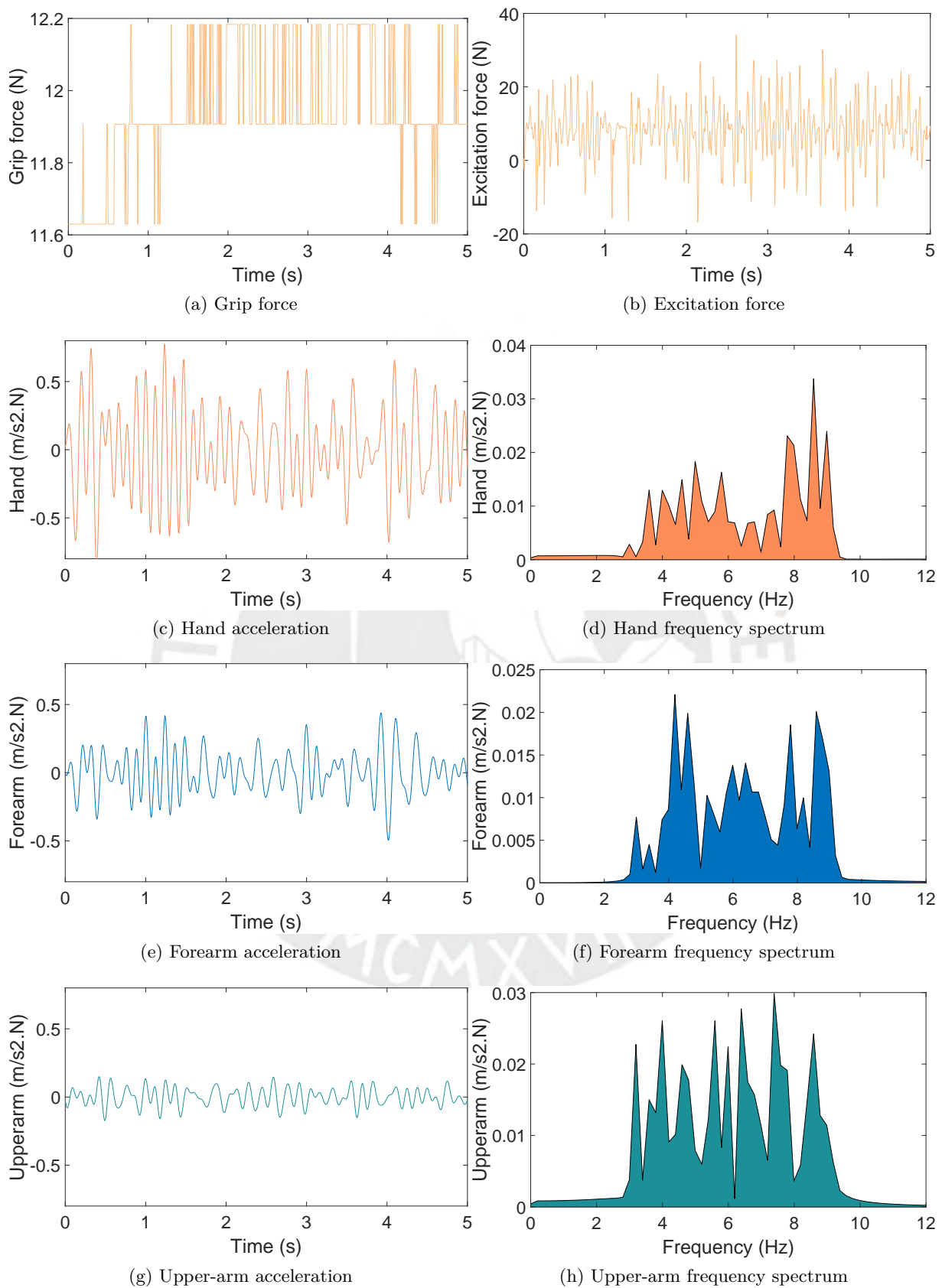


Figure 8.3.: Dynamic response during a 50% grip force condition with 90° posture: (a-b) force measurement, (c-d) hand, (e-f) forearm, (g-h) upper-arm

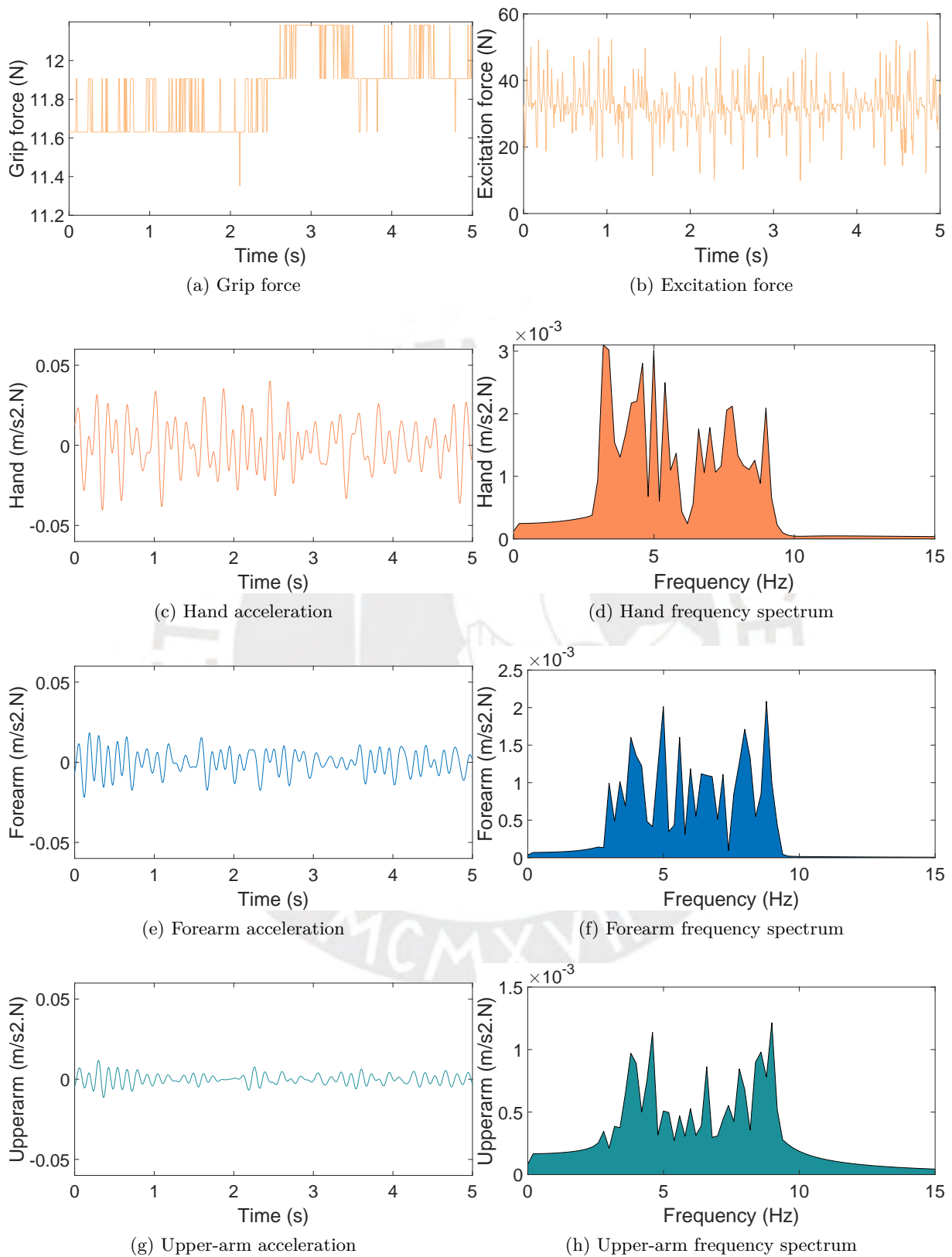


Figure 8.4.: Dynamic response during a 50% grip force condition with 180°: (a-b) force measurement, (c-d) hand, (e-f) forearm, (g-h) upper-arm

Influence on the dynamic response

The dynamic response for each grip force condition and posture is summarized in Figure 8.5 with the acceleration value calculated as the rms of the signal for hand, forearm and upper-arm acceleration. It can be seen that the highest acceleration were found in the posture 90° case. In these graphs, a higher negative slope shows lower transmissibility through each wrist and elbow joint. The highest transmissibility were found in the highest muscle tension level in both postures. This behaviour was also reflected during the transient dynamics in Table 8.1. In both postures, it can be seen a general tendency to decrease the acceleration response as the grip force increased. In posture 90° case (a), there were grip force conditions out of tendency. On the other hand, in posture 180° case (b), grip force 50 and 75% were out of tendency. Figure 8.6 shows the frequency spectrum of each grip force condition. Frequency spectra showed also the lowest acceleration values in the highest grip force condition. It can be seen the different frequencies peak presented in each case around the nominal excitation frequency of 6Hz. The peaks position in each spectrum shows that these different frequencies had the origin in the shaker excitation signal, which is equal to the hand spectrum.

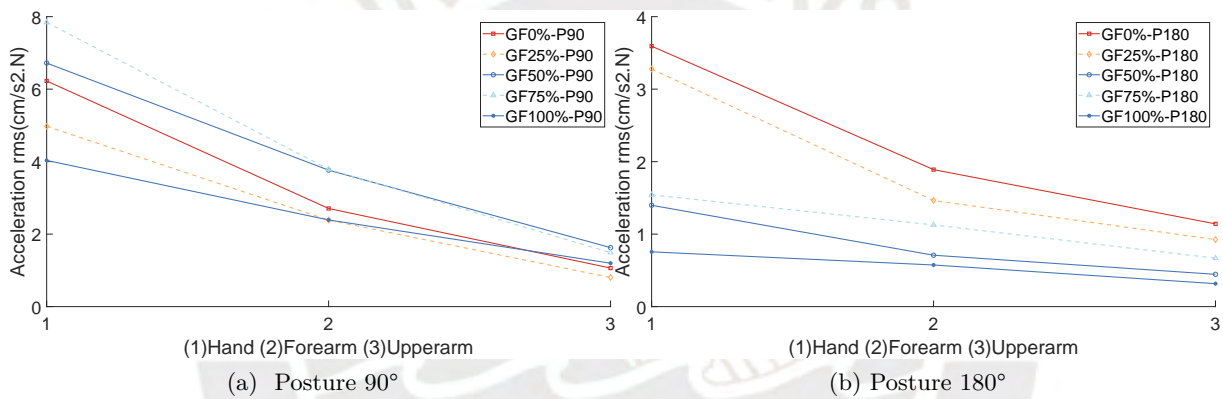


Figure 8.5.: Influence of the grip force on the acceleration response along the hand-arm-system with a posture (a) 180° and (b) 90°

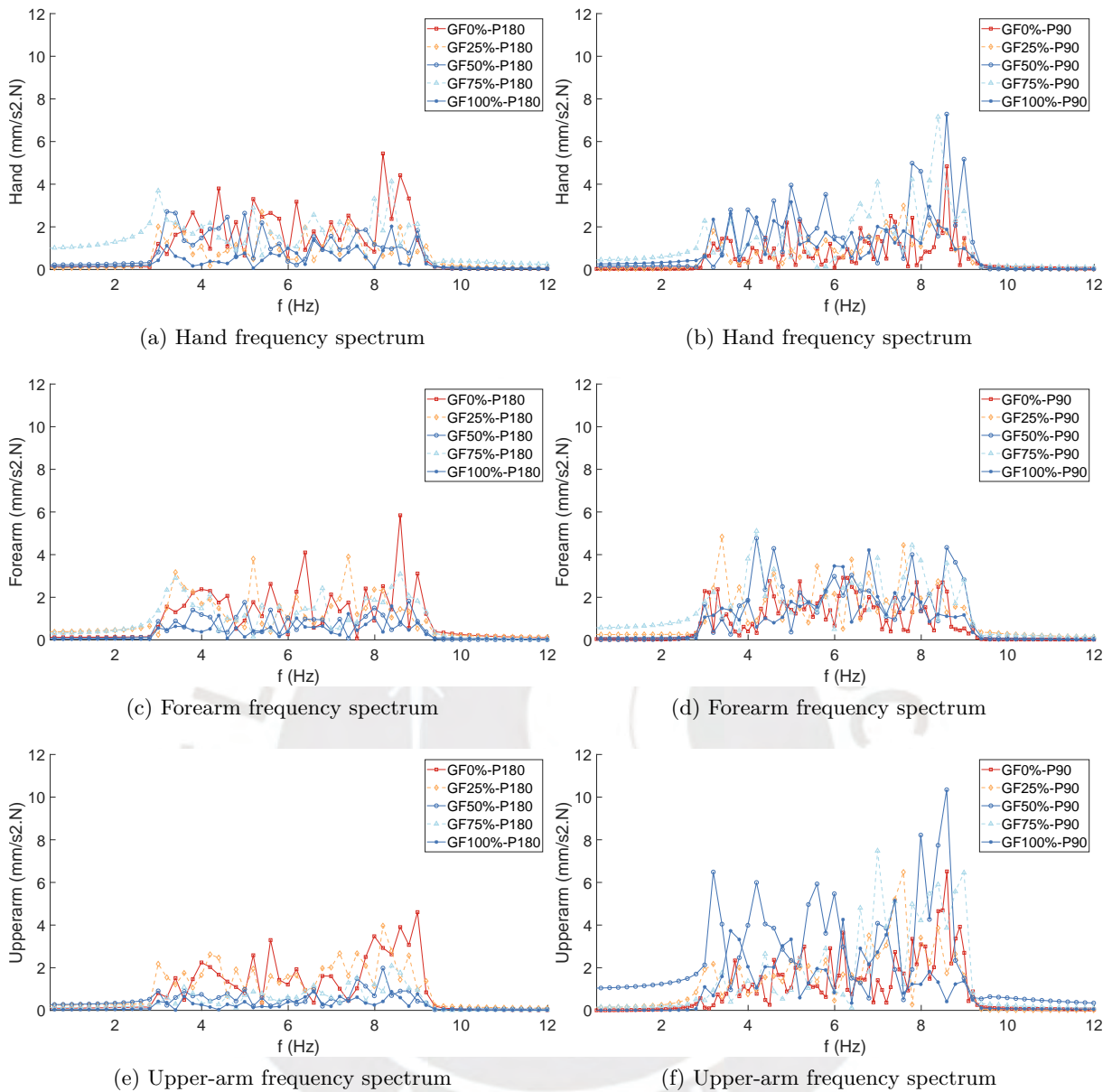


Figure 8.6.: Influence of the grip force on the frequency spectrum along the hand-arm-system with a posture of (a), (c), (e) 180° and (b), (d), (f) 90°

8.3. Frequency influence

The dynamic response of the test subject was measured with a grip force of 50 % and a reaction force of 0% (as close as possible to relaxed condition) and the HAS posture was set in 180°. Three values of perturbation frequency were tested while the other variables were fixed. The stationary period of the dynamic response was selected for the analysis. Figure 8.7 shows the dynamic response for each perturbation. In (a), it can be noticed that the acceleration magnitude increases as the perturbation frequency decreases, where the highest value was reached with 3Hz. The frequency spectra in (b), (c) and (d) show this behavior in detail. During experiments, it was observed that shaker performance tended to produce an excitation around the nominal value as shown in (b), where the hand is fixed to the shaker motion and its reflected in the forearm and upper-arm, (c) and (d) respectively. However, these peaks were not necessarily presented on the whole time simple and are not reflected in the rms value of the whole signal in (a).

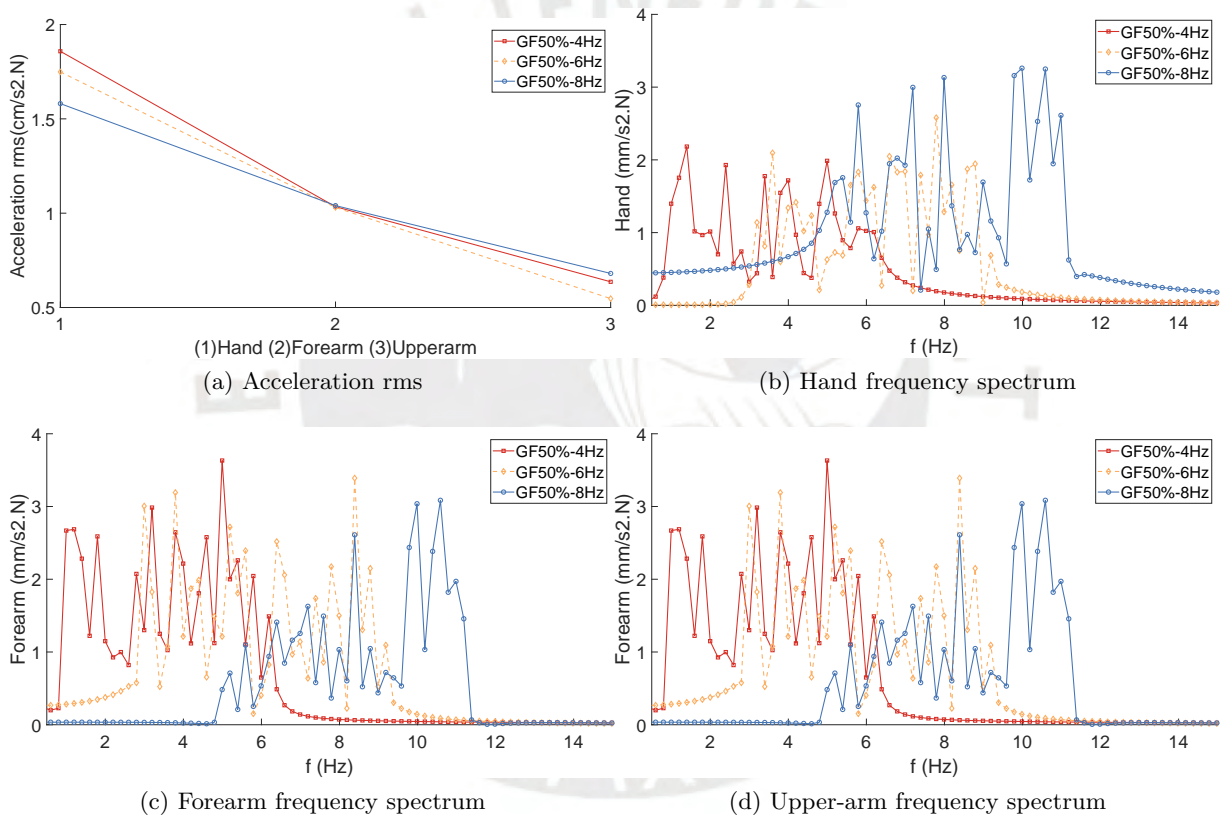


Figure 8.7.: Influence of the perturbation frequency on the dynamic response the hand-arm-system with a posture of 180°, (a) acceleration in rms, (b), (c) and (d) the frequency spectrum of the acceleration signal of hand, forearm and upper-arm respectively

8.4. Estimation of dynamic parameters

A first approach to the estimation of the dynamic parameters based on analytic model elaborated in Section 5 was carried out. The analytical model allows to modify the geometry of the hand-arm-system for each posture either 180° or 90°. A linearization of the model was performed around the specific positions. The motion and force signals measured in each condition of grip

force, posture and perturbation were used for the determination of the stiffness and damping of the wrist, elbow and shoulder. Due to the non-linear characteristics of the arm behavior, a specific time period of motion of each dataset was selected for the identification algorithm. It was selected a time period as stationary as possible. The estimated dynamic parameters of the test subject are shown in Table 8.2. If the grip force is isolated, it can be noticed that the stiffness value of each joint tends to increase as the grip force increases. The wrist stiffness was the most influenced value by the grip force. Table 8.3 shows the estimated natural frequencies of the HAS calculated with the biomechanical model and the stiffness values. It can be identified that the lowest natural frequency corresponded to a modal shape with mainly the rotation of the arm with respect to the shoulder while the highest natural frequency corresponded to the rotation of the hand with respect to the wrist. It also shows that the increase of the grip force slightly impacts to the first and second frequency; however, it impacts significantly on the third frequency.

Table 8.2.: Estimated joint stiffness and damping for each condition

| Condition | k (Nm/rad) | | | c(Nm.s/rad) | | |
|-----------------|------------|-------|-------|-------------|-------|-------|
| | Shoulder | Elbow | Wrist | Shoulder | Elbow | Wrist |
| GF 0% - P 90 | 2.2 | 32.7 | 21.9 | 9.5 | 9.9 | 0.3 |
| GF 25% - P 90 | 7.6 | 39.6 | 36.4 | 15.5 | 18.4 | 1.6 |
| GF 50% - P 90 | 10.3 | 24.6 | 38.8 | 17.7 | 15.9 | 2.6 |
| GF 75% - P 90 | 4.1 | 20.9 | 52.8 | 18.9 | 20.5 | 1.2 |
| GF 100% - P 90 | 9.2 | 30.1 | 76.4 | 8.1 | 18.1 | 11.8 |
| GF 0% - P 180 | 22.5 | 39.2 | 15.1 | 4.6 | 10.1 | 3.1 |
| GF 25% - P 180 | 26.4 | 48.5 | 30.7 | 4.5 | 14.7 | 8.4 |
| GF 50% - P 180 | 28.5 | 33.3 | 29.2 | 4.6 | 14.9 | 12.3 |
| GF 75% - P 180 | 29.4 | 44.7 | 42.4 | 4.9 | 8.4 | 10.1 |
| GF 100% - P 180 | 28.8 | 45.3 | 55.9 | 4.8 | 13.3 | 8.8 |

Table 8.3.: Estimated natural frequencies for each condition with a posture 180°

| Condition | 1st (Hz) | 2nd (Hz) | 3rd (Hz) |
|-----------------|----------|----------|----------|
| GF 0% - P 180 | 1.10 | 7.54 | 20.79 |
| GF 25% - P 180 | 1.19 | 8.68 | 28.55 |
| GF 50% - P 180 | 1.21 | 7.49 | 27.41 |
| GF 75% - P 180 | 1.25 | 8.57 | 32.92 |
| GF 100% - P 180 | 1.24 | 8.68 | 37.47 |

9. Discussion

9.1. Setup prototype performance

The materialized concept for performing the method was able to quantify the different conditions of the hand-arm-system (HAS) under the presence of vibrations. The validation of the measurement setup developed was carried out through the measurement of the dynamic response of a test subject and a characterization with the experimental data obtained with the setup. This characterization was focused on the estimation of the main variables influence previously defined in Chapter 5 for a test subject.

The first test that verified the different ranges of dynamic response measurement was the transition state, which is a close behaviour to the natural motion, where the characteristics of the HAS are continuously adapting to the instant requirements. In a muscle tension transition, the transient influence on the dynamic response could be effectively measured. The setting time in the grip force and excitation force showed the measured short period, where the HAS tried to reach the desired state while the system was retro-alimented by feedback provided by the natural senses of the test subject and a correction signal is performed through the actuators of the HAS, in this case, the local muscle tension that produced the grip force.

In stationary tests, where conditions are maintained as stationary as possible, the prototype was also able to quantify the change produced by the variation of the muscle tension, posture and perturbation as selected variables of this study. The selection of these parameters were made by the assumption that they were the most significant variables in the natural performance of motion in the HAS. The measured influence of each variable verified the assumption of the variables selection in Chapter 5.

The grip force was limited to 25N as maximal due to mechanical behaviour of the PLA elements of the measurement device in the prototype since it was found a significant deformation from this value of force. This also impacted on the measurement of the grip force since the force measurement with the type of sensor used depends on the deformation produced to it. If the sensor base is deformed, as in this case, part of the grip force is addressed to maintain the deformation state of the instrument is not measured by the sensor. Previous research has measured the range of grip force in group and established values until 700N Nilsen et al. (2012). In this sense, in next versions of the device, selection of materials with high stiffness and low weight as the aluminum alloy is required.

Adjustment of the lever was necessary in order to produce a comfortable grip action for the hand. This depended on the test subject characteristics. It could be adjusted by the length of the force sensor at the top. However, a more sophisticated mechanism should be implemented for an adjustment without the need of hand tools before each measurement. This would be also a design requirement for next versions.

It must be noticed that the non desired mechanical performance in presence of vibrations of the measurement setup was produced by the characteristics of the existent equipment used. The existent equipment was not specific acquired for the setup working range. In this line, the mechanical performance was not as good as desired. Although a nominal frequency was

set, the shaker provided a range around the nominal value, behaviour that is not stationary and introduces non-linearity to the HAS dynamic response. This behaviour can be seen in the frequency spectra in Figure 8.6, where different frequency peaks were manifested in the hand acceleration signal. Hand acceleration signal also represents the acceleration signal of the excitation from the shaker since hand and measurement device are fixed, Figure 7.4. Therefore, the different peaks were originated in the shaker. Likewise, it can be seen in the results a non-linearity behavior, natural to the HAS as expected, in transient and stationary dynamics. This complicated the maintaining of each condition during the tests. Results in Figure 8.4(b) and 8.3(b) can illustrate how difficult the maintain of the reaction force could be for a test subject. In this sense, it is important to produce a well controlled behaviour of the shaker as stationary as possible.

In conclusion, the concept of the measurement setup fulfils the list of requirements established and allows the quantification of the vibration characteristics of the HAS; however, the implementation of a more sophisticated shaker and a manufacturing of the measurement device with higher stiffness material is crucial for further analysis and tendencies quantification.

9.2. Characterization method

Part of the development was the establishment of the characterization method of the HAS's dynamic behaviour under presence of vibration. The experimental results showed that the HAS can be effectively quantified through its dynamic response and a bio-mechanic model can be elaborated with the experimental estimation of its parameters.

The motion response is the expression of how the system responses to a determined excitation input. Through the measurement of the these variables of motion under different conditions, the method was able to quantify the influence of a determined condition. The strategy of each selected variable isolation was correct. Figure 8.6 showed how the local muscle tension is closely related to the dynamic response. This corresponded to the anatomic study of the HAS where each group of muscles are addressed to the control determined DoF of the HAS Gerhard (2010).

The experimental results also showed that the test subject tends to increase in each case the muscle tension along the whole HAS unintentionally and required a setting time to isolate only the grip action, Figure 8.1(a). The influence of the muscle tension was not only a local phenomenon, but also tended to impact to the dynamic response of the forearm and upper-arm with a lower intense and vice versa, as shown Figure 8.5(b). This behaviour depended on the quality of control of the test subject. Due to the high setting time (difficult isolation) of the muscle tension that produces grip force from the muscle tension that produces the reaction force against the shaker, the transient dynamic response was preferred in the method to be more intuitive than managing the exact force percentage. In this transient case with sequential force increment, it was easier for the test subject to increase the muscle tension along the whole arm, this involves grip and reaction force (also measured as excitation force) in parallel instead only the grip force while isolating the reaction force.

Once the dynamic response was measured, the method allowed a system identification of the dynamic parameters which govern the response of the HAS. The fact that the HAS can be represented through a biomechanical model with its fundamental parameters experimentally determined allows the explanation of the dynamic behaviour through them. In this sense, the prediction of the response to different conditions is possible. This is specially useful for the study of tremor behavior and the design of assisting devices that could improve the motion control in presence of pathological conditions. Vibration absorption devices developed in the literature,

see Section 3.2, could use specific dynamic parameters for the design calculations and numerical simulation. Due to the high non-linear behaviour of the HAS, optimization of tremor absorption devices for specific posture and muscle tension conditions is also possible, specially for passive device solutions which are unable to be adapted and active devices which must be optimized to reduce its volume Mo & Priefer (2021).

9.3. Vibration characteristics of the hand-arm-system

The dynamic response of the (HAS) depends on its own parameters and any external conditions due to its biologic and non-linear nature which allows its adaptability to the physical task requirements. In this research, it was proposed the study of the response of the HAS under controlled conditions as a method to characterize its dynamic behavior. The characterization was focused on the influence of three variables: muscle tension, posture and perturbation. Each variable corresponded to a specific study detailed in Section 7.2, designed to quantify the dynamic response change which is produced by a change of each variable. Results have demonstrated that these variables have a significantly influence on how the dynamic response is produced and strategy of each variable isolation can explain the mechanics of its influence.

The influence of these different conditions were manifested on tangible variables that can be measured directly as the dynamic response as shown in Figure 8.5. Additionally to this, a more quantitative and systematic relation can be explained from a biomechanical perspective through the use of the estimated dynamic parameters after the system identification process, Table 8.2. These parameters conform the mechanical impedance of system as the stiffness which quantifies force value required to produce a deformation of the system, an action that is controlled by the muscle tissue net.

In the study of the transient behaviour, frequency domain analysis as frequency spectrum and spectrogram provided useful information for identifying a change in a signal over time. Thus it was used for the quantification of the influence in the transition period of muscle tension and posture. In a transition condition, in contrast to a steady state, the characteristics of the HAS were setting until they found a dynamic balance. The subject continuously tried to set the characteristics with the feedback provided by the senses. This behaviour was shown in Figure 8.1 and 8.2 were a short setting period was identified in each change. In a muscle tension transition, the increase of both grip and reaction force, which represented the whole muscle tension level, produced a decrease of the dynamic response. The transmissibility in Table 8.1, calculated as the rate between the rms values of acceleration signals shows this behaviour. The wrist transmissibility was the lowest in a relaxed condition where there is a high difference between hand and forearm acceleration and the highest in a high muscle tension since the whole HAS tends to behave as one rigid body with the acceleration proportional to the distance to the rotational center, in this case the shoulder. This behaviour also corresponded to the findings for each stationary case of muscle tension level in Figure 8.5 where the transmissibility can be represented as the slope between hand-forearm and forearm-upperarm.

In the case of a posture transition in Figure 8.2, it is shown the spectrogram of the acceleration during the transition of the posture from 180° to 90° from 19s. The dynamic response of the HAS during a transition of the posture shows that there is a significant decrease of the vibration amplitude (measured as the vector projection in the vertical axis) as flexion angle of 90° is reached. The acceleration of the upper-arm was the most influenced and decreased since the position of 90° is almost fixed for the upper arm during a perturbation in the vertical direction. The parallelism between the perturbation force and the upper arm reduces the presence of

torques at the shoulder joint. Then, only wrist and elbow joints works and the dynamic response depends mainly on them.

In the stationary study of the muscle tension, quantified through the grip and reaction force produced by the HAS. As a general tendency, there was a significant decrease of the acceleration amplitude in the whole dynamic response as the muscle tension increased. This was clearly identified in Figures 8.5(a) and (b). However, there were some cases out of tendency, especially in Figure 8.5(a). The out of tendency cases were due to the difficulty of the local muscle tension of the grip force isolation and the non-intentional increase of the reaction force produced by the rest of the HAS which corresponded to a higher stiffness of the system. This demonstrated that the dynamic response depended on the mechanical impedance of the whole system. Likewise, the production of grip forces over 50% tended to produce fatigue on the test subject arm, which decreased the quality of control over the muscle tension and posture. Additionally to this, the non-linearity introduced by the shaker, as explained in the Section 9.1, makes a stationary value of muscle tension and posture more difficult to maintain. This behaviour can be seen in the excitation force signal, which represents also the reaction force, Figure 8.4 and Figure 8.3. More excitation forces behaviour can be found in the Appendix, Section B. Therefore, all the non-controlled conditions could impact each particular case with the posture 90° , especially the reported fatigue along the hand-arm-system reflected in low values of elbow stiffness in Table 8.2 despite the high grip force.

The study of the perturbation frequency quantified the lower excitation frequencies produced higher values of dynamic response, represented by the acceleration value in rms, Figure 8.7. This behaviour can be explained with the fact the lower frequencies are close to first natural frequencies, which are characterized by higher amplitudes. This finding shows the importance of a characterization of the HAS in low frequency conditions, in contrast with studies in occupational diseases where excitation frequencies from tools and machines are commonly high. The frequency spectra, in general, showed how peaks of different frequencies were manifested. Some of them, specially the farthest from the nominal value, only appeared for short moments during the experiment and its contribution is not reflected in the acceleration rms which evaluates the complete signal.

A first approach to the dynamic parameters estimation was carried out with the data from the stationary tests of the grip force study. In terms of dynamic parameters of the biomechanical model, there was a clear increase tendency of the system stiffness as the muscle tension increases for the posture 180° in Table 8.2 . In this context the system stiffness can be represented as joint stiffness in the wrist, elbow and shoulder since these joints represent the DoF of motion Gerhard (2010), more detail can be found in Chapter 2. The estimated stiffness values were consistent with the ranges reported in previous study oriented to a static condition Kistemaker et al. (2007) and a study of the stiffness during a reflex period Zhang & Rymer (1997). Numerical values were also consisted to the reported in a dynamic study in Piovesan et al. (2013) where the posture was different, but the flexion motion of the forearm was similar to the test configuration carried out in this work. The shoulder stiffness estimated for the posture 90° in Table 8.2 was affected to the relative motion between the skin and bone found in this vertical position of the upper-arm. In this sense, it makes sense that the model estimates small values since the motion corresponds to the flexible skin.

The estimated natural frequencies showed that the HAS has a low frequency behaviour as expected. The posture 180° corresponded essentially to a modal shape with a rotational motion with respect to the shoulder. In presence of a high wrist stiffness due to a high muscle tension, the more flexible motion was with respect to the shoulder. The natural frequencies in a low frequency also corresponded to the frequency study in Figure 8.7, where the highest amplitudes

are found close to low frequencies. The low frequency behaviour and modal shapes corresponds to the first modes of vibration calculated with FEM simulations in Adewusi et al. (2014). However, the numerical values are significantly different. Since the muscle tissues properties and geometric distribution are highly non-linear and non-isotropic, the numerical results of the FEM simulation are not comparable, but qualitatively the tendency is the same. Other studies as in Aldien et al. (2006) and Wu et al. (2022) have quantified the transmissibility showing natural frequencies in a high frequency range due to the experimental procedure in a rigid direction as the excitation force in the the direction of the HAS axis.

9.4. Observations and limitations

Regarding the experimental part, the inherent relation of the muscle tension along the hand-arm-system made the isolation of the variables difficult to maintain. An increase of grip force tends to also produce an increase of the muscle tension level along the arm. This was noticed on the increase of the reaction force performed again the shaker. This behaviour was a special characteristic during the measurement of a transition condition. The skin motion could affect the measurement of the acceleration and angular velocity signals with the IMUs, specially in other planes additional to the vertical plane.

During the experiments, it was found the applying high grip forces can produce fatigue of the test subject arm and the quality of the variables control as muscle tension can be affected, which is part of the variables isolation strategy, needed for the quantification of the influence

Regarding the performance and limitations of the measurement setup implementation, the use of existent components and instrument were sometimes not in the work range. Then, it can be expected a dynamic behaviour as not accurate as it should be with components specially selected for the work range. A well controlled excitation signal from the shaker was possible only for higher frequencies due to the large frequency range of the shaker. However, this study corresponded to a low frequency range until 8 Hz. The actuator of the system didn't produce a excitation signal as stationary as desired.

The characterization method was designed to perform in a vertical plane. However, the shaker internal bearing was not as accurate as expected. There were also components of motion in a 3D space. This behavior could affect directly to the calculation of the dynamic parameters since the bio-mechanic model was developed in a vertical plane as assumption.

The validation of the measurement setup was carried out with polymer materials due to manufacturing limitations. Polymer materials showed a significant deformation which could impact on the measurement of the grip and excitation force over time. Ideally, the components should be made by aluminum alloy for its mechanical strength and light weight relation. The shaker for the case posture 90° did not have a stable frame since the lifting platform manifested perceptible vibrations and could have affected the measurement with the accelerometers that are very sensitive.

10. Conclusions and Outlook

It was proposed a method for the characterization of the hand-arm-system dynamics during vibration conditions and a measurement setup was developed in order to carry out the method. This measurement setup was evaluated through a first approach to the experimental characterization of the hand-arm-system with data from a test subject in transient and stationary dynamics studies. The performance of the measurement setup showed that it is able to quantify the dynamic response under different conditions of muscle tension, posture and perturbation.

The experimental procedure demonstrated that the characterization method can effectively quantify the influence of the specific conditions on the dynamic response. The experimental procedure was implemented in Matlab in order to carry out the measurements and use the measured data to estimate the parameters of a hand-arm-system biomechanical model. The estimated dynamic parameters in this first approach with one test subject were consistent with values and tendencies reported in previous studies. It was found in the experimental part significant level of non-linear behaviour. The isolation of variables strongly depended on the quality of control produced by the test subject.

As a first approach to the quantification of the vibration characteristics, tendencies in the dynamic behavior were obtained and showed that the muscle tension, posture and perturbation frequency have a significant influence on the dynamic response. As a tendency, the increase of the muscle tension, in terms of the biomechanical model, increases the stiffness of the hand-arm-system joints. The perturbation frequency study with a posture of 180° (extended arm) reported that higher acceleration magnitudes are produced by lower perturbation frequencies. This behaviour corresponded to the proximity to the estimated natural frequencies which were found within a low frequency range from 1.1 to 8.7 Hz (first two natural frequencies). The estimated stiffness and damping along the mass of the hand-arm-system provide a deep comprehension of the mechanical impedance in a specific condition.

Further measurement of different groups of people is necessary in order to quantify average values of the hand-arm-system impedance. Large ranges of variable conditions should be evaluated as well as the entire range of possible grip force. This information could provide useful data not only for the development of tremor absorption devices which requires models for numerical simulation and optimization, but also as an indicator of the hand-arm-system state. A next version should be carried out with sturdier implementation of the measurement setup with components specially selected in the working range in order to reduce mechanical deformations and possible sources of errors. Sophisticated system identification procedures can be also carried out without the simplification of 2D motion as well as non-linear analytical models.

Bibliography

- Adewusi, S., Thomas, M., Vu, V. H. & Li, W. (2014), 'Modal parameters of the human hand-arm using finite element and operational modal analysis', *Mechanics and Industry* **15**, 541–549.
- Aldien, Y., Marcotte, P., Rakheja, S. & Boileau, P. E. (2006), 'Influence of hand-arm posture on biodynamic response of the human hand-arm exposed to zh-axis vibration', *International Journal of Industrial Ergonomics* **36**, 45–59.
- Basaraba, S. (2024), 'Measuring grip strength for health'. Accessed: 2024-06-5.
URL: <https://www.verywellhealth.com/what-is-grip-strength-2224061>
- Bhatia, K. P., Bain, P., Bajaj, N., Elble, R. J., Hallett, M., Louis, E. D., Raethjen, J., Stamelou, M., Testa, C. M. & Deuschl, G. (2018), 'Consensus statement on the classification of tremors. from the task force on tremor of the international parkinson and movement disorder society', *Movement Disorders* **33**, 75–87.
- Dempster, W. T. & Gaughran, G. R. (1967), 'Properties of body segments based on size and weight', *American Journal of Anatomy* **120**, 33–54.
- Deuschl, G., Raethjen, J., Hellriegel, H. & Elble, R. (2011), 'Treatment of patients with essential tremor', *The Lancet Neurology* **10**, 148–161.
- Diaz, N. L. & Louis, E. D. (2010), 'Survey of medication usage patterns among essential tremor patients: Movement disorder specialists vs. general neurologists', *Parkinsonism and Related Disorders* **16**, 604–607.
- Earthlabs (2019), 'Ulna bone'. Accessed: 2024-06-15.
URL: <https://www.earthslab.com/anatomy/ulna/>
- Fayyad, S. M., Salam, A., Alsabagh, Y., Al-Rawashdeh, M. O., Alsabagh, A. S. & Rawashdeh, M. O. (2020), 'Research on the estimation of natural frequency of mechanical structures, machines, automobiles and bio-systems', *International Journal of Mechanical and Production* .
- Fivemicrons (2021), 'Tremelo'. Accessed: 2023-07-10.
URL: <https://fivemicrons.com/tremelo/>
- Formica, D., Charles, S. K., Zollo, L., Guglielmelli, E., Hogan, N. & Krebs, H. I. (2012), 'The passive stiffness of the wrist and forearm', *J Neuro-physiol* **108**, 1158–1166.
- Fromme, N. P., Camenzind, M., Riener, R. & Rossi, R. M. (2020), 'Design of a lightweight passive orthosis for tremor suppression', *Journal of NeuroEngineering and Rehabilitation* **17**.
- Gerhard, A. (2010), *Anatomie*, Vol. 2, 2 edn, Thieme.
- Herrnstadt, G. & Menon, C. (2016), 'Voluntary-driven elbow orthosis with speed-controlled tremor suppression', *Frontiers in Bioengineering and Biotechnology* **4**.

- Hosseini, R., Firoozbakhsh, K. & Naseri, H. (2014), 'Optimal design of a vibration absorber for tremor control of arm in parkinson's disease'.
- Kaiser, A. (2018), *Modellierung maximaler menschlicher Muskelmomente auf Basis digitaler Menschmodelle : am Beispiel der oberen Extremitäten*, Technische Universität Chemnitz.
- Kistemaker, D. A., Soest, A. J. V. & Bobbert, M. F. (2007), 'A model of open-loop control of equilibrium position and stiffness of the human elbow joint', *Biological Cybernetics* **96**, 341–350.
- Kuchenbecker, K. J., Park, J. G., Niemeyer, G. . U., Kuchenbecker, K., Park, J. & Niemeyer, G. (2003), 'Characterizing the human wrist for improved haptic interaction', *Proceedings of IMECE'03* .
- Lang, G. F. & Snyder, D. (2001), 'Understanding the physics of electrodynamic shaker performance'.
- Lukšys, D., Jonaitis, G. & Griškevičius, J. (2018), 'Quantitative analysis of parkinsonian tremor in a clinical setting using inertial measurement units', *Parkinson's Disease* **2018**.
- Matsumoto, Y., Seki, M., Ando, T., Kobayashi, Y., Nakashima, Y., Iijima, H., Nagaoka, M. & Fujie, M. G. (2013), 'Development of an exoskeleton to support eating movements in patients with essential tremor', *Journal of Robotics and Mechatronics* **25**, 949–958.
- Messsysteme (n.d.), 'Druck kraftmessdose'. Accessed: 2024-06-15.
URL: <https://www.me-systeme.de/de/km26z-20n>
- Mo, J. & Priefer, R. (2021), 'Medical devices for tremor suppression: Current status and future directions', *Biosensors* **11**.
- Morrison, S., Kerr, G. & Silburn, P. (2008), 'Bilateral tremor relations in parkinson's disease: Effects of mechanical coupling and medication', *Parkinsonism and Related Disorders* **14**, 298–308.
- Napier, J. (1956), 'The prehensile movements of the human hand'.
- Nilsen, T., Hermann, M., Eriksen, C. S., Dagfinrud, H., Mowinckel, P. & Kjeklen, I. (2012), 'Grip force and pinch grip in an adult population: Reference values and factors associated with grip force', *Scandinavian Journal of Occupational Therapy* **19**, 288–296.
- Pappalardo, C. M. & Guida, D. (2018), 'System identification and experimental modal analysis of a frame structure', *Engineering Letters* .
- Piovesan, D., Pierobon, A., Dizio, P. & Lackner, J. R. (2013), 'Experimental measure of arm stiffness during single reaching movements with a time-frequency analysis', *J Neurophysiol* **110**, 2484–2496.
- Puschmann, A. & Wszolek, Z. K. (2011), 'Diagnosis and treatment of common forms of tremor', *Seminars in Neurology* **31**, 65–77.
- Reynders, E. (2012), 'System identification methods for (operational) modal analysis: Review and comparison', *Archives of Computational Methods in Engineering* **19**, 51–124.
- Rincon, C. & Alencastre, J. (2023), 'Analytical modelling of a dynamic vibration absorber for parkinson disease', *60th Ilmenau Scientific Colloquium* .

- Rincon, C., Alencastre, J. & Rivera, R. (2023), ‘Analytical modelling of an active vibration absorber for a beam’, *Mathematics* **11**.
- Rocon, E., Andrade, A. O., Pons, J. L., Kyberd, P. & Nasuto, S. J. (2006), ‘Empirical mode decomposition: A novel technique for the study of tremor time series’, *Medical and Biological Engineering and Computing* **44**, 569–582.
- Rocon, E., Belda-Lois, J. M., Ruiz, A. F., Manto, M., Moreno, J. C. & Pons, J. L. (2007), ‘Design and validation of a rehabilitation robotic exoskeleton for tremor assessment and suppression’, *IEEE Transactions on Neural Systems and Rehabilitation Engineering* **15**, 367–378.
- Rudraraju, S. & Nguyen, T. (2018), ‘Wearable tremor reduction device (trd) for human hands and arms’, *Proceedings of the 2018 Design of Medical Devices Conference* .
- Scales, C. (2024), ‘R11380 stainless steel single point load cells’. Accessed: 2024-06-15.
URL: <https://products.carolinascals.com/viewitems/rice-lake-load-cells-2/r11380-stainless-steel-single-point-load-cells>
- Taheri, B., Case, D. & Richer, E. (2015), ‘Adaptive suppression of severe pathological tremor by torque estimation method’, *IEEE/ASME Transactions on Mechatronics* **20**, 717–727.
- Tekscan (2016), ‘Pressure mapping, force measurement tactile sensors’. Accessed: 2024-06-15.
URL: <https://www.tekscan.com/resources/whitepaper/load-cell-vs-force-sensor>
- Tira (n.d.), ‘Schwingprüftechnik’. Accessed: 2024-06-10.
URL: <https://www.tira-gmbh.de/schwingprueftechnik/schwingpruefanlagen/standard-schwingpruefanlagen/>
- Tsotsis, G. (1987), *Entwicklung eines biomechanischen Modells des Hand-Arm-Systems*, Springer Berlin Heidelberg.
- Vectornav (2024), ‘What is an internal measurement unit?’. Accessed: 2024-06-15.
URL: <https://www.vectornav.com/resources/inertial-navigation-articles/what-is-an-inertial-measurement-unit-imu>
- Veluvolu, K. C. & Ang, W. T. (2011), ‘Estimation of physiological tremor from accelerometers for real-time applications’, *Sensors* **11**, 3020–3036.
- Wu, M., Jia, S. & Lin, Z. (2022), ‘An experimental study on the vibration transmission characteristics of wrist exposure to hand transmitted vibration’, *Applied Sciences (Switzerland)* **12**.
- Xu, X. S., Welcome, D. E., McDowell, T. W., Warren, C. & Dong, R. G. (2009), ‘An investigation on characteristics of the vibration transmitted to wrist and elbow in the operation of impact wrenches’, *International Journal of Industrial Ergonomics* **39**, 174–184.
- Yang, S., MacLachlan, R. A. & Riviere, C. N. (2015), ‘Manipulator design and operation of a six-degree-of-freedom handheld tremor-canceling microsurgical instrument’, *IEEE/ASME Transactions on Mechatronics* **20**, 761–772.
- Zamanian, A. H. & Richer, E. (2017), ‘Adaptive disturbance rejection controller for pathological tremor suppression with permanent magnet linear motor’, *Proceedings of the ASME 2017 Dynamic Systems and Control Conference* .

Zhang, L.-Q. & Rymer, W. Z. (1997), 'Simultaneous and nonlinear identification of mechanical and reflex properties of human elbow joint muscles', *IEEE TRANSACTIONS ON BIOMEDICAL ENGINEERING* 44.

Zhou, Y., Jenkins, M. & Naish, M. (2016), 'The measurement and analysis of parkinsonian hand tremor'.



Appendix



A. Matlab codes

Hand-arm-system model

```
1
2 clc
3 clear
4 close all
5
6 syms theta1(t) theta2(t) theta3(t) theta4(t) theta5(t)
7 syms m1 m2 m3 l1 l2 l3 lg1 lg2 lg3 Ig1 Ig2 Ig3
8
9 % Generalized coordinates
10
11 theta1_t(t) = diff(theta1,1,t)
12 theta2_t(t) = diff(theta2,1,t)
13 theta3_t(t) = diff(theta3,1,t)
14
15 theta1_t_t(t) = diff(theta1_t,1,t)
16 theta2_t_t(t) = diff(theta2_t,1,t)
17 theta3_t_t(t) = diff(theta3_t,1,t)
18
19 % dynamic parameters
20
21 syms k_theta1 k_theta2 k_theta3 k_theta4 k_theta5
22 syms c_theta1 c_theta2 c_theta3 c_theta4 c_theta5
23
24 %Kinematics
25
26 %% Position S1
27
28 x_1g=lg1*cos(theta1)
29 y_1g=lg1*sin(theta1)
30
31 x_A=l1*cos(theta1)
32 y_A=l1*sin(theta1)
33
34 r_1g=[x_1g y_1g 0]
35 r_A=[x_A y_A 0]
36
37 %% Position S2
38
39 r_2g=r_A+(lg2)*[cos(theta2) sin(theta2) 0];
40 r_B=r_A+(l2)*[cos(theta2) sin(theta2) 0];
```

```

41
42 %% Position S3
43 r_3g=r_B+(lg3)*[cos(theta3) sin(theta3) 0];
44
45 %% Velocity
46
47 v_1g=diff(r_1g,1,t);
48 v_2g=diff(r_2g,1,t);
49 v_3g=diff(r_3g,1,t);
50
51 %Velocities
52
53 w_1=theta1_t(t);
54 w_2=theta2_t(t);
55 w_3=theta3_t(t);
56
57 T_pos =
58 (m1/2)*v_1g*transpose(v_1g)+
59 (m2/2)*v_2g*transpose(v_2g)+
60 (m3/2)*v_3g*transpose(v_3g);
61
62 T_rot = (I_g1/2)*w_1^2 +
63 (I_g2/2)*w_2^2 +
64 (I_g3/2)*w_3^2;
65
66 T=T_pos+T_rot;
67
68 V= (k_theta1/2)*(theta1)^2+
69 (k_theta2/2)*(theta2-theta1)^2+
70 (k_theta3/2)*(theta3-theta2)^2;
71
72 D=(c_theta1/2)*theta1_t(t)^2+
73 (c_theta2/2)*(theta2_t(t)-theta1_t(t))^2+
74 (c_theta3/2)*(theta3_t(t)-theta2_t(t))^2
75
76 % Equations for theta1
77 T_theta1_t = (diff(T,1,theta1_t));
78 T_theta1_t_t= (diff(T_theta1_t,1,t));
79 T_theta1= diff(T,1,theta1);
80 V_theta1=diff(V,1,theta1);
81 D_theta1_t=(diff(D,1,theta1_t))
82
83 L_theta1=vpa(T_theta1_t_t-T_theta1+V_theta1+D_theta1_t); %Equation of motion
84
85 % Equations for theta2
86 T_theta2_t = (diff(T,1,theta2_t));
87 T_theta2_t_t= (diff(T_theta2_t,1,t));
88 T_theta2= (diff(T,1,theta2));
89 V_theta2=diff(V,1,theta2);
90 D_theta2_t=(diff(D,1,theta2_t))

```

```

91
92 L_theta2=vpa(T_theta2_t_t-T_theta2+V_theta2+D_theta2_t,3); %Equation of motion
93
94 % Equations for theta3
95 T_theta3_t = (diff(T,1,theta3_t));
96 T_theta3_t_t= (diff(T_theta3_t,1,t));
97 T_theta3= (diff(T,1,theta3));
98 V_theta3=diff(V,1,theta3);
99 D_theta3_t=(diff(D,1,theta3_t))
100
101 L_theta3=vpa(T_theta3_t_t-T_theta3+V_theta3+D_theta3_t,3); %Equation of motion
102
103 %Linearization
104 var=[theta1, theta2, theta3,
105      theta1_t, theta2_t, theta3_t,
106      theta1_t_t,theta2_t_t,theta3_t_t];
107
108 svar=diag([1 1 1 1 1 1 1 1 1])
109 Ls= [L_theta1 L_theta2 L_theta3 ];
110 sL=diag([1 1 1 ])
111
112 for i=1:3;
113 for j=1:9;
114
115 Eq(i,j)=diff(Ls*transpose(sL(i,:)),1,var*transpose(svar(j,:)));
116
117 [i,j]
118 end
119 end
120
121 Eq_s=subs(Eq, [theta1 ], [0]);
122 Eq_s=subs(Eq_s, [ theta1_t ], [0]);
123 Eq_s=subs(Eq_s, [theta1_t_t ], [0]);
124 Eq_s=subs(Eq_s, [ theta2 ], [0]);
125 Eq_s=subs(Eq_s, [ theta2_t ], [0]);
126 Eq_s=subs(Eq_s, [ theta2_t_t ], [0]);
127 Eq_s=subs(Eq_s, [ theta3 ], [0]);
128 Eq_s=subs(Eq_s, [ theta3_t ], [0]);
129 Eq_s=subs(Eq_s, [ theta3_t_t ], [0]);
130
131 M=[ Eq_s(1,7) Eq_s(1,8) Eq_s(1,9);
132     Eq_s(2,7) Eq_s(2,8) Eq_s(2,9);
133     Eq_s(3,7) Eq_s(3,8) Eq_s(3,9)]
134
135 C=[ Eq_s(1,4) Eq_s(1,5) Eq_s(1,6);
136     Eq_s(2,4) Eq_s(2,5) Eq_s(2,6);
137     Eq_s(3,4) Eq_s(3,5) Eq_s(3,6)]
138
139 K=[Eq_s(1,1) Eq_s(1,2) Eq_s(1,3);
140     Eq_s(2,1) Eq_s(2,2) Eq_s(2,3);

```

```
141 Eq_s(3,1) Eq_s(3,2) Eq_s(3,3)]
```

```
142
```

Main code

```
1
2 %%%%%%%%% Code for the analysis of results by using the measurement setup B
3 %%%%%%%%% It is required 3 data sets with motion signals, grip force and
4 %%%%%%%%% excitation force over time
5
6 %%%% Version: 01 22.03.2024 Feliz cumplea;os mamita
7 %%%% Some minor corrections in descriptions and axis indexing 27.03.24
8 %%%% Calibration intention in order to get logical results in the system
9 %%%% identification
10 %%%% Version: 02 18.04.2024 Range of data for the analysis added.
11 %%%% Frequency band added
12 %%%% Version: 02 12.05.24
13 %%%% Bandfilteradded to system identification
14 %%%% Version: 2.1 18.05.24 Spectrogram added
15 %%%% Version 2.2 26.05.24 accelerometer in shoulder added
16 %%%% Force pre processing and filtering added, force with
17 %%%% acceleration synchronization
18 %%%% Version 2.3 30.05.24 iden2 added for system identification with
19 %%%%functions costFunction and odesystem.
20 %%%% HASModel used for the differential equations determination
21 %%%% Version: 2.4 04.06.24 Calibration constants added
22 %%%% Version: 2.5 14.06.24 Test 6 and 7 processed.
23 %%%% Version: 3 22.06.24 Test 8 processed.
24
25 clear all
26 close all
27 set(groot,'defaultAxesFontName','Helvetica')
28 set(groot,'defaultAxesFontSize',16)
29
30 %%%%%%%%%%%%% Input parameters %%%%%%%%%%%%%
31
32 test='7_10'
33 load('unter.mat') % Dataset of force measurement between device and shaker
34 load('oben.mat') % Dataset of force measurement on the Hand
35 load('bel.mat') % Data set of acceleration, angular velocity over time
36
37 %% Sensor parameters
38
39 Fs = 150 ; % Sampling frequency of MPUs
40 Fs_force = 100 ; % Sampling frequency of force sensors
41 k_handforce = -131.4015 ; % Force transformation from Volts to N
42 k_excforce = 27.9233 ; % Force transformation from Volts to N
43 kgrip = 0.207 ; % Lever constant
```

```

44
45 %% Measured data
46 acc1 = accelbuff1; % Acceleration MPU1
47 gyro1 = gyrobuff1; % Angular velocity MPU1
48 xyz1 = [2,3,1]; % Directions according to the model
49
50 acc2 = accelbuff2; % Acceleration MPU2
51 gyro2 = gyrobuff2; % Angular velocity MPU2
52 xyz2 = [2,3,1]; % Directions according to the model
53
54 acc3 = accelbuff3; % Acceleration MPU3
55 gyro3 = gyrobuff3; % Angular velocity MPU3
56 xyz3 = [2,3,1]; % Directions according to the model
57 [2,3,1] fuer 180, [3,2,1]
58
59 handforce(1,:) = oben(1,:); % Time range of grip force
60 handforce(2,:) = oben(2,:);
61
62 excforce(1,:) = unter(1,:); % Time range of excitation force
63 excforce(2,:) = unter(2,:);
64
65
66 %%%%%%%%%%% Pre-processing %%%%%%%%%%%
67
68 %% Raw signals for setting the parameters for filtering and synchronization
69
70 L = length(acc1(:,1)); % Length of signal
71 xlimt = [0.5 15]; % Axis limits
72 ylimt = [0 20]; % Axis limits
73
74 %%% Plots %%%
75 rawSignals
76
77 %%%%%%%%%%% Processing %%%%%%%%%%%
78
79 %% Input Data
80 Fc = [5 11]; %Cut frequency for bandpass filter
81 excforce0 = 4.07428; % Excitation force without proband
82 handforce0 = 0.6847; % Grip force without proband
83
84 %% Input for measured data synchronization
85
86 setMPU0 = 580 % Startpoint of mpu signal
87 setMPUf = 5975 % Endpoint of mpu signal
88 setForce0 = 2*Fs_force % Startpoint of force signal
89 setForcef = 58.3*Fs_force % Endpoint of force signal
90
91 %% synchronization
92 deltasetMPU = (setMPUf - setMPU0) /Fs
93 deltasetForce = (setForcef - setForce0) /Fs_force

```

```

94 Fs_setforce = round(((setForcef - setForce0) /deltasetMPU),0)
95 deltat      = setMPU0/Fs           % Time difference for synchronization
96 deltatforce = setForce0/Fs_setforce
97
98 handforce(2,:) = (handforce(2,:) - handforce0)*k_handforce*kgrip;
99 excforce(2,:)  = (excforce(2,:) - excforce0 )*k_excforce;
100
101 acc1=signalCorrection(acc1); %Mean value removed
102 acc2=signalCorrection(acc2); %Mean value removed
103 acc3=signalCorrection(acc3); %Mean value removed
104
105 %%%% Plots %%%%
106 filteredSignals
107 frequencyAnalysis
108 spectro
109
110 %%%% Isolating a specific time range for analysis %%%%
111
112 t0 = 20 % Start time of analysis
113 tf = 25 % End time of analysis
114
115 sprange_mpu = Fs* ([t0 tf]); % Sample range for identification
116 sprange_force = Fs_setforce*([t0 tf] + deltatforce);
117
118 frequencyAnalysisSpecificRange
119 spectroSpecificRange
120
121 %%%% Muscle tension and motion response %%%%
122
123 Fc_force = Fc; % Cut frequency for bandpass filter
124 t0 = 20; % Start time for dynamic parameters estimation
125 tf = 22; % End time for dynamic parameters estimation
126
127 range_mpu = Fs* ([t0 tf] ); % System identification range.
128 range_force = Fs_setforce*([t0 tf] + deltatforce);
129
130 %%%% Plots %%%%
131 force
132
133 %%%% System Identification %%%%
134 %% Procedure explained in Chapter Method of Characterization
135 iden2

```



B. Grip study results

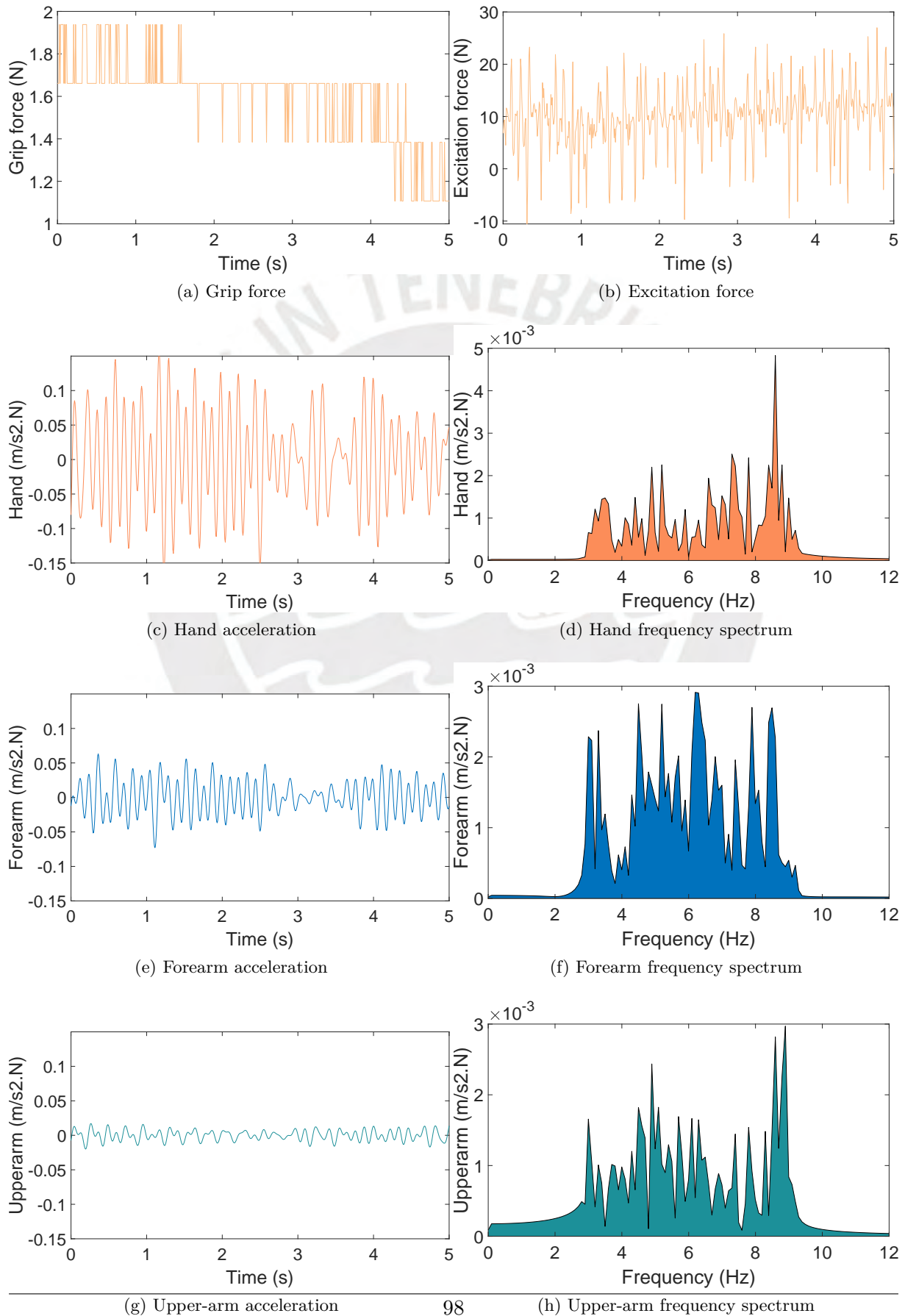


Figure B.1.: Dynamic response during a relaxed condition (0% grip force) with a posture of 90°:

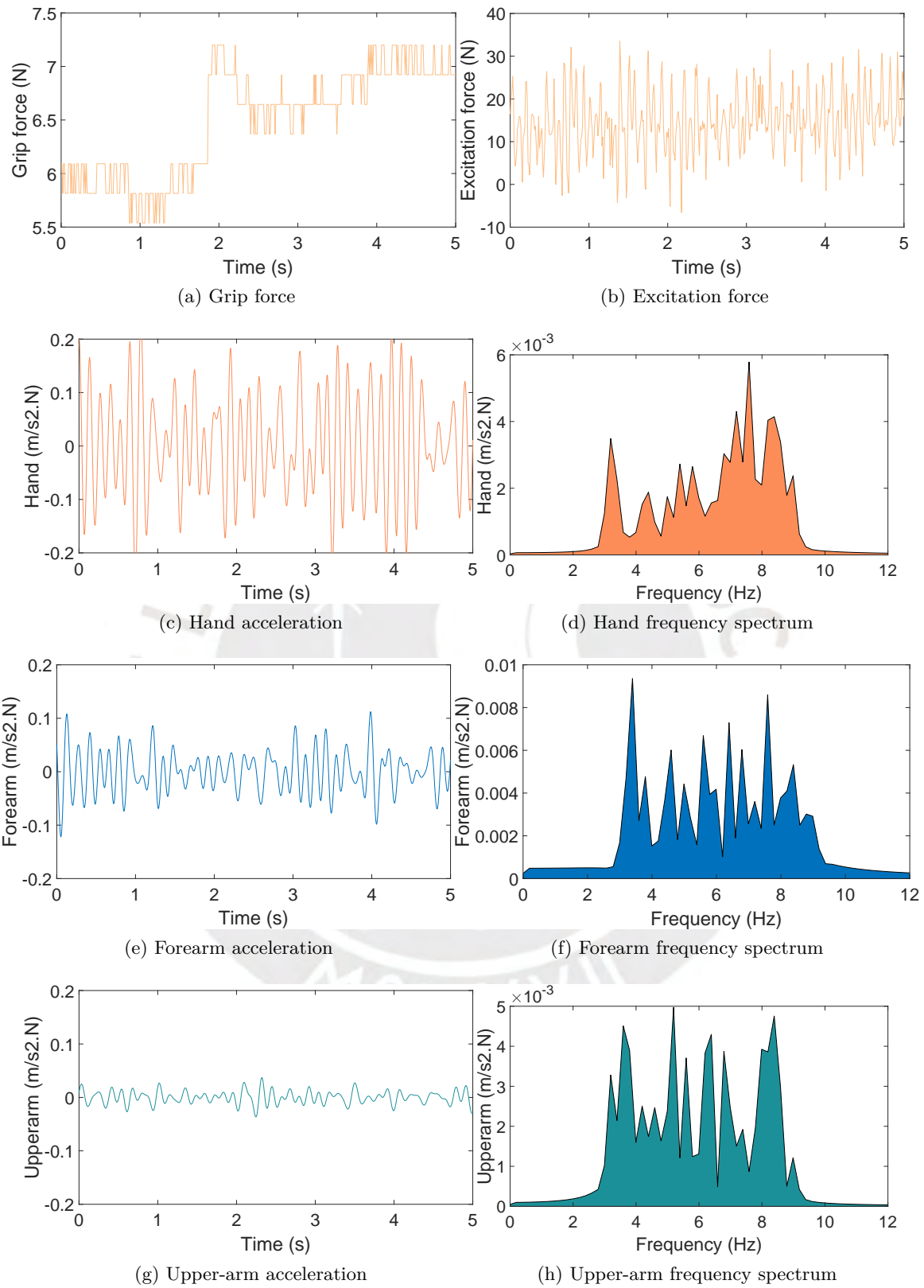


Figure B.2.: Dynamic response during a 25% grip force condition with a posture of 90° : (a-b) force measurement, (c-d) hand, (e-f) forearm (g-h) upper-arm acceleration and frequency spectrum

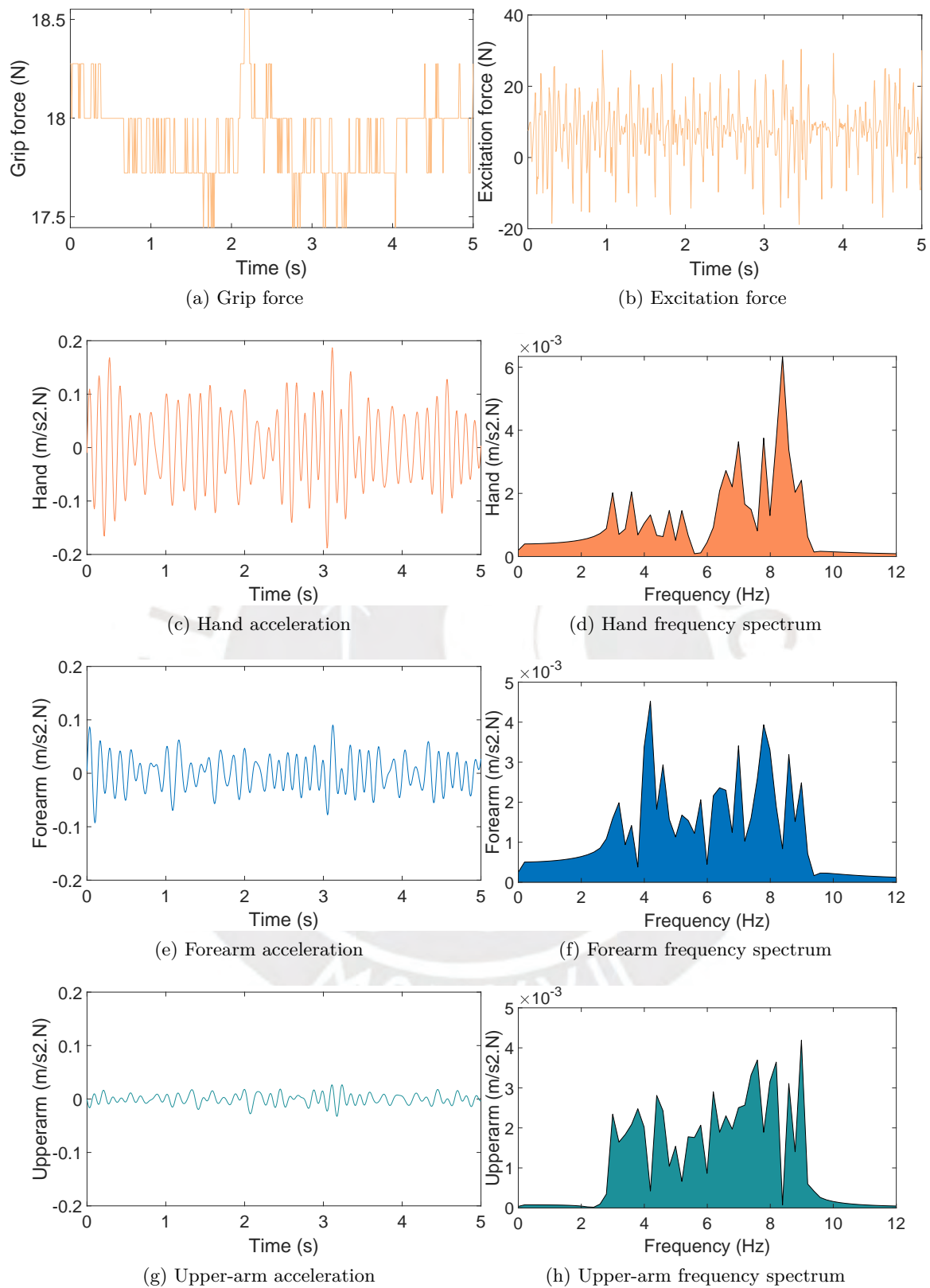


Figure B.3.: Dynamic response during a 75% grip force condition with a posture of 90°: (a-b) force measurement, (c-d) hand, (e-f) forearm (g-h) upper-arm acceleration and frequency spectrum

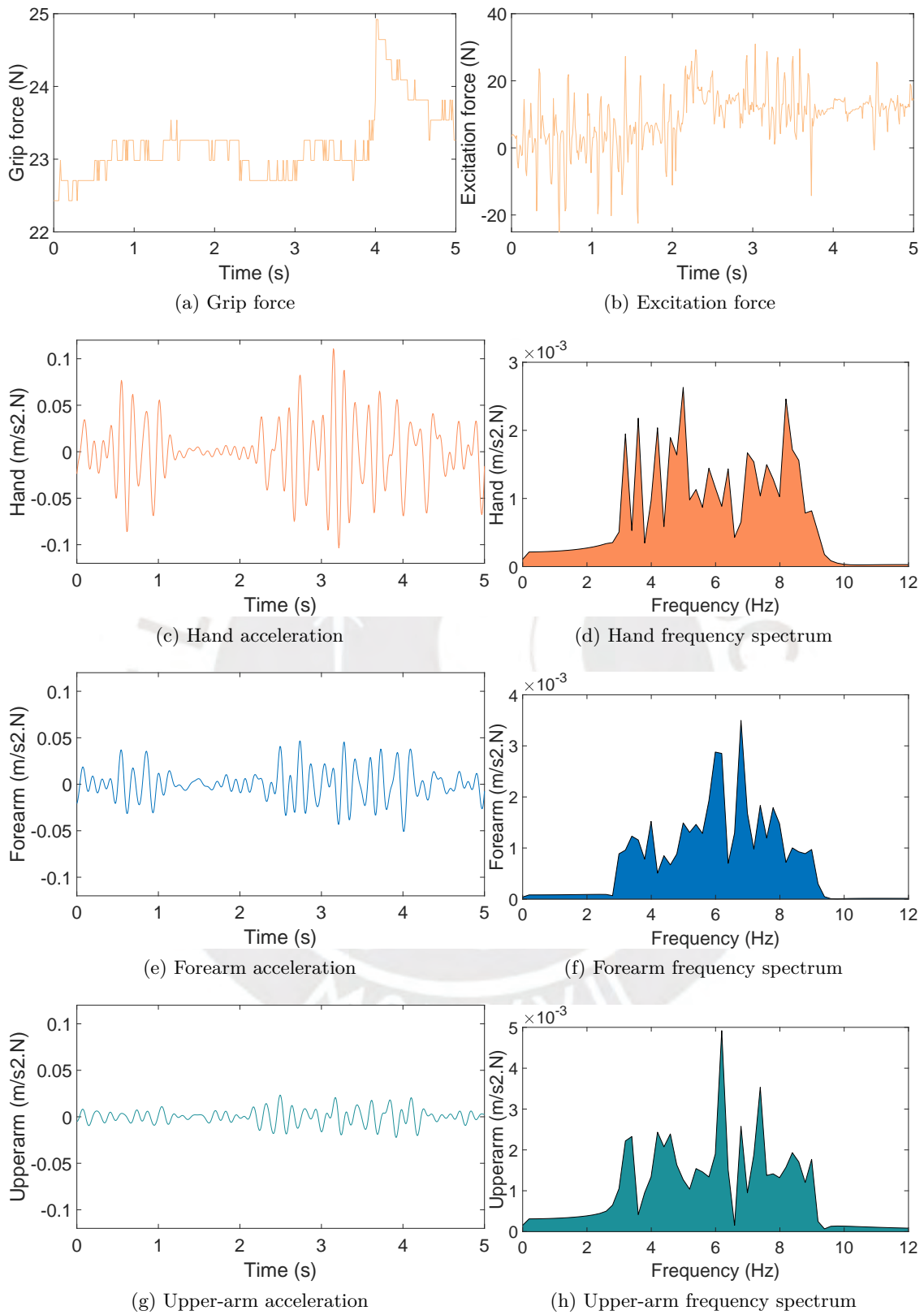


Figure B.4.: Dynamic response during a 100% grip force condition with a posture of 90°: (a-b) force measurement, (c-d) hand, (e-f) forearm (g-h) upper-arm acceleration and frequency spectrum

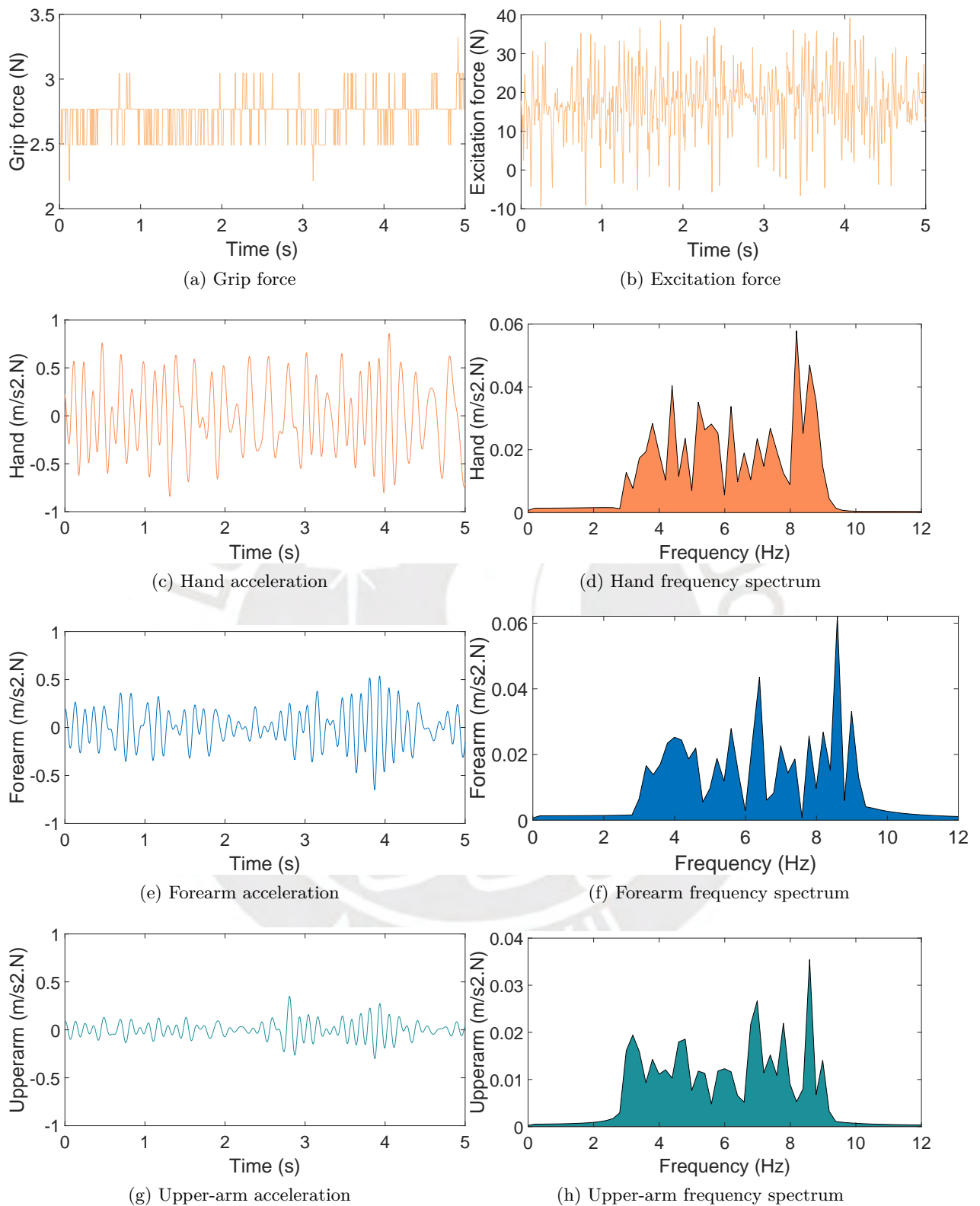


Figure B.5.: Dynamic response during a relaxed muscle tension condition and posture 180°:(a-b) force measurement, (c-d) hand, (e-f) forearm (g-h) upper-arm acceleration and frequency spectrum

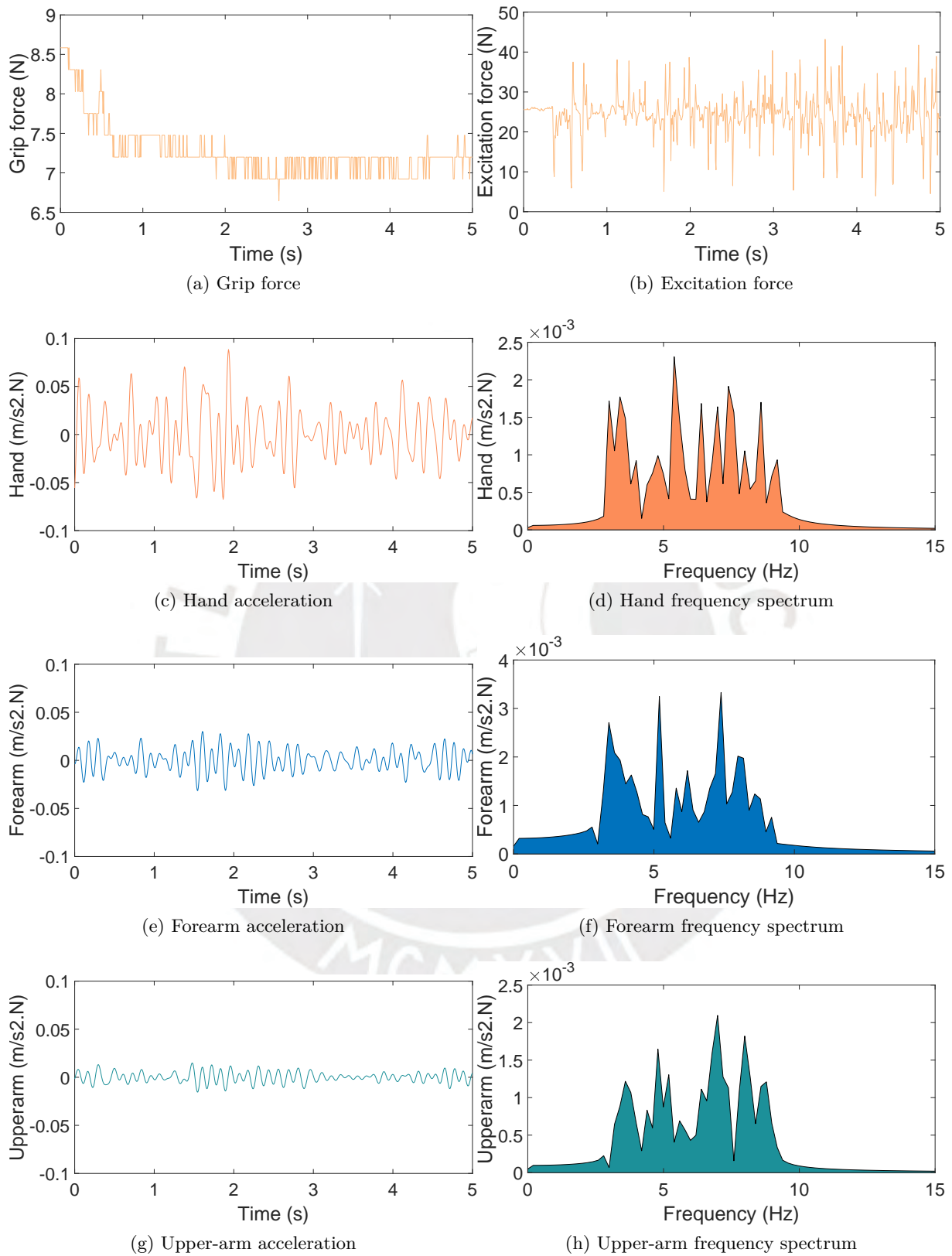


Figure B.6.: Dynamic response during a 25% grip force condition with a posture of 180: (a-b) force measurement, (c-d) hand, (e-f) forearm (g-h) upper-arm acceleration and frequency spectrum

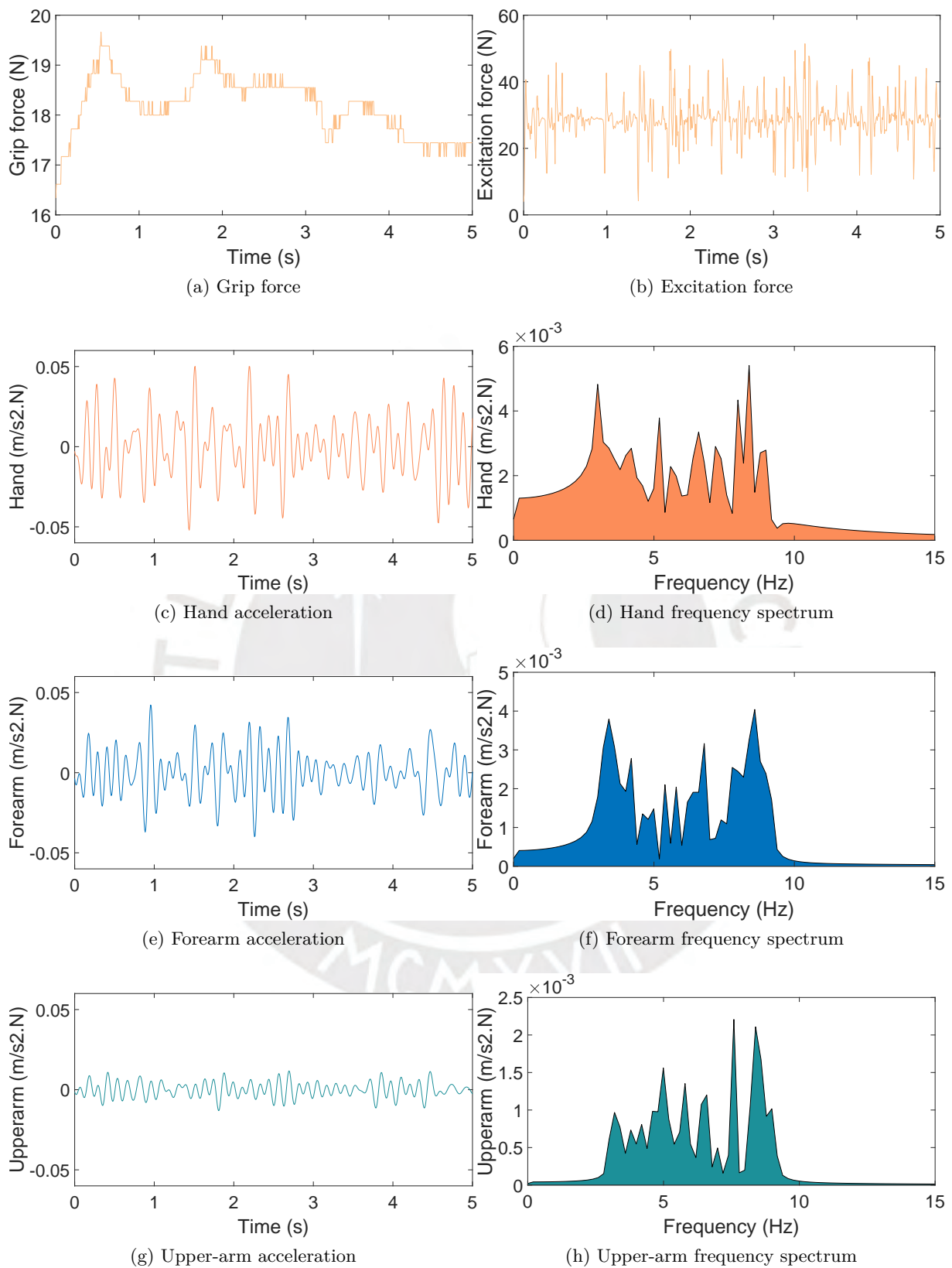


Figure B.7.: Dynamic response during a 75% grip force condition and posture 180°: (a-b) force measurement, (c-d) hand, (e-f) forearm (g-h) upper-arm acceleration and frequency spectrum

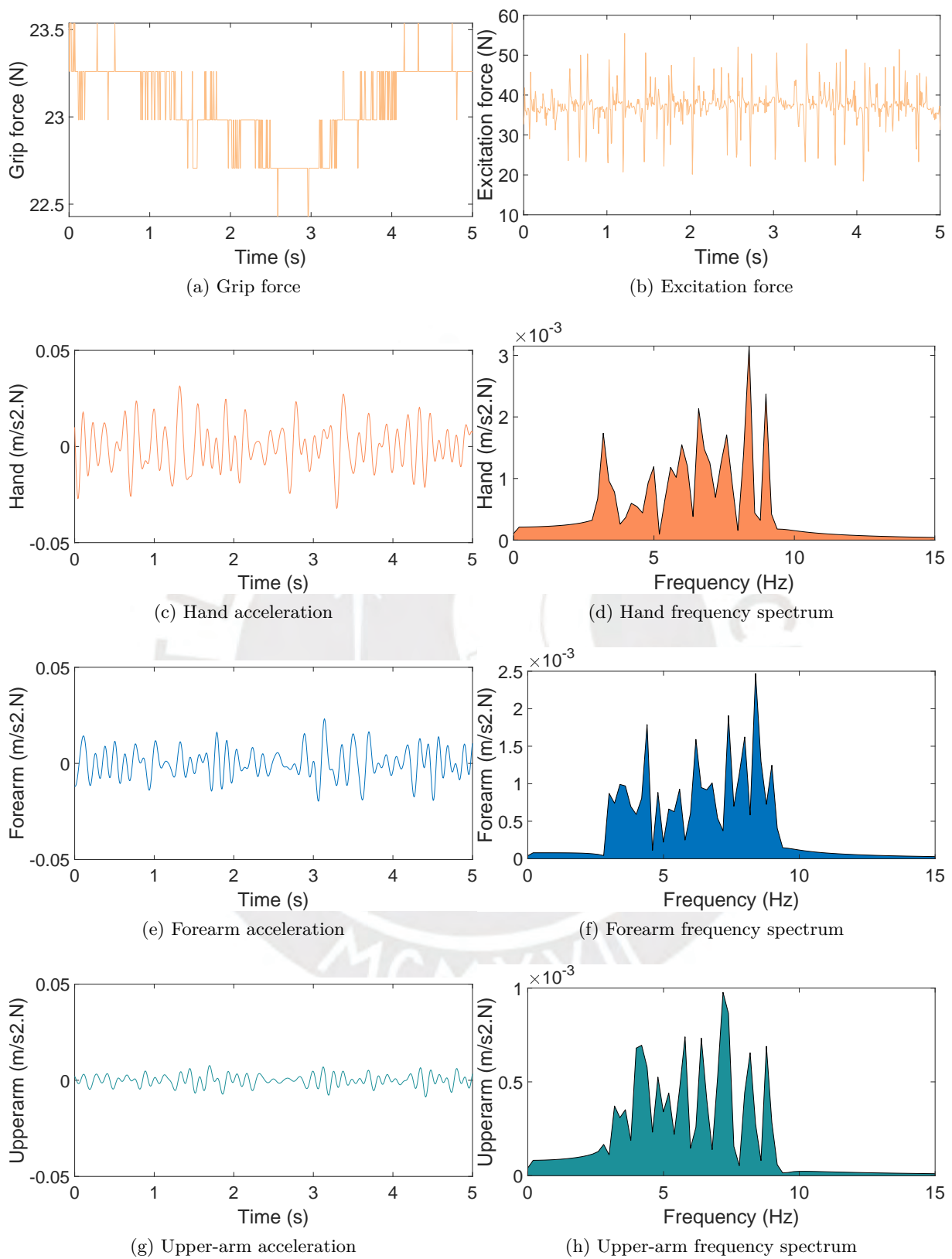


Figure B.8.: Dynamic response during a 100% grip force condition and posture 180°: (a-b) force measurement, (c-d) hand, (e-f) forearm (g-h) upper-arm acceleration and frequency spectrum

C. DVD

The DVD content is organized as shown in Figure C.1 with the following description of the items:

- Thesis document: It contains the PDF document.
- Design: It contains the three measurement setup developed in STEP format.
- Data-sheets of components: It contains the data-sheets of all the components implemented.
- Matlab codes: It contains all the matlab files used for the processing of the experimental data.
- Experimental results: It contains the raw data and the processed data in csv. files used for the plots.
- Figures: It contains all the figures used in the thesis document.
- Literature: It contains the Citavi project file and the PDFs of the literature used.
- Technical documents of the design: It contains all the formal documents from the conception until the final design.

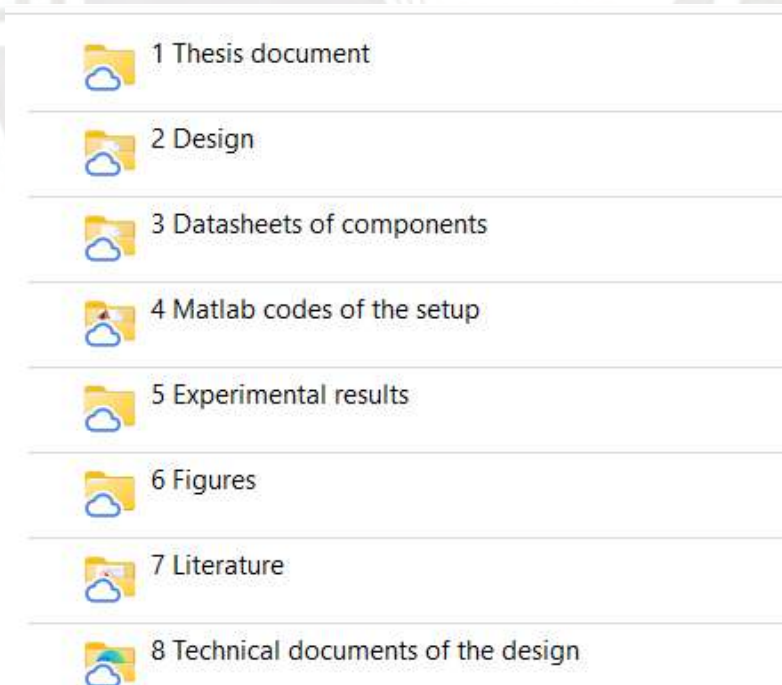


Figure C.1.: DVD files

D. Technical documents



A

A

B

C

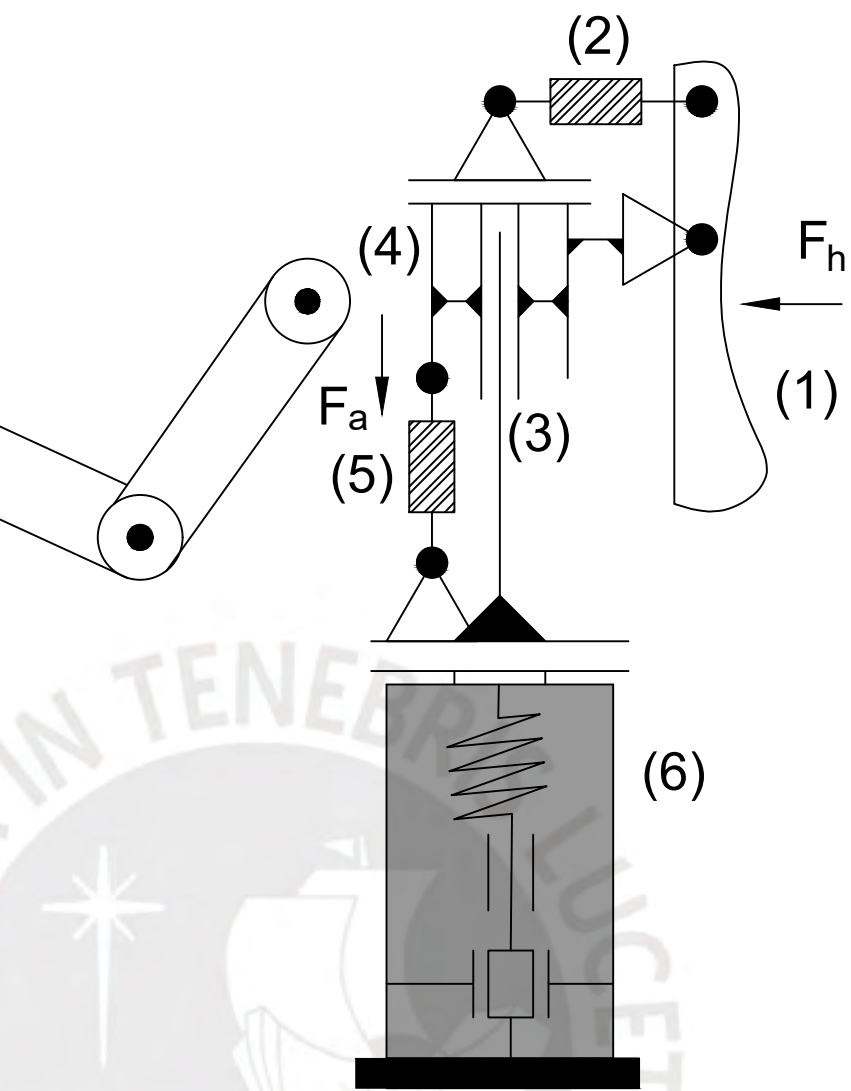
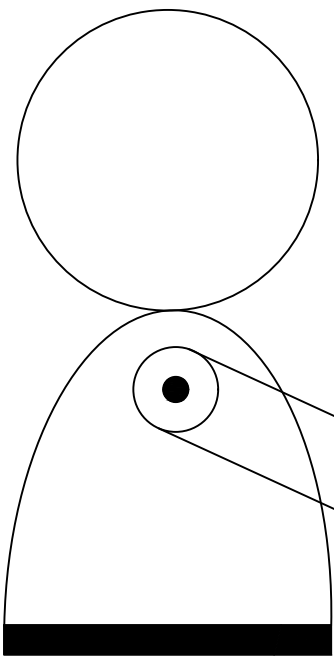
D

E

E

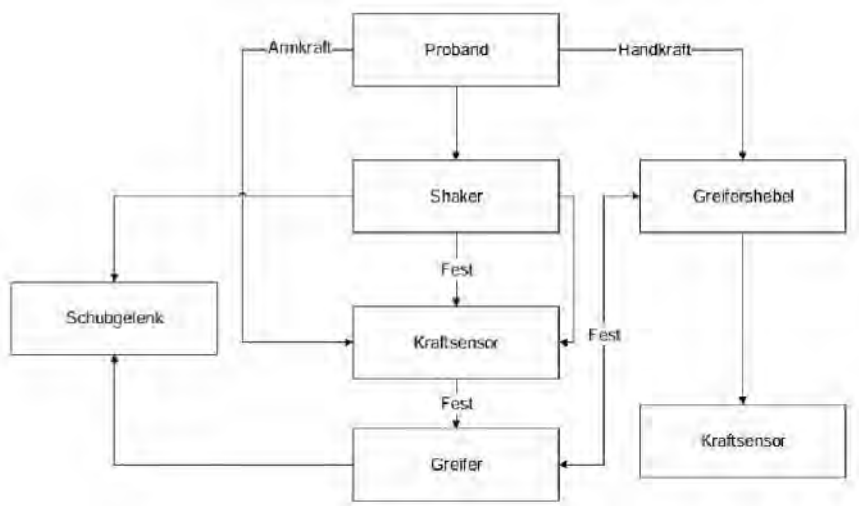
F

F

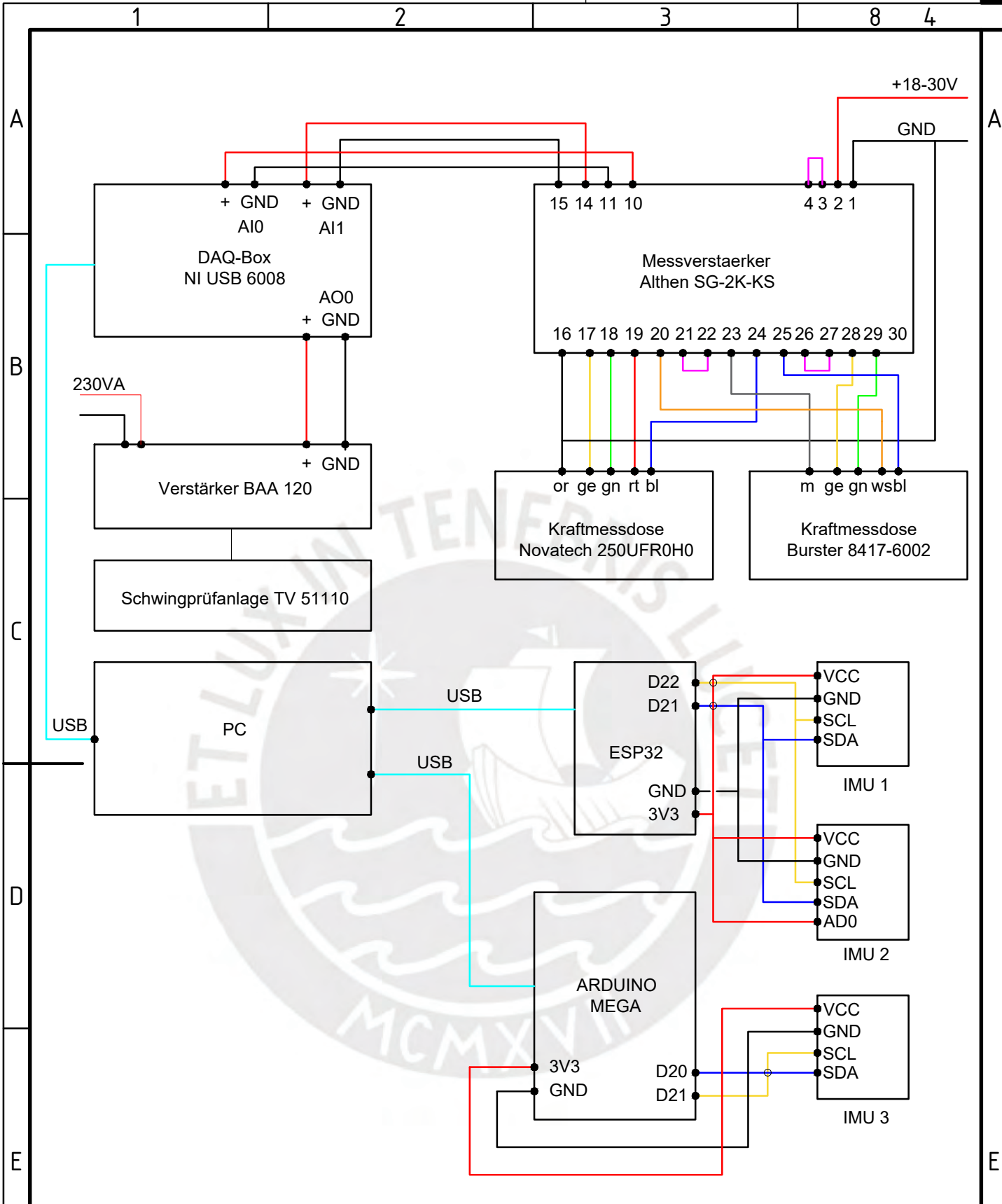


- (1) Greifershebel
- (2) Kraftsensor
- (3) Schubgelenk
- (4) Greifer
- (5) Kraftsensor
- (6) Shaker

F_h : 0...60kg
 F_a : 0...50kg



| | | | | | |
|----------------------------------------------------------------|----------------------------------|-----------------------------------------------------------------------------|---------------------------------|------------------------------------------------|---------------------|
| Allgemeintoleranzen- DIN ISO 2768- | | | | | |
| Werkstückkanten- DIN ISO 13715- | | Material:- Halbzeug:- | | Maßstab:- Masse ca.:- | |
| Verantwortliche Abt.: | Technische Referenz:- | Erstellt durch: Carlos Rincon | | Genehmigt von: Sabine Bruchmueller | |
| Technische Universität Ilmenau Fakultät für Maschinenbau | | Dokumentenart Konzept | | Dokumentenzustus Ver03 | |
| | | Titel, zusätzlicher Titel Konkretisiertes Technisches Prinzip | | | |
| | | Änd. | Ausgabedatum 29.06.24 | Spr. de | Blatt 1/1 |



| | | | |
|----------------------------------------------------------------|---------------------------------|------------------------------------------------|----------------------------------------------|
| Allgemeintoleranzen DIN ISO 2768- | | | |
| Werkstückkanten DIN ISO 13715- | | Material: _____ | Maßstab: _____ |
| | | Halbzeug: _____ | Masse ca.: _____ |
| Verantwortliche Abt. | Technische Referenz | Erstellt durch: Carlos Rincon | Genehmigt von: Sabine Bruchmueller |
| Technische Universität Ilmenau Fakultät für Maschinenbau | | Dokumentenart Schaltplan | Dokumentenstatus Ver01 |
| | | Titel, zusätzlicher Titel Messaufbau | |
| And. | Ausgabedatum 29.06.24 | Spr. de | Blatt 1/1 |

| 1 | | 2 | | 3 | | 4 | |
|----------------------------------------------------------------|-------|------------------------------|---------------------------|--------------------------|------------------------------------|---------------------|-----------|
| Pos. | Menge | Benennung | | Sachnummer/Norm-Kurzbez. | | Bemerkung | |
| A | 1 | 1 | Buchse des Gelenks | | | | Vorhanden |
| | 2 | 1 | Separator des Hebels | | | | PLA |
| | 3 | 1 | Buchse des Gelenkkoepf | | | | PLA |
| | 4 | 1 | Obenkupplung | | | | PLA |
| | 5 | 1 | Befestigungsmasseoben2 | | | | PLA |
| B | 6 | 1 | Adaptor | | | | PLA |
| | 7 | 1 | Greifer | | | | PLA |
| | 8 | 1 | Befestigungsmasse | | | | PLA |
| | 9 | 1 | Vibrationsplatte | | | | PLA |
| | 10 | 4 | Plain washers | | ISO 7089 - 6 | | |
| C | 11 | 4 | Hexagon Socket Screw | | ISO 4762 - M5 x 16 | | |
| | 12 | 7 | Plain washers | | ISO 7089 - 5 | | |
| | 13 | 4 | Hexagon Socket Screw | | ISO 4762 - M4 x 20 | | |
| | 14 | 2 | Hexagon nuts | | ISO 4032 - M4 | | |
| | 15 | 6 | Plain washers | | ISO 7089 - 4 | | |
| D | 16 | 2 | Hexagon Socket Screw | | ISO 4762 - M4 x 35 | | |
| | 17 | 1 | Kraftsensor der Handkraft | | BURSTER 8417-6002 KLBM-06-1 | | |
| | 18 | 1 | IMU mit Case | | MPU6050 | | |
| | 19 | 1 | Welle | | LHFRF13H | | |
| | 20 | 1 | Linearfuehrung | | LHFRF13H | | |
| E | 21 | 1 | Kraftsensor der Störung | | NOVATECH F250 UFR0H0 KLBM-05-M4 | | |
| | 22 | 1 | Shaker | | TIRA TV 51110 | | |
| | 23 | 1 | Parallel pins | | ISO 8734 - 6 x 40 | | |
| | 24 | 4 | Hexagon Socket Screw | | ISO 4762 - M6 x 12 | | |
| | 25 | 1 | Hexagon Socket Screw | | ISO 4762 - M5 x 25 | | |
| F | 26 | 2 | Hexagon nuts | | ISO 4032 - M5 | | |
| | 27 | 1 | Hexagon Socket Screw | | ISO 4762 - M5 x 40 | | |
| | 28 | 2 | Parallel pins | | ISO 8734 - 5 x 30 | | |
| | 29 | 2 | Hexagon nuts | | ISO 4032 - M3 | | |
| | 30 | 2 | Hexagon Socket Screw | | ISO 4762 - M3 x 30 | | |
| | 31 | 6 | Plain washers | | ISO 7089 - 3 | | |
| | 32 | 2 | Hexagon Socket Screw | | ISO 4762 - M3 x 10 | | |
| | 33 | 4 | Hexagon Socket H Screw | | ISO 4762 - M4 x 16 | | |
| | 34 | 1 | Hebel | | Ducati Desert X 65803003 | | |
| Verantwortliche Abt. | | Technische Referenz | | Erstellt durch: | | Genehmigt von: | |
| | | | | Carlos Rincon | | Sabine Bruchmueller | |
| Technische Universität Ilmenau Fakultät für Maschinenbau | | Dokumentenart | | Dokumentenstatus | | | |
| | | Technischer Entwurf | | VerB-06 | | | |
| | | Titel, zusätzlicher Titel | | | | | |
| | | Messaufbau Geraetprototyp | | And. | Ausgabedatum | Spr. | Blatt |
| | | | | | 30.06.24 | de | 1/1 |